THE M_w 7.8 GORKHA, NEPAL EARTHQUAKE OF 25 APRIL 2015

A FIELD REPORT BY EEFIT

THE M_w 7.8 GORKHA, NEPAL EARTHQUAKE OF THE 25TH APRIL 2015

A FIELD REPORT BY EEFIT

Sean Wilkinson

Matt DeJong

Viviana Novelli

Paul Burton

Sarah Tallet-Williams

Michael Whitworth

Franco Guillermo

Tim White

Arthur Trieu

Barnali Ghosh

Suryanarayana Datla

Additional contributions by
Yebang Xu
School of Environmental Sciences, University of East Anglia, Norwich

Thomas R. Hall
National Oceanography Centre, University of Southampton, Southampton

Report reviewed by
Diana Contreras
School of Engineering, Newcastle University

Earthquake Engineering Field Investigation Team
c/o The Institution of Structural Engineers
International HQ
47–58 Bastwick Street
London EC1V 3PS
Tel: +44 (0) 20 7235 4535
Fax:+44 (0) 207235 4294
Email: eefit@istructe.org.uk
Website: http://www.eefit.org.uk

August 2019

ACKNOWLEDGEMENTS

The authors would like to express their thanks to the many individuals and organisations that have assisted with the Earthquake Engineering Field Investigation Team (EEFIT) mission to Nepal and in the preparation of this report.

We firstly thank AIR Worldwide, AECOM and Arup for enabling, Suryanarayana Datla, Michael Whitworth and Tim White to attend this mission. We would also like to thank the Engineering and Physical Sciences Research Council, Grant Number EP/I01778X/1 for providing funding for Sean Wilkinson, Matt DeJong, Paul Burton, Viviana Novelli and Arthur Trieu to join the team. Their continued support in enabling UK academics to witness the aftermath of earthquakes and the effects on structures and the communities they serve is gratefully acknowledged. We also thank other members of EEFIT who provided support in getting the mission to Nepal and for providing support while the team members were there. In particular, we would like to acknowledge the support of Berenice Chan and Tristan Lloyd.

The authors would also like to thank Carlos Geha, Susan Robertson and Alexandra Lazau-Ratz from the United Nations Office for the Coordination of Humanitarian Affairs (UNOCHA) for housing the team in Gorkha. They provided valuable information on sites to visit and for organising the helicopter flights that made the observations in the remote mountains communities possible, Brian Tucker, Jitanda Bothara, Peeyush Sekhsaria, Juliet Lang, and Bijan Khazai. We would also like to thank Kumar Talluri and the staff of Verisk whose assistance to the team while in Kathmandu greatly increased the quantity and quality of the observations made. We are additionally grateful to Jean-Philippe Avouac for supplying Figure 2-10 and other invaluable information and to Tim Wright of the NERC Centre for the Observation and Modelling of Earthquakes, Volcanoes and Tectonics (COMET). Further thanks are due to L. B. Adhikari for vital discussion and disclosure of information and to other scientists at the National Seismological Centre, Kathmandu (NSC)

Finally, the EEFIT Corporate Sponsors extend its thanks for their support over the years to URS-AECOM, AIR Worldwide, Arup, Atkins, British Geological Survey (BGS), CH2M Hill, Guy Carpenter, Mott MacDonald, Risk management Solutions (RMS), Sellafield Ltd and Willis Towers Watson (WTW).

TABLE OF CONTENTS

INDEX OF FIGURES

INDEX OF TABLES

ACRONYMS

BGS	British Geological Survey
CEA	China Earthquake Administration
CEDIM	Centre for Disaster Management and Risk Reduction Technology.
CRR	Cyclic Resistance Ratio
CSR	Cyclic Stress Ratio
CGI	Corrugated Galvanised Iron
CTR	Current Tectonic Regime
DUDBC	Department of Urban Development and Building Construction
EEFIT	Earthquake Engineering Field Investigation Team
EERI	Earthquake Engineering Research Institute
GEER	Geotechnical Extreme Events Reconnaissance
GSHAP	Global Seismic Hazard Assessment Program
GMPE	Ground Motion Prediction Equation
ISC	International Seismological Centre
KVPT	Kathmandu Valley Preservation Trust
MoHP	Ministry of Health and Population
M_w	Moment Magnitude Scale
MBT	Main Boundary Thrust
MCT	Main Central Thrust
MFT	Main Thrust Fault
NEIC	National Earthquake Information Center
NGO	Non-Governmental Organization
NSC	National Seismological Centre
NEIC	National Earthquake Information Center
NSET	National Society for Earthquake Technology
PDNA	Post-Disaster Needs Assessment
PGA	Peak ground acceleration
PSHA	Probabilistic Seismic Hazard Analysis
RC	Reinforced Concrete
RLD	Subsurface Rupture Length
SESAME	Site Effects Assessment using Ambient Excitations
STDS	The South Tibetan Detachment System
UN	United Nations
UNESCO	United Nations Educational, Scientific and Cultural Organization
UNOCHA	United Nations Office for the Coordination of Humanitarian Affairs

URM	Unreinforced Masonry.
USGS	United States Geological Survey
WH	World Heritage
WTW	Willis Towers Watson

1. INTRODUCTION

1.1. THE GORKHA EARTHQUAKE

At 11:56 NST (06:11 UTC) on the 25th April 2015, an earthquake with a moment magnitude scale of M_w7.8 struck Nepal. The epicentre was located at 28.147°N, 84.708°E near the town of Gorkha approximately 80 km West of Kathmandu and had a focal depth of 19 km (USGS 2015). The earthquake was reported to have caused widespread damage between the epicentre and an area stretching to the East of Kathmandu. The earthquake also triggered numerous landslides in the hills and mountains in the affected region as well as causing an avalanche on Mt. Everest, which resulted in the deaths of 19 *Sherpas* and climbers (April 2015 Nepal earthquake, 2015). As is usual with these events, the region was also hit by a number of aftershocks. The most noticeable occurring on the 12th of May 2015 at 12:51 NST with a moment magnitude of M_w 7.3 and with an epicentre near the Chinese border between the capital of Kathmandu and Mt. Everest (USGS 2015).

1.2. THE MISSION

The Earthquake Engineering Field Investigation Team (EEFIT) management committee decided to send a team to investigate the impacts of this earthquake, how it affected Nepalese communities and their economy. Mission members covering a wide range of disciplines. The mission included seismologists, engineers and architects selected from the EEFIT membership and are the authors of this report. The mission had the objectives of 1) obtaining available recorded ground motion data, 2) making observations of the performance of buildings, geotechnical structures and lifelines, 3) assessing the impact of landslides on remote mountain communities, and 4) Gaining an understanding of insurance and other economic consequences resulting from this event. The team left the UK on the 12th June and returned on the 20th June spending seven days in the field making observations and meeting local engineers, scientists and government officials. This earthquake was of international significance, therefore visited by a number of other international reconnaissance teams, most notably the Earthquake Engineering Research Institute (EERI) and by the Geotechnical Extreme Events Reconnaissance (GEER) group. Valuable exchanges of knowledge occurred between the teams.

The mission visited Kathmandu and surrounds as well as Sangachok located approximately 40 km east of Kathmandu before travelling to Gorkha to observe damage near the epicentre. During the week of the mission, survey time was shared approximately equally between Kathmandu and surrounding districts and the Gorkha region and surrounding districts, with one trip in the region of the village of Sangachok. The location of the sites visited during the mission are depicted in Figure 1-1.

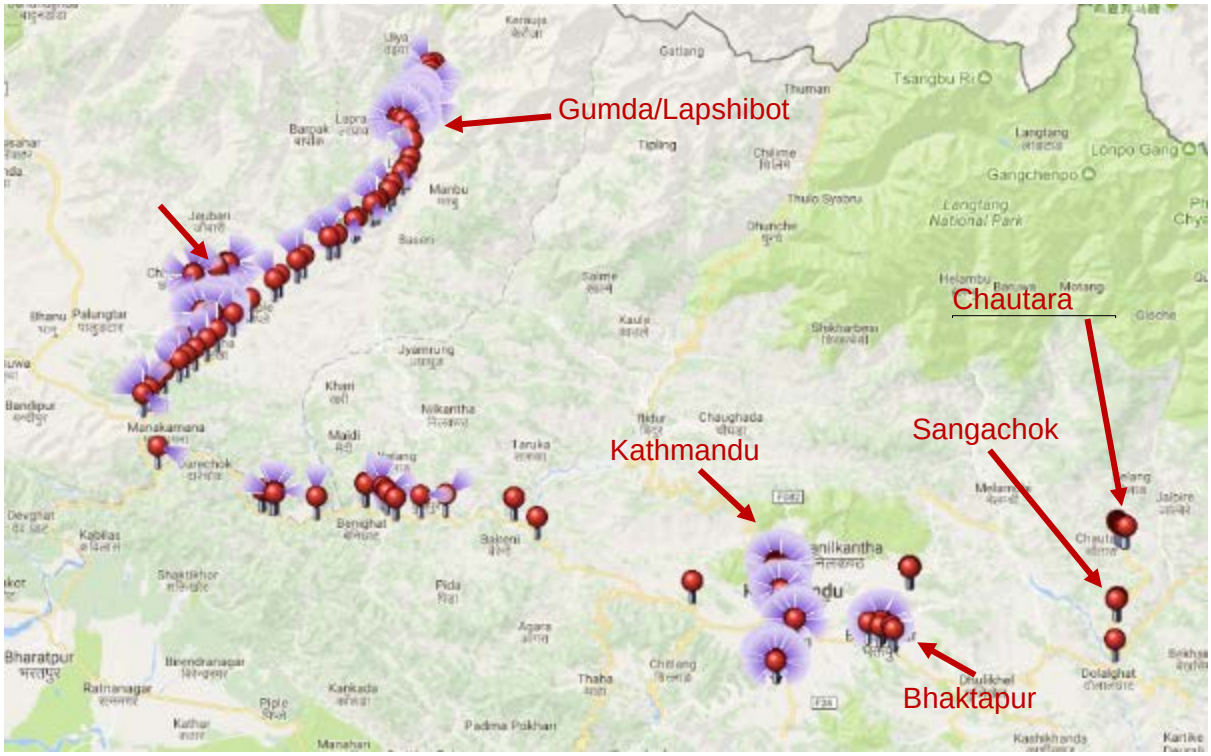

Figure 1-1 Map of visited locations.

Figure 1-2 EEFIT team members.
From left to right: Matt DeJong, Arthur Trieu, Sarah Tallet-Williams, Tim White, Michael Whitworth, Paul Burton, Viviana Novelli (front), Guillermo Franco (back), Sean Wilkinson, Suryanarayana Datla, (absent) Barnali Ghosh .

2. TECTONICS, SEISMOLOGY AND SEISMIC HAZARD

The Himalayan arc is a well-known zone of high seismicity that includes large and great earthquakes that can exceed magnitude 8. It has formed as a result of a long tectonic process dating back 225 million years when the India Plate broke away from Pangea in the southern hemisphere, eventually docking north of the equator against Eurasia. Presently, the India plate still thrusts northwards and subducts below the overriding Eurasia plate. This is continent-continent collision in the current tectonic regime.

This northward thrusting of the India plate maintains the height of the Himalaya Mountains and causes large earthquakes along the Himalayan arc. These earthquakes are associated with thrust or reverse faults that run the length of the Himalayan arc and mark the decollement between the India plate and the overriding Eurasia plate. Nepal occupies the central third of the arc for about 800 km. These through-going fault systems are longer than Nepal.

The Gorkha earthquake of the 25th April, 2015 is also known as the Nepal earthquake or the Kathmandu earthquake. Its epicentre was located at 36 km east of Khudi, Nepal, about 80 km northwest of Kathmandu, the capital of Nepal (USGS). It had moment magnitude M_w 7.8. The biggest aftershock was on the 12th May, had magnitude M_w 7.3, with epicentre 19 km southeast of Kodari, about 75 km east northeast of Kathmandu. Both the Gorkha earthquake and its main aftershock were thrust faulting earthquakes associated with the main fault system and decollement between India and Eurasia plates along the arc with epicentres approximately 150 km apart.

Many aftershocks followed the Gorkha earthquake. In addition to the large M_w 7.3 aftershock, examination of The United States Geological Survey (USGS) seismicity data sets through to mid-October 2015 reveals about 300 aftershocks of magnitude 4 or larger, including four exceeding magnitude 6. A simple measurement of the extent of these aftershocks along the spine of Nepal is almost 200 km long and stretches from west of the Gorkha epicentre to just east of the main aftershock. This extent of the aftershock swarm suggests a subterranean rupture length of ~200 km, which is compatible with an earthquake approaching magnitude 8 within a large seismic zone.

It is difficult to capture instrumental recording of earthquake strong ground shaking. There is an installation in the compound of the US Embassy in Kathmandu that records strong ground shaking, and the recorded accelerogram shows a peak of ~160 cm s^{-2}. Although there is an embryonic strong motion recording network in Nepal, run by the National Seismological Centre (NSC), Kathmandu, there are few Nepalese accelerograms to date, and such a database will take many years to gather and develop to form independent ground motion prediction equations (GMPE's).

The NSC, Kathmandu, has published the national seismic hazard map of Nepal. This map contours the peak ground acceleration (PGA) in gal or cm s^{-2} for the usual 500 year return period. The NSC map is based on probabilistic seismic hazard analysis (PSHA). Their PSHA allows for occurrence of earthquakes in excess of magnitude 8, and includes underlying models for seismic zonation and for ground motion. There are two other recently published seismic hazard maps for Nepal, which have been derived using alternative seismic zonations and ground motion equations. All these maps show their higher values along the spine of Nepal but they differ in detail and in the range of PGS (at bedrock level) that they embrace.

The NSC map indicates peak ground acceleration ~200 cm s^{-2} (500 years) near Kathmandu and ~400 cm s^{-2} near Gorkha. The other two published maps indicate higher values of PGA near to Kathmandu. We have carried out our own exploratory test work on seismicity data since 1900 to explore hazard mapping and seismic zonation in Nepal in order to explore issues in parallel to the three existing maps. Our exploratory hazard mapping adopts the same ground motion model as NSC but differs in methodology and in that it excludes any seismic zonation scheme. This exploratory hazard map indicates a PGA acceleration ~475 cm s^{-2} near Kathmandu and considerably higher values in western Nepal, reaching to ~650 cm s^{-2}. A

second but quite different examination to partition these seismicity data into separate earthquake clusters that can then be compared with seismic zone models used in production of the three published seismic hazard maps. Whereas the earthquake clusters we observe can readily accommodate the subsurface rupture length of a magnitude 8 earthquake, the individual zones along the spine of Nepal in existing seismic zone models cannot. Thus, in view of the differences between the published seismic hazard maps, we conclude there is a case to re-examine the magnitude of the older larger earthquakes in Nepal and to continue to develop the seismic zone model, in addition to the ubiquitous issue of ground motion models. While we see ways forward to develop PSHA in Nepal, at this time it is appropriate to recognise that the national seismic hazard map produced by the NSC, Kathmandu, is reasonable and carefully produced, although there are caveats e.g. this seismic hazard map may indicate values of PGA that may be too low in western Nepal and Kathmandu.

2.1. TECTONICS OF THE HIMALAYA, SEISMICITY, AND NEPALESE GEOLOGY

Nepal occupies the centre of the Himalayan arc. The Himalayan arc is the zone of continent-continent collision between the India and Eurasia plates. The thrust faults arising from this process provide the structures with which the earthquakes of the 25th April, 2015 (M_w 7.8) and the 12th May, 2015 (M_w 7.3) were both associated. How did this situation develop through ancient geological times to the present?

The progress of Indian plate movement is mapped from 275 million years ago (Permian) to the present in Figure 2-1. The nascent India plate was far south of the equator in the Permian and became detached about 200 million years ago (Triassic) and began to move northwards. Northwards movement continued 125 million years ago (Jurassic) and the Indian plate arrived at the equator about 65 million years ago (Cretaceous), eventually docking against the Eurasian plate as part of the current tectonic regime (CTR). In the CTR, the continuing northwards pressure of the India plate against Eurasia provides the force that maintains the uplift and elevation of the modern Himalaya.

Two cross-sections in Figure 2-2 depict the final 'moments' of this continent-continent collision with the 'AFTER' collision schematic being the CTR (USGS; also see EEFIT, 2006, 2008, for discussion of the October 8, Kashmir earthquake of magnitude M_w 7.6). The Indian plate subducts under the Eurasia plate, and this subduction has raised the Tibetan plateau (circa 4,600 m above sea level), and raised the mountains of the Himalaya pushing Mt. Everest up to about 8,850 m (29,035 ft) at rock head. The smaller arrows in Figure 2-2 indicate direction of motion of the many schematic thrust faults that have been created in this process and also the relative movement and decollement between the India and Eurasia plates at depth.

Rapid dynamic movement on these thrust planes or faults is synonymous with earthquakes in the CTR. Epicentral regions of some of the larger known historical earthquakes along the Himalayan earthquake belt are illustrated in Figure 2-3. The approximate epicentre of the April 25, 2015 Gorkha (Nepal) earthquake, amidst these historical earthquakes, is indicated by arrow in Figure 2-3.

Focussing on Nepal, its geology and main faults in the CTR are summarised in Figure 2-4 (Upreti, 1999; Chaulagain et al., 2015). Following Chaulagain et al. (2015) there are four major fault systems or structural units that are conventionally identified, these are: main thrust fault (MFT), main boundary thrust (MBT), main central thrust (MCT), the south Tibetan detachment system (STDS). Both Kathmandu and Pokhara are labelled in Figure 2-4 with the approximate epicentre of the M_w 7.8 Gorkha earthquake identified by the larger yellow star between them. The smaller earthquake of May 12, 2015 with magnitude M_w 7.3 has epicentre located by the smaller yellow star. This is about 60 miles (95 km) west of Mt. Everest.

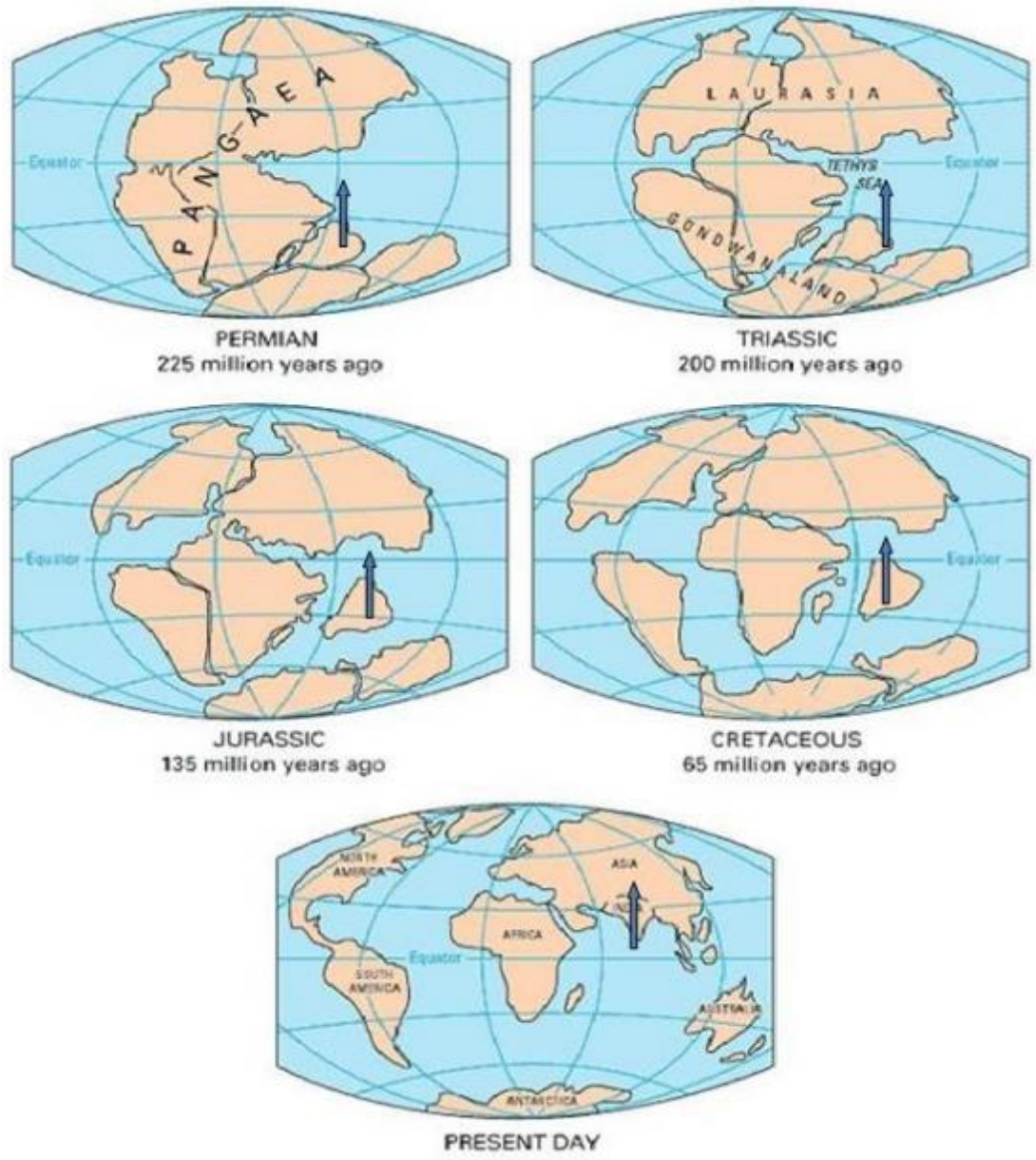

Figure 2-1 Ancient and modern tectonics.

Pangea begins to break up and the Indian plate begins to move northwards in the Permian (225 MYBP). Follow the green arrows. The India plate moves northwards during the Triassic (200 MYBP) and Jurassic (135 MYBP), arriving at the equator in the Cretaceous (65 MYBP). The India plate then finally docks against the Eurasia plate and continues to thrust forward in continent-continent collision, under thrusts the Eurasia plate and maintains the height of the Himalaya in the current tectonic regime (CTR).

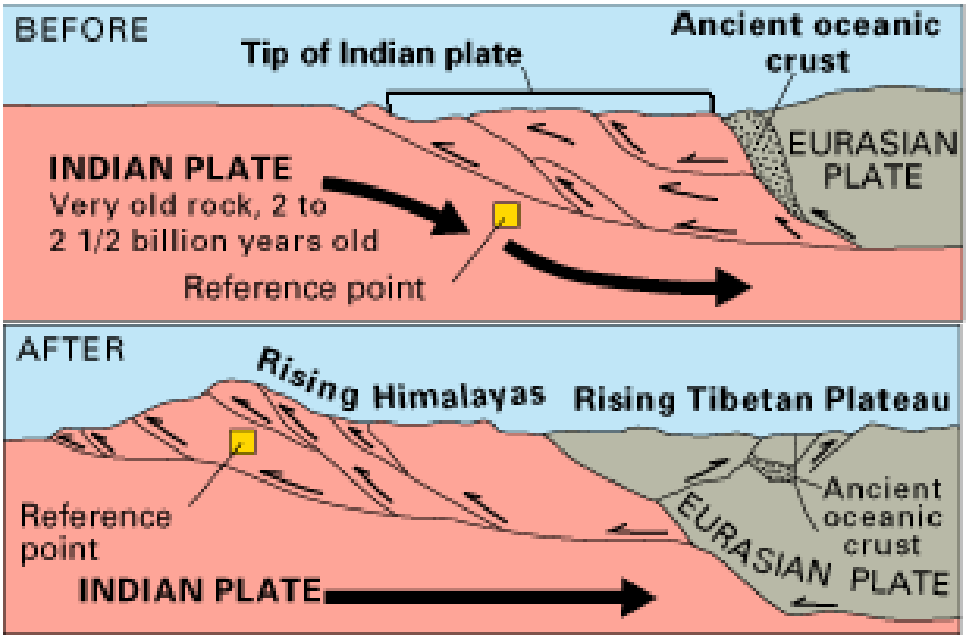

Figure 2-2 Final stages of formation of the Himalaya.

Final stages of formation of the Himalaya: just before and just after the continent-continent collision between the northwards moving India plate and the Eurasia plate at the start of the CTR. This is effectively an S-N cross-section through the final stage of Figure 2-1 (see EEFIT, 2006, 2008, and after the USGS).

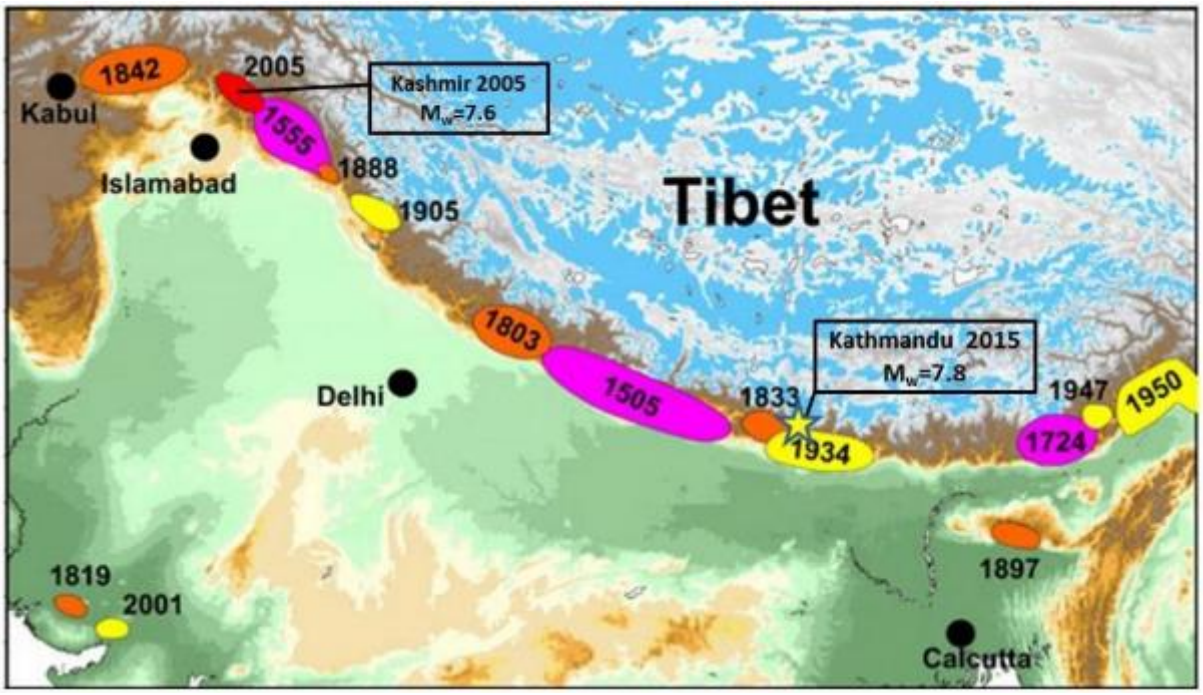

Figure 2-3 Historical earthquakes along the Himalayan arc.

Continent-continent collision is accompanied by subduction of the India plate from the south below the over-riding Eurasia plate to the north. This is accompanied by uplift of the Tibetan plateau and the Himalaya. In the zone of collision is the Himalayan arc – a zone of very high seismicity. The ellipses identify some of the major earthquakes in this zone. There was an EEFIT mission to the disastrous Kashmir earthquake of October 8, 2005 (Mw 7.6). (Peiris, N., Rossetto, T., Burton, P., & Mahmood, S. ,2005). Note the location of the April 25, 2015 Kathmandu (Gorkha) earthquake (M_w 7.8).

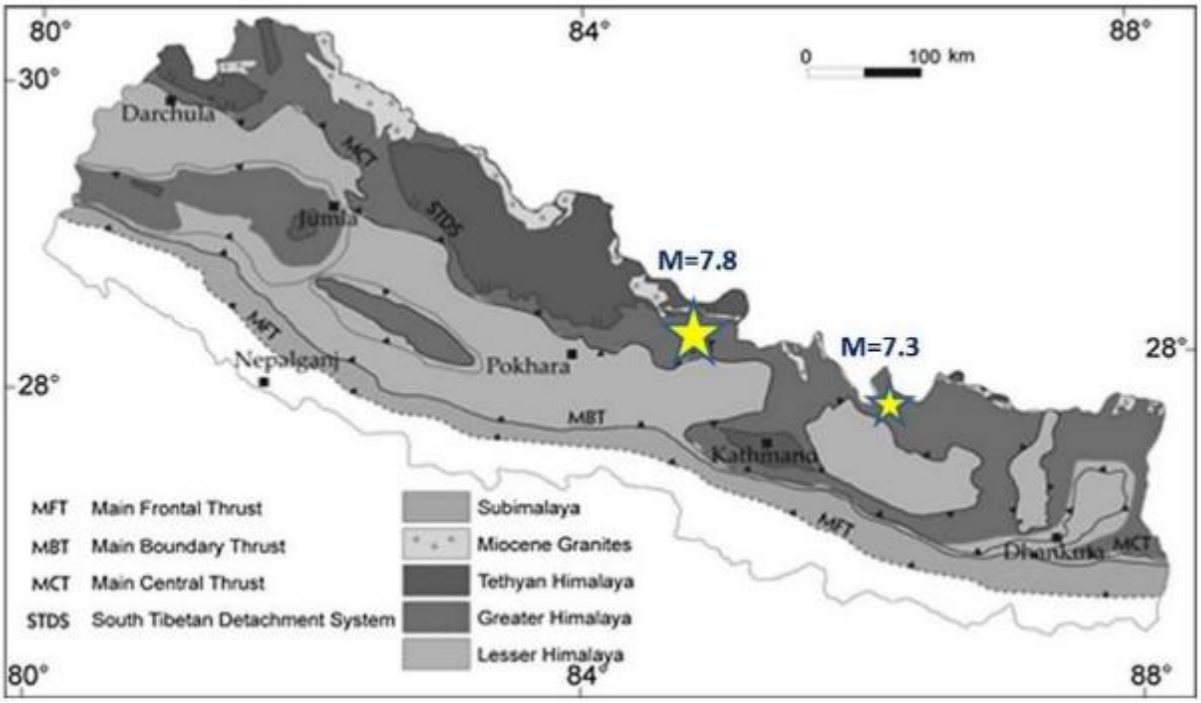

Figure 2-4 Geological map of Nepal.

Geological map of Nepal indicating the main faulting structures associated with thrust mechanism seismicity along the spine of Nepal (from Chaulagain et al., 2015, and adapted from Upreti, 1999). These thrust faults extend along the length of the Himalayan arc. Nepal is 800 km long and occupies the central third of the Himalayan arc. The larger yellow star indicates the epicentre of the 25th April 2015 Gorkha earthquake (M_w 7.8) and the smaller yellow star is the epicentre of its main aftershock on the 12th May, 2015 (M_w 7.3). The epicentre of the Gorkha earthquake is about 80 km northwest of Kathmandu and 75 km east of Pokhara, the main aftershock is approximately 75 km east northeast of Kathmandu. Everest is about 85 km further east of the main aftershock epicentre.

2.2. SEISMICITY IN NEPAL AND THE GORKHA 2015 EARTHQUAKE

2.2.1. Seismicity and Gorkha 2015

Seismicity in Nepal from 1900 to the 25th April 2015 is summarised by the epicentral map in Figure 2-5. The epicentral parameters were extracted from the National Earthquake Information Center (NEIC) of (USGS). This time interval is windowed to cut off just prior to the Gorkha earthquake and nominally corresponds to the period of instrumental observation of earthquakes in seismology, earlier reporting relying on macro-seismic data rather than instrumental data. The broad lineation of earthquakes along the central spine of Nepal is very clear in Figure 2-5. This spatial belt of seismicity corresponds to the spinal lineation of the main faults in Nepal (Figure 2-4) arising from subduction of the India plate (south) below the overriding Eurasia plate (north) accompanied by mechanisms of thrust faulting. Marked in Figure 2-5 are the epicentres of the large 1916 (M = 7) and 1934 (M = 8) earthquakes.

Including seismicity through to the 12th October 2015, which spans the main Gorkha shock of April 25, its main aftershock of the 12th May 2015, and many smaller aftershocks, results in Figure 2-6. Epicentres of the main shock and main aftershock are labelled. Comparing Figure 2-5 and Figure 2-6 underlines the high seismicity rates stimulated by the Gorkha earthquake which includes recorded aftershocks in 6, 5, and 4 magnitude ranges (and lower), clearly suggesting that our knowledge of seismicity following earlier earthquakes, like 1934, is very deficient. The main Gorkha shock, in this newly ruptured zone, is to the west, and the main aftershock is in the east of the zone.

The difference in content between Figure 2-5 and Figure 2-6 is the seismicity generated by Gorkha 2015 and aftershocks during the 25th April to the 12th October 2015, is displayed in Figure 2-7. A very large rupture zone is apparent and these aftershocks and their relation to both fault length and to fault segmentation will be included in later discussion.

2.2.2 Fundamental seismological parameters of the Gorkha earthquake

The principle parameters of the Gorkha earthquake are listed in Table 2-1 and these have been extracted from the USGS website list of "most preferred data available". The USGS describes the epicentre as being at 36 km east of Khudi, Nepal.

PARAMETER	VALUE
Magnitude	M_w 7.8
Location	28.231°N 84.731°E ± 7.3 km
Depth	8.2 ±2.9 km
Origin time	2015-04-25 06:11:25.950 UTC
Number of seismic phases	446
Minimum distance of seismic station	206.72 km (1.86°)
Travel time residual	0.96 sec
Azimuthal gap	12°
Flinn-Engdahl region	NEPAL (310)

Table 2-1 Seismological parameters of the Gorkha earthquake.

The magnitude of the Gorkha earthquake is 7.1 m_b and 7.9 M_s respectively. These values are determined by averaging observations from many seismological observatories worldwide, however, when comparing the size of very large earthquakes the moment magnitude value M_w 7.8 will usually be adopted when possible.

2.2.3 Fundamental seismological parameters of the main aftershock of the 12th May, 2015

The principle parameters of the main aftershock are also listed, in Table 2-2, and these have been extracted similarly from the USGS website. The USGS describes this epicentre as at 19 km southeast of Kodari, Nepal. The preferred moment magnitude is M_w 7.3 and on the other scales the values are 6.8 m_b and M_s 7.6 respectively.

PARAMETER	VALUE
Magnitude	M_w 7.3
Location	27.809°N 86.066°E ± 7.4 km
Depth	15.0 ± 1.7 km
Origin time	2015-05-12 07:05:19.730 UTC
Number of seismic phases	496
Minimum distance of seismic station	75.36 km (0.68°)
Travel time residual	0.92 sec
Azimuthal gap	11°
Flinn-Engdahl region	NEPAL (310)

Table 2-2 Seismological parameters of the main aftershock of the 12th May 2015.

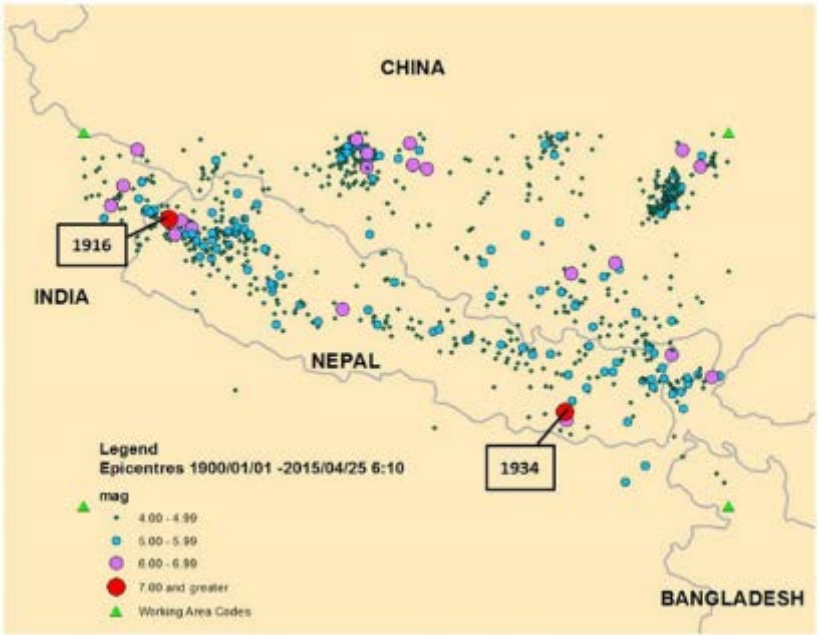

Figure 2-5 Seismicity of Nepal since 1900 until just before the Gorkha earthquake.

The first earthquake in this data set is in 1911. All magnitudes displayed have either been measured on, or converted to, the moment magnitude scale. The 1916 and 1934 earthquakes have magnitude 7 or greater in the database (1916 Nepal-India border earthquake M_w 7); 1934 Nepal-Bihar earthquake M_w 8.0).

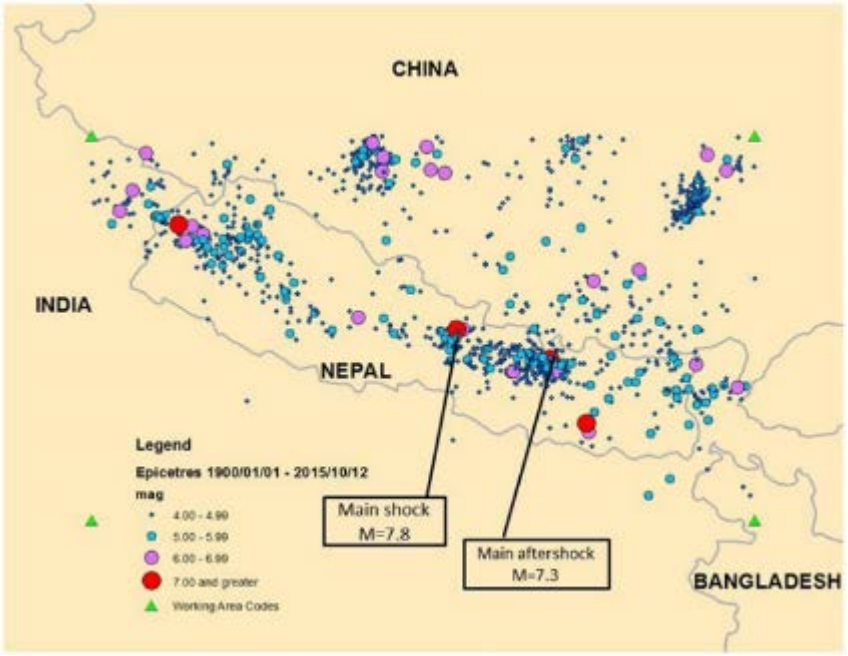

Figure 2-6 Seismicity of Nepal since 1900 until the 12th October 2015.

Source: (NEIC, USGS and see caption to Figure 2-5). This period extends well beyond the occurrence of the Gorkha M_w 7.8 main shock on the 25th April 2015 and embraces many aftershocks, including the main aftershock M_w 7.3 on the 12th May 2015. The red epicentral symbols indicate four earthquakes with magnitude 7.0 or greater that are now in this data set for Nepal.

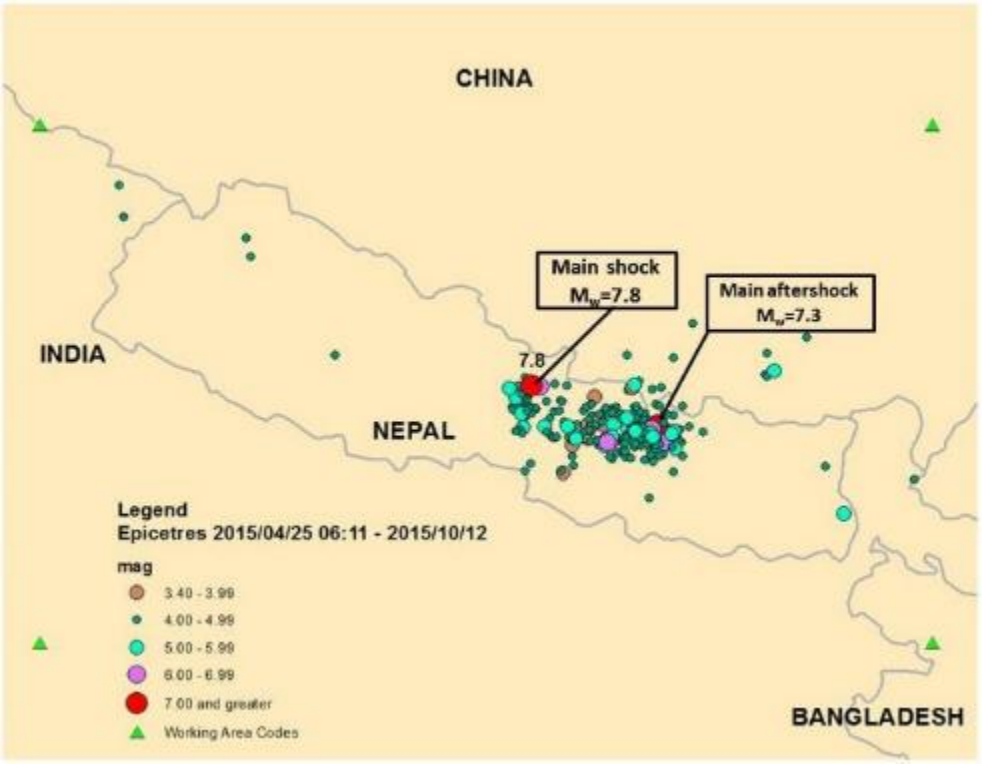

Figure 2-7 Seismicity of Nepal since (including) the Gorkha earthquake.
Seismicity of Nepal since (including) the Gorkha earthquake of the 25th April, 2015 until the 12th October, 2015 (NEIC, USGS and see captions to Figure 2-5 and Figure 2-6). This seismicity is composed nearly entirely of aftershocks of the Gorkha earthquake, extending from slightly west of its epicentre to slightly east of the main aftershock. Aftershock extent helps to delineate the extent of the subsurface rupture area.

2.2.4. Aftershocks and fault rupture length: observations and empirical equations

It is a common assumption in seismology to consider that a very large earthquake sweeps through a rupture plane and thus relieves stress through the ruptured area, subsequent smaller aftershocks are localised minor readjustments or stress releases within the newly ruptured rock mass. Thus aftershocks, if well recorded as a body of smaller events, serve to map the newly ruptured area. Hence, the linear length of the aftershock swarm can provide an estimate of the rupture length below ground. The seismicity is again mapped as an epicentral map, down to magnitude 3, in Figure 2-8, with contours of calculated slip (on the rupture) superimposed centred on the Gorkha epicentre. The length of the aftershock swarm, along the direction of the spine of Nepal in Figure 2-8, is almost 200 km. This suggests the subsurface rupture length (RLD) was ~200 km.

There are several published empirical equations that link earthquake magnitude to a variety of earthquake rupture geometry parameters e.g. surface and subsurface rupture length, down dip rupture length and rupture area. The equations of Wells and Coppersmith (1994) provide a commonly used source of these equations, which they prepared for normal, strike slip and reverse fault types and all fault types combined. A set of Wells and Coppersmith's equations is used in Table 2-3 to calculate and illustrate geometrical rupture properties for a few large values of magnitude. An RLD of 200 km in Table 2-3 corresponds directly to magnitude about M_w 8.0. The formulae in Table 2-3 have a logarithmic relationship between magnitude and fault geometry with standard deviation around 0.2. The aftershock derived RLD of ~200 km is thus quite consistent with Table 2-3 for the magnitude M_w 7.8 (M_s 7.9) Gorkha earthquake. A value of about 200 km is reasonable for the subsurface rupture length.

There is an issue here concerning epicentre and rupture length. Smaller magnitude earthquakes tend towards point sources; larger earthquakes do not. The modern definition of epicentre e.g. "The epicenter is the point on the earth's surface vertically above the hypocenter (or focus), point in the crust where a seismic rupture begins (USGS)" or the epicentre is the point on the Earth's surface that is directly above the hypocentre or focus, the point where an earthquake or underground explosion originates allows a seismologist to put a point on a map.

Robert Mallet is attributed with originating the word epicentre in the middle of the 19th Century when the epicentre was taken to be the centre of the meizoseismal area (the area of maximum damage). The Gorkha earthquake has a focus or hypocentre from which seismic waves appear to originate, that notwithstanding the rupture then propagated ~200 km to the East causing damage along an extensive rupture length, not just around the epicentre.

FORMULA†	MAGNITUDE				FORMULA'S OBSERVED M_W RANGE
	7.8	8.0	8.3	8.5	
	Fault lengths for given magnitude (km)				
R: logRLD = -2.42 + 0.58M	127	166	248	324	4.8-7.6
All: logRLD = -2.44 + 0.59M	145	191	286	376	4.8-8.1
R: logSRL = -2.86 + 0.63M	113	15	234	-	5.4-7.4
All: logSRL = -3.22 + 0.69M	145	200	321	-	5.2-8.1
R: logRA = -3.99 + 0.98M	4508‡	7079‡	13932‡	-	4.8-7.6
All: logRA = -3.49 + 0.91M	4055‡	6168‡	11561‡	-	4.8-7.9
R: logRW = -1.61 + 0.41M	39	48	62	-	4.8-7.6
All: logRW = -1.01 + 0.32M	31	35	44	-	4.8-8.1

† Table 2-3 Estimates of fault rupture length for various large magnitudes of earthquake.

Formulae from Wells and Coppersmith (1994). Standard deviations on these formulae are around 0.2. M_w is the moment magnitude. ‡ fault area km^2. R = reverse or thrust fault, All = all fault types, RLD = subsurface rupture length km, SRL = surface rupture length km, RA = rupture area km^2, RW = down dip rupture length km.

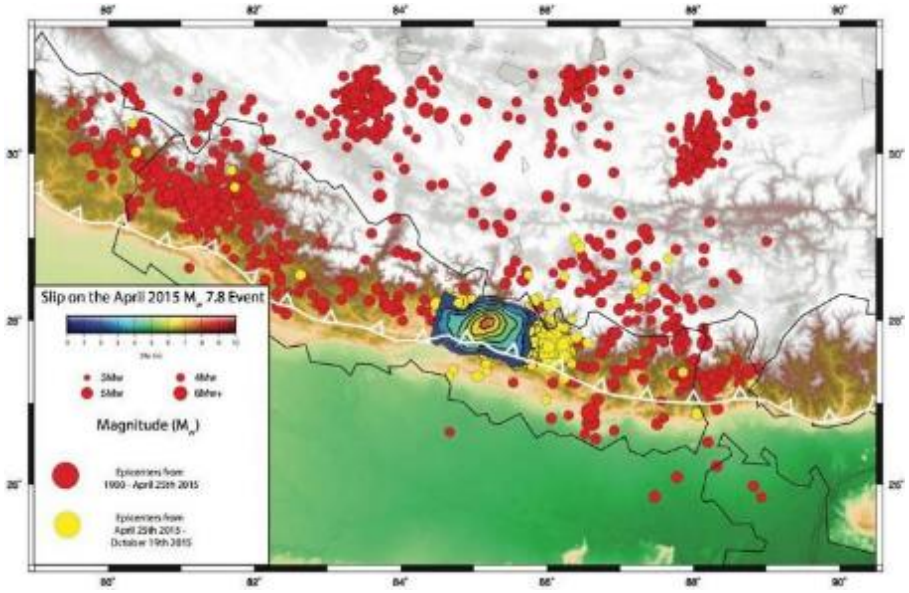

Figure 2-8 Slip on the Gorkha earthquake rupture and extent of the aftershocks.
Seismicity of Nepal, slip on the Gorkha earthquake rupture and extent of the aftershocks. Seismicity and aftershock epicentres following the 26th April, 2015 Gorkha earthquake are mapped through to the 19th October, 2015 and marked in yellow, earlier epicentres prior to the Gorkha earthquake is marked in red. Slip on the Gorkha subterranean rupture is contoured and shaded in metre intervals.

2.3. SEISMIC HAZARD ANALYSIS AND ZONATION IN NEPAL

2.3.1. Existing seismic hazard maps and seismic zonations of Nepal

There are three PSHA studies and related maps available for Nepal. These were prepared by: Pandey et al. (2002), Thapa and Guoxin (2013) and Chaulagain et al. (2015). The latter analysis (Chaulagain et al. 2015) was published about the time that the EEFIT mission was in the field in Nepal. All of these analyses lead to ground motion expectations expressed in terms of PGA and include results for the estimated PGA with 10% probability of exceedance in 50 years (the seismic hazard parameter for the traditional, approximately “500 year” occurrence). There is a fourth set of results available through the Global Seismic Hazard Assessment Program (GSHAP, 1999) which incorporated the analyses of Zhang et al. (1999) into a final GSHAP map for continental Asia. The first three sets of PSHA results, the resulting maps, adopted strong ground motion prediction equations and the underlying seismic source zonations will be described here.

Until very recently, the only available and generally accepted “Seismic Hazard Map of Nepal” was that of Pandey et al. (2002) and prepared by the Department of Mines and Geology at the National Seismological Centre, Kathmandu. This map has been made generally available in an NSC publication in 2012 (NSC, 2012) and is reproduced in Figure 2-9 and shall be referred to as the NSC2002 map. This remains the nationally accepted map.

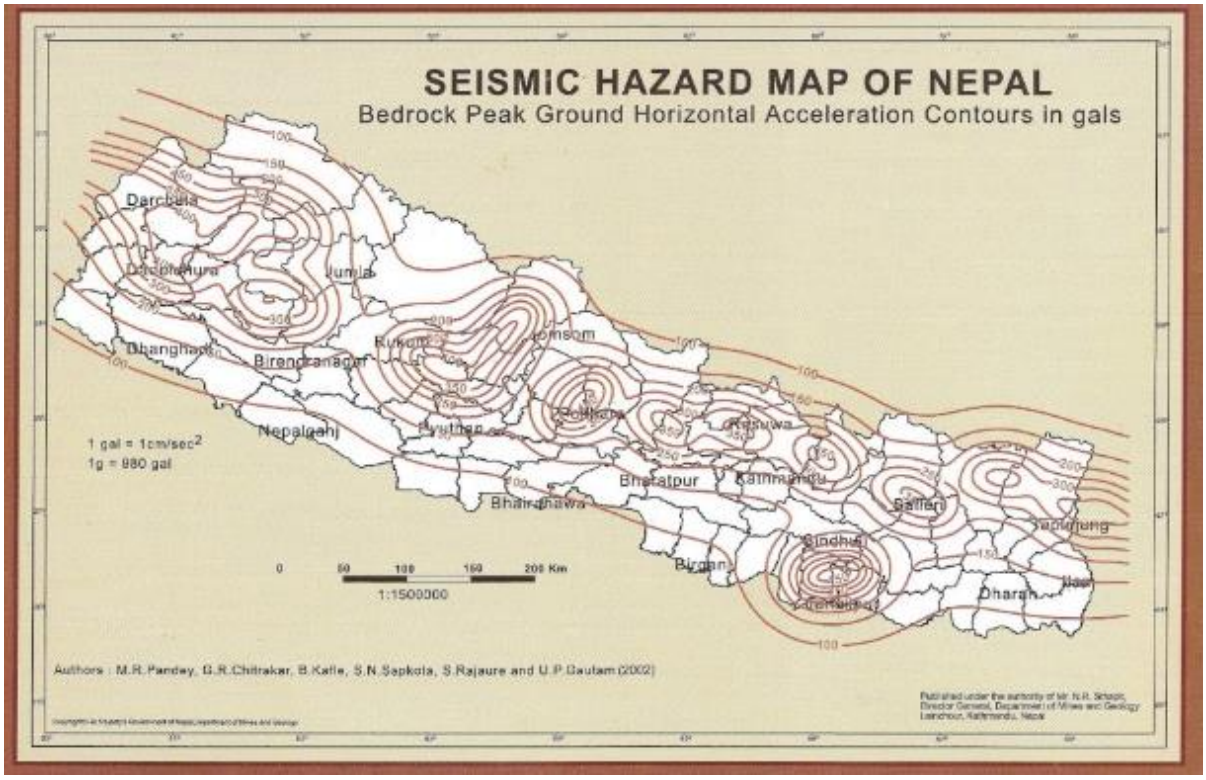

Figure 2-9 Seismic hazard map (NSC2002).

Seismic hazard map (NSC2002). The national seismic hazard map was prepared by the NSC and published by Pandey et al. (2002). This was made generally available in the publication NSC (2012). The map contours peak ground horizontal acceleration in gal (1 gal = 1 cm s-2), nominally for the usual 500 year expectation i.e. 90% probability of non-exceedance in 50 years, viz, a 1-in-10 chance of exceedance in 50 years on average. The results are at bedrock. There is an underlying seismic zonation scheme with 12 zones circumscribing the major detachment earthquakes into zones along he spine of Nepal (see text).

The NSC2002 map contours PGA with a 10% probability of exceedance in 50 years. This map is at bedrock, viz, it does not account for site effects or surface geology, which will influence local ground motions and should be a subject of localised studies when specific site assessments are required. NSC2002 shows high PGA expectations as a ridge with pinnacles

of higher PGA reaching ~400 cm s^{-2} along the spine of Nepal. NSC adopt the ground motion model of Youngs et al. (1997) in their PSHA

$$\ln (PGA) = 0.2418 + 1.414M_w - 2.552\ln(r_{rup} + 1.7818e^{0.554Mw}) + 0.00607H,$$

where M_w is the moment magnitude, r_{rup} km is the closest distance to rupture and H km is focal depth. The selection of this equation is justified through its approximate fit to peak horizontal accelerations observed from two earthquakes in Nepal (magnitudes 6.8 M_w and 6.6 M_w).

The sources of seismicity in the underlying NSC zonation for PSHA is primarily built on the seismotectonic investigations of Pandey et al. (1995), Bilham et al. (1997), Cattin and Avouac (2000) and Lave and Avouac (2000), supplemented by observations from a seismic monitoring network embracing all Nepal (Pandey et al., 1999). The ensuing zonation is in two parts. A first set of 12 zones accounts for the major detachment earthquakes, extending up to the great earthquakes, with six zones east of 82°E along the spine of Nepal and six zones west of 82°E arranged along Nepal's spine with three to the north and three to the south of the spine. The second component of zonation is for the smaller thrust earthquakes ($M_w < 6.3$) that correspond to circa 40 km segment lengths, which are accounted for by 24 faults in NSC zonation mapping. These 24 faults are themselves divided into two segment belts east and west of 82°E.

The NSC2002 hazard map indicates an expectation of ~400 cm s^{-2} near to Gorkha and ~200 cm s^{-2} near to Kathmandu.

The second PSHA analysis is Thapa and Guoxin's (2013). Their analysis method is fundamentally Cornell's (1968, and McGuire, 1976) method but primarily references the China Earthquake Administration (CEA, 2005, in Chinese) for the exact details of their methodology.

The results of Thapa and Guoxin's (2013) analyses are illustrated as maps (here referred to as TG2013) in Figure 2-10. There are three TG2013 maps published corresponding respectively to 63%, 10% and 2% probabilities of exceedance in 50 years. All three maps are for PGA expectation at bedrock level. Because observations of earthquake strong ground motion are in short supply for Nepal, TG2013 is based on a ground motion model that CEA (2005) developed for western China. This is an elliptical model of attenuation with major and minor axes and is of form

$$\ln(PGA(Ra)) = 5.912025 + 1.836588M_s - 2.84658\ln(R_{Ra} + 3.400\exp^{0.451Ms})$$

and

$$\ln(PGA(Rb)) = 2.509012 + 1.360759M_s - 1.79151\ln(R_{Rb} + 1.046\exp^{0.451Ms})$$

where M_s is the surface wave magnitude, PGA(Ra) cm s^{-2} and PGA(Rb) cm s^{-2} are PGA along the major and minor axes at hypocentral distances R_{Ra} km and R_{Rb} for major and minor axes.

Thapa and Gouoxin (2013) created an earthquake catalogue for Nepal based on a string of earlier publications on seismicity plus data from the International Seismological Centre (ISC), the NEICand the NSC. This resulted in a data base containing local, body wave, surface wave and moment magnitudes. All of these were then rendered onto the surface wave magnitude scale to facilitate the CEA (2005) ground motion model adopted in their PSHA analysis.

Thapa and Guoxin (2013) study the spatial distribution of earthquakes and major faults and recognise that the "vast majority of earthquakes are located near the Main Central Thrust", and based on this distribution of data, along with pattern recognition analysis (Gelfand et al., 1972), they produce an underlying zonation with 23 seismic sources as illustrated in Figure 2-11.

The TG2013 map of PGA (expressed in g, acceleration due to gravity) with 10% probability of exceedance in 50 years indicates a value contained in the range 0.475-0.525 g near Kathmandu.

The third and most recently published PSHA study is Chaulagain et al.'s (2015). They investigate both hazard and risk. The seismic hazard component draws on an earthquake catalogue of Nepal referenced as www.seismonepal.gov.np for 1255-2011, adopts Thapa and Guoxin's (2013) underlying zonation (Figure 2-11) along with a *b*-value of 0.85 (also drawn

from Thapa and Guoxin). Chaulagain et al. (2015) provide four seismic hazard maps of PGA with 10%, 5%, 2% and 1% probability of exceedance in 50 years, see C2015 maps in Figure 2-12. In order to arrive at the suite of PSHA maps of C2015 from Thapa and Guoxin's underlying zonation, Chaulagain et al. classify the region as "active shallow crust and subduction interface". They then chose ground motion models from Boore and Atkinson (2008), Chiou and Youngs (2008), Campbell and Bozorgnia (2008), Atkinson and Boore (2003) and Youngs et al. (1997), absorbed into a logic tree.

The coloured contoured C2015 map of PGA with 10% probability of exceedance in 50 years indicates a value of around ~0.33 g near Kathmandu.

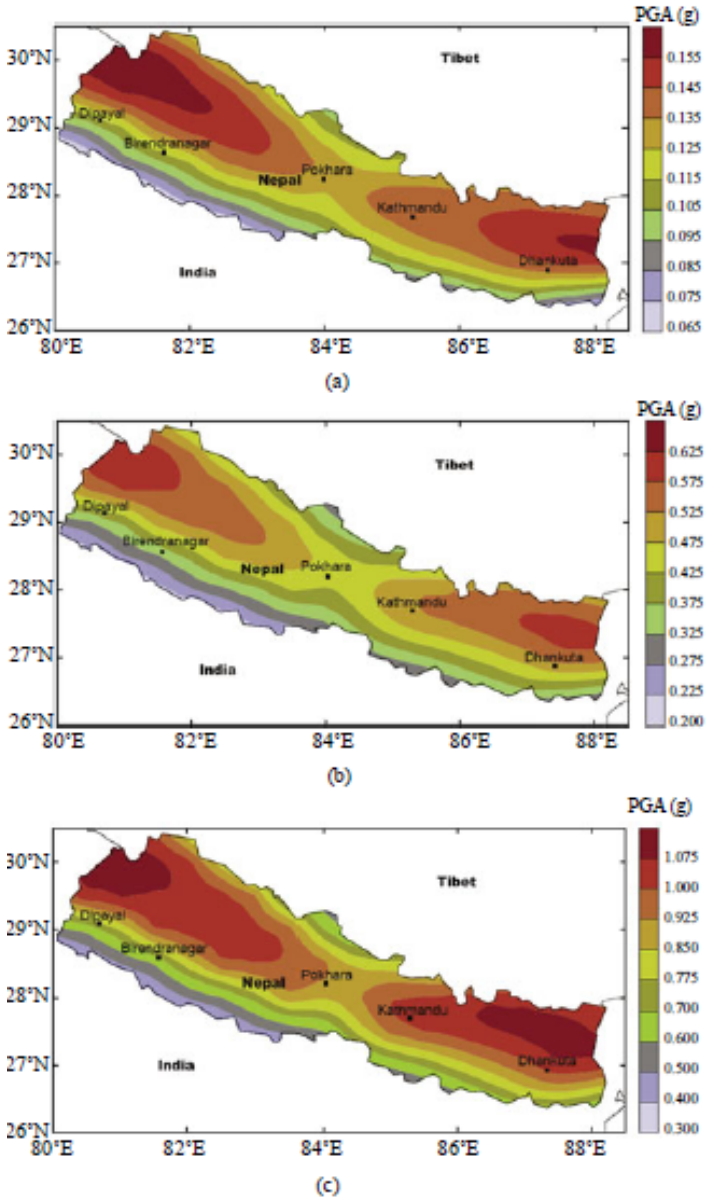

Figure 2-10 Seismic hazard map (TG2013).
These seismic hazard maps show the peak ground acceleration at bedrock level for (a) 63% probability of exceedance, (b) 10% probability of exceedance, and (c) 2% probability of exceedance, all in 50 years. Thus the middle map corresponds to the usual 500 year average expectation (see caption to Figure 2-9). The values are contoured in intervals of the acceleration due to gravity or g. There is an underlying seismic zonation scheme with 23 zones as illustrated in Figure 2-11. These maps are published by Thapa and Guoxin (2013).

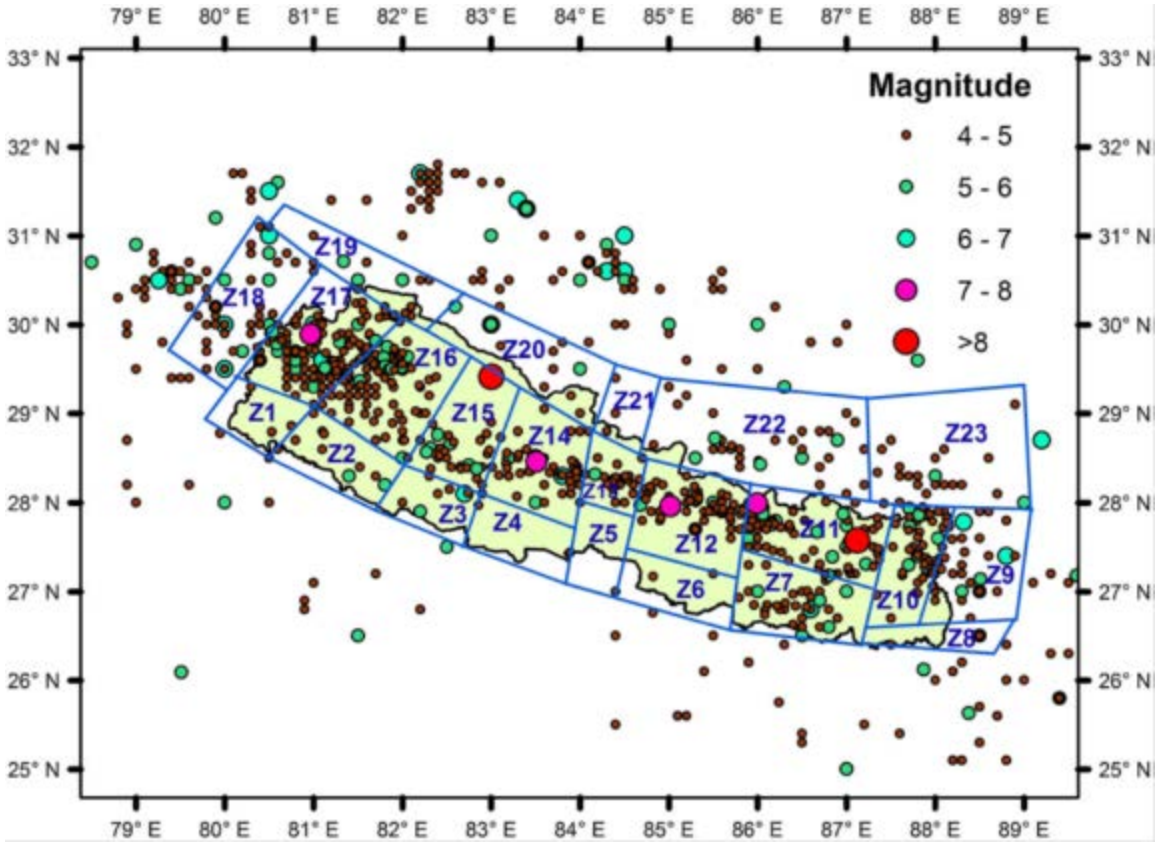

Figure 2-11 Seismic source zones in Nepal.

Seismic source zones in Nepal. Thapa and Guoxin (2013) developed a seismic source zonation scheme with 23 zones (illustration from Chaulagain et al., 2015, adapted from Thapa and Guoxin, 2013). The zonation model necessarily extends beyond Nepal so that subsequent probabilistic seismic hazard analysis embraces earthquakes beyond Nepal that cause strong ground shaking within Nepal

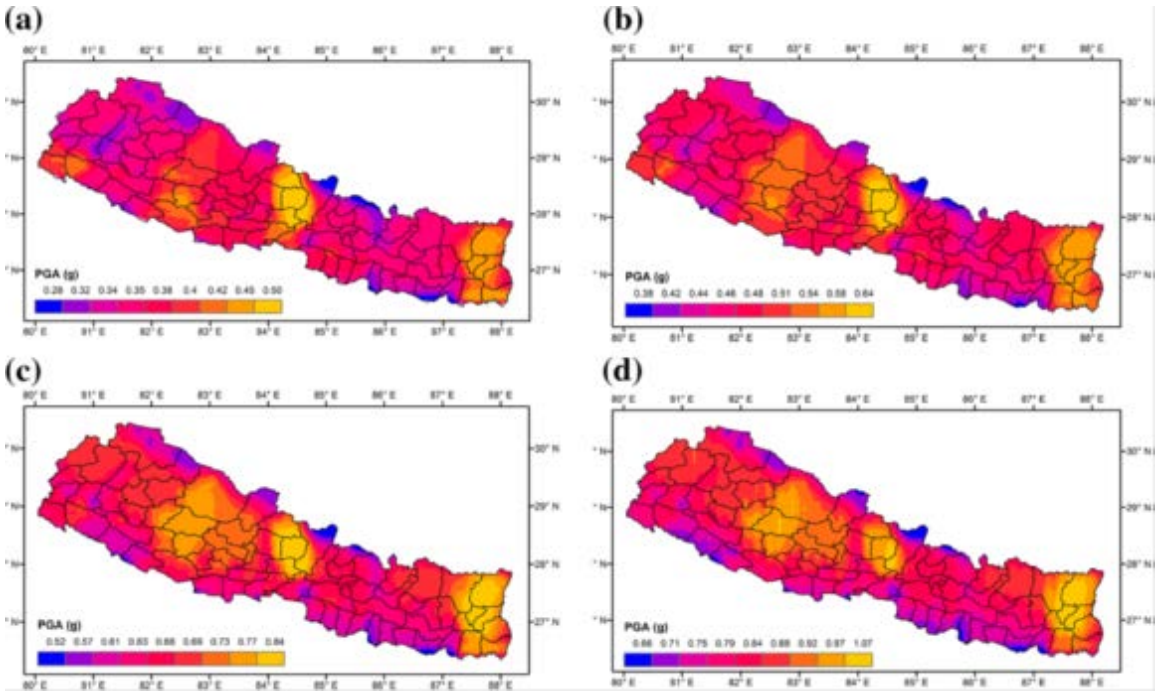

Figure 2-12 Seismic hazard maps (C2015).

Seismic hazard maps (C2015). These seismic hazard maps show the peak ground acceleration at bedrock level for (a) 10% probability of exceedance, (b) 5% probability of exceedance, (c) 2% probability of exceedance, and d) 1% probability of exceedance, all in 50 years. The top left map corresponds to the usual 500 year average expectation (see caption to Figure 2-9). There is an underlying seismic zonation scheme with the 23 zones in Figure 2-11. These maps are published by Chaulagain et al. (2015).

2.3.2.Strong ground motion accelerogram recorded at Kathmandu

The three maps of seismic hazard described above indicate PGA values with 10% probability of exceedance near Kathmandu of ~200 gal (NSC2002), 0.475-0.525 g (TG2013) and ~0.33 g (C2015), respectively. All of these apply to bedrock level.

We are aware of one accelerogram of strong ground motion recorded at Kathmandu during the Gorkha earthquake. This accelerogram was recorded at an installation inside the compound of the US Embassy in central Kathmandu. The three components of this recording are reproduced in Figure 2-13. The large pulse arriving early in the horizontal traces of strong ground shaking indicate a PGA around ~160 cm s^{-2} inside the Embassy compound. We did not access the installation.

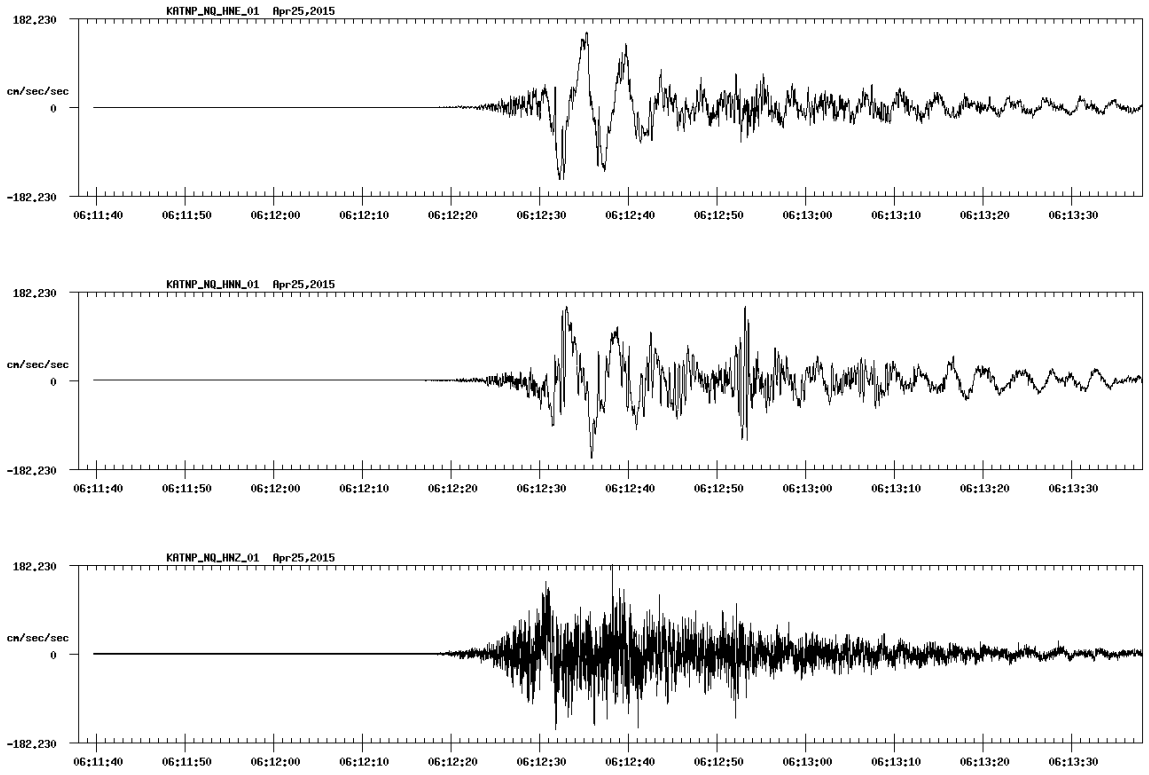

Figure 2-13 Strong ground motion accelerogram recorded at Kathmandu.
The Gorkha earthquake recorded on a strong ground motion accelerometer inside the compound of the US Embassy in central Kathmandu. The upper trace is the E-W component of strong ground motion, the middle trace is N-S and the lower trace is the Vertical component. The biggest value of acceleration in the large pulse on the two horizontal components is ~160 cm s-2.

2.3.3. Seismic hazard mapping and seismic zonation in Nepal

An EEFIT mission provides opportunity not only to visit sites of building damage and geological change but also gives opportunity to discuss with local experts and to hear their views on seismotectonics, seismicity, seismic hazard and earthquake monitoring needs in general in Nepal. Discussion at the NSC, Kathmandu, provided a knowledge base for EEFIT to explore, post-field mission, into existing hazard mapping and zonation. The map prepared by NSC (Figure 2-9) is the national standard for Nepal – is this a reasonable and viable map? This question implies a need to begin exploring the existing seismic hazard mapping provided by different authors with a view to seeing what is reliable and reasonable (to some extent considered in the above review material) and to try to see where useful developments might be made.

2.3.4 Seismic hazard map

To produce a new provisional seismic hazard map the basic earthquake catalogue data drawn on are those of the NEIC. Most of the data in the ensuing earthquake catalogue for magnitude 6.1 and greater already have magnitude estimated on the moment magnitude scale, but where this was not the case the GMPE of Scordilis (2005) have been used to convert m_b and M_s values to M_w. Conversions at smaller magnitudes also drew on the GMPE of Scordilis (2005). NSC, to develop their seismic hazard map, adopted the GMPE of Youngs et al. (1997, see Section 2.3.1), and we have done likewise to ease comparison. The results obtained using Youngs et al.'s attenuation model and then mapped for the whole region are illustrated in Figure 2-14, which can be compared with the NSC2002 map of Figure 2-9. This PSHA, for which the map of Figure 2-14 is the contoured illustration, first estimates point values of PGA over a matrix of many points, using a moving cell strategy, on which the PGA hazard is estimated, and then the matrix of hazard values subsequently contoured. The analysis uses extreme values based on long standing techniques most recently applied and described in Burton and Bayliss (2013) and Bayliss and Burton (2013). The seismic hazard map of Figure 2-14 is the result of this strategy and analysis. The mapped contoured values are PGA cm s^{-2} with the usual 10% probability of exceedance in 50 years, identical to the maps described above. There are broad underlying consistencies between the three "500 year" maps of NSC2002 (Figure 2-9), TH2013 (Figure 2-10), C2015 (Figure 2-12) and Figure 2-14. Generally the maps of NSC2002 and C2015 have slightly lower PGA values but the most significant difference seems to be in western Nepal for which Figure 2-14 indicates ~600 cm s^{-2}, whereas NSC2002 and C2015 indicate ~400 cm s^{-2} and ~350 cm s^{-2} respectively, whereas TG2013 (Figure 10) does indicate a higher value ~600 cm s^{-2} in western Nepal. The earthquake of August 28, 1916 was on the Nepal-India border and has been variably reported; it is this earthquake that may have a significant role to play in differences in result between the maps for western Nepal. In our preliminary analysis of Figure 2-14 it was included with a magnitude 7.0 M_w drawn from the NEIC database.

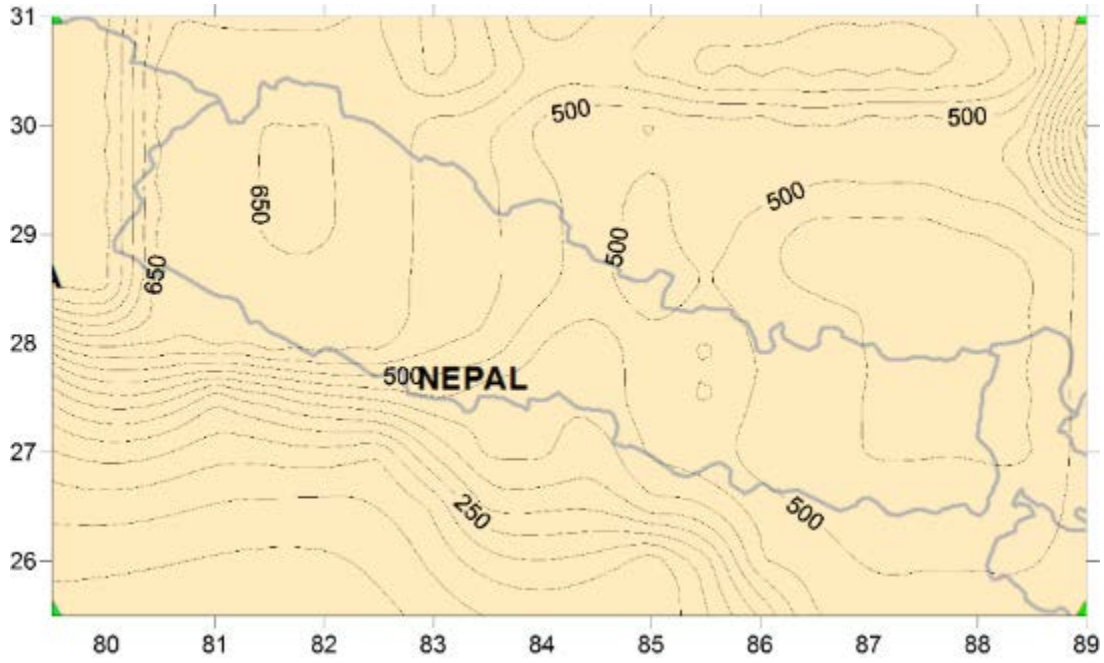

Figure 2-14 Seismic hazard map (this report).
This is a preliminary result designed to explore seismic hazard in Nepal. It is developed using the techniques most recently described in Burton and Bayliss (2013) and does not rely on an underlying seismic zonation scheme, instead the hazard value is calculated at a matrix of points through Nepal and then contoured. The ground motion model used follows the lead of the National Seismological Centre, Kathmandu in Pandey et al. (2002, who adopted the model of Youngs et al., 1997). The map contours PGA in cm s-2, at 50 cm s-2 intervals, nominally for the usual 500 year expectation i.e. 10% probability of exceedance in 50 years. The results are at bedrock.

2.3.5 Seismic zonation

Nepal occupies the central third of the Himalayan arc and is about 800 km long. Nevertheless, the faults that run through the length of Nepal (Figure 2-4) are longer than Nepal and are through-going the length of the Himalayan arc. The seismicity that these faults generate as individual earthquakes in Nepal have been zoned into 12 zones by Pandey et al. (2002, used by NSC seismic hazard mapping) and into 23 zones by Thapa and Guoxin (2013, used by Thapa and Guoxin in seismic hazard mapping, and also used by Chaulagain et al.). Clearly, through-going faults exceeding 800 km length are not expected to rupture in entirety in a single earthquake. These faults are geologically segmented as described for other fault systems by Bellier et al. (1997) and De Joussineau and Aydin (2009). In Figure 2-15, we reproduce the zonation of Thapa and Guoxin and compare these to a hypothetical rectangular rupture area (using the Wells and Coppersmith, 1994, calculations of Table 2-3) of a magnitude 8 earthquake. Such an earthquake would have rupture length along the spine of Nepal that spanned two zones or more of Thapa and Guoxin's zonation model, a single zone would not contain an earthquake rupture of this size.

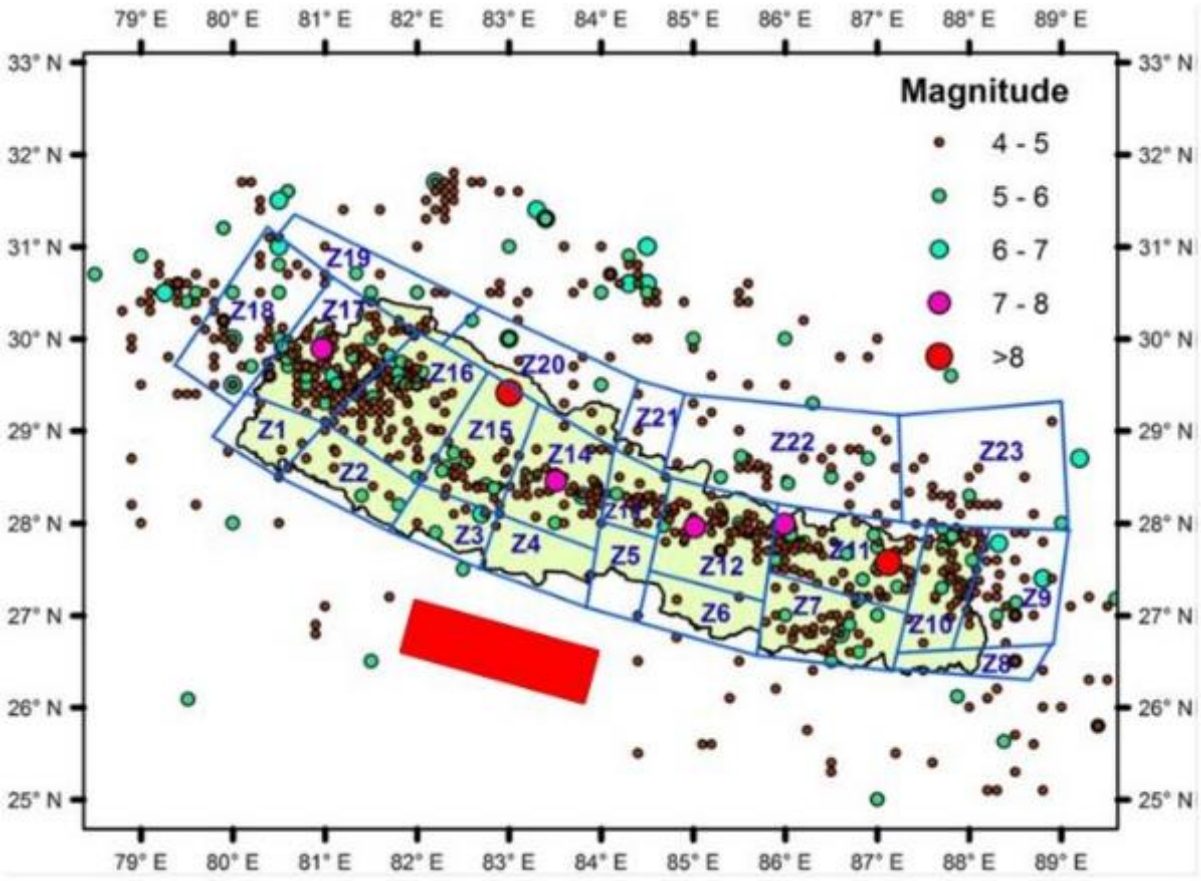

Figure 2-15. Subterranean rupture size and seismic zones.

Subterranean rupture size and seismic zones. The red rectangle represents a hypothetical rupture area for an earthquake of magnitude 8, calculated using the equations of Wells and Coppersmith (1994) as in Table 2-3. Such a rupture area would straddle two or more seismic zones, along the spine of Nepal, in this zonation scheme (Thapa and Guoxin, 2013). Seismic hazard analysis procedures for Nepal usually allow for occurrence of magnitudes in excess of 8 and although the NEIC USGS database assigns a magnitude 8 to the 1934 Nepal-Bihar earthquake (see Figure 2-3 and Figure 2-5 for this epicentre), some assessments for this earthquake exceed this magnitude value (Gupta, 2000)

It is possible to partition a regional seismicity into clusters of earthquakes, and then into seismic zones e.g. Greece (Weatherill and Burton, 2009). Indeed, it is possible to partition the seismicity on a long fault into clusters of seismicity that are comparable with the geometry of a geological segmentation. This has been done for the 1,800 km long Sumatran fault (Burton and Hall, 2014) where the partitioned seismicity (or earthquake clusters), hence fault segments, complements the geological segmentation of Sieh and Natawidjaya (2000), while differing in some important details.

The procedure to partition seismicity into earthquake clusters is described in detail by Weatherill and Burton (2009), and Burton and Hall (2014) but the gist is as follows. A cluster is envisaged with a centroid and surrounding earthquakes, as cartooned in the upper-left part of Figure 2-16. The geographical location of trial centroids are chosen randomly using Monte Carlo techniques and the procedure starts with two cluster centroids (k = 2), then three, four and so on until a reasonable limit has been passed. For each family of clusters (k = 2, 3, 4, 5….) the positions of the centroids are adjusted to minimise the total within-cluster sum of squares (TWCSS). This takes many thousand repetitions to achieve the optimum centroid locations for each cluster family. At this stage of the procedure, the analysis indicates that some sets of centroids and cluster partitions fit the whole seismicity better than others (Krzanowski and Lai, 1988). A preliminary result from this developing analysis is illustrated in Figure 2-16 in which nine clusters of earthquakes have been identified. Within Figure 2-16 the rectangular rupture area corresponding to a notional magnitude 8 earthquake is superimposed. These cluster dimensions along the spine of Nepal are larger than those proposed by either Pandey et al. (2002) or Thapa and Guoxin (2013) and can accommodate such a very large earthquake.

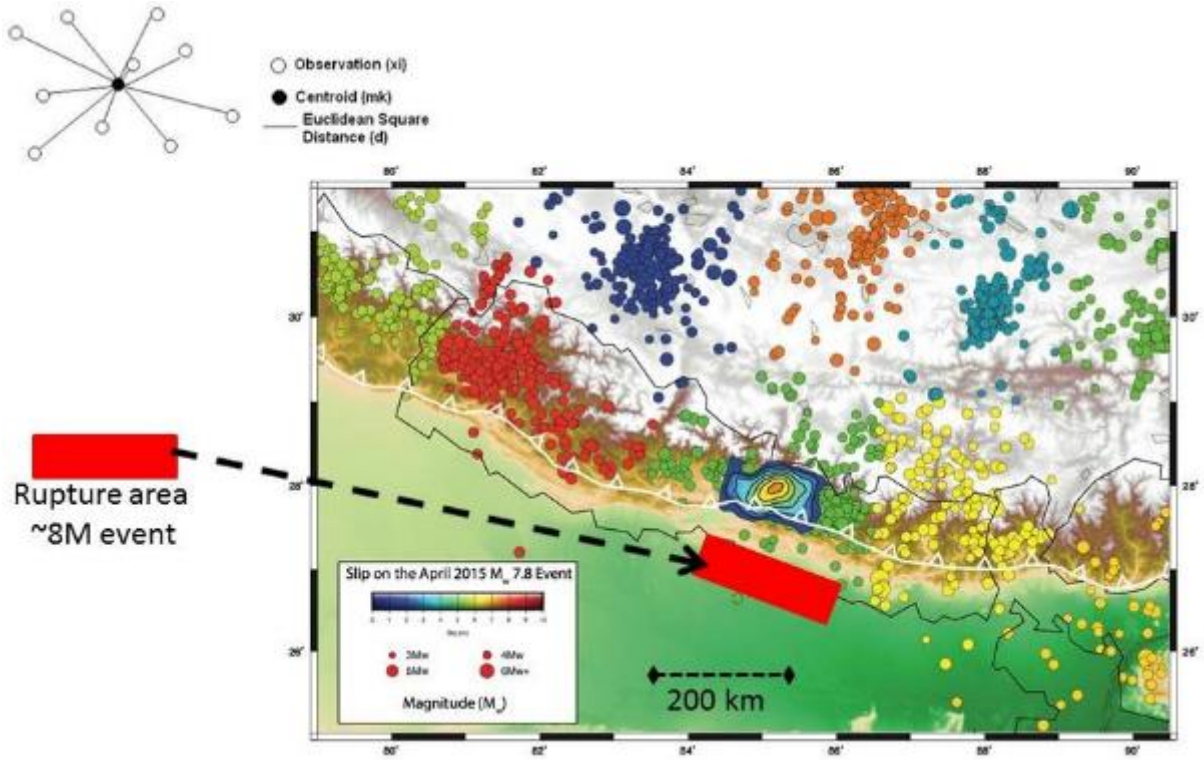

Figure 2-16 Earthquake clusters in Nepal.
The diagram at top-left of this Figure visualises a simple cluster of earthquakes around a centroid. Seismicity in a region, or along a large fault, can be partitioned into a series of clusters (Weatherill and Burton, 2009; Burton and Hall, 2014) by minimising the "total within cluster sum of squares" (TWCSS), first assuming two clusters (k = 2), then three clusters (k = 3) and so on (k = 2, 3, 4, 5…) and the optimum number of clusters is then determined at the end of this process (Krzanowski and Lai, 1988). The initial latitude and longitude at each cluster centroid is chosen by Monte Carlo methods and then adjusted over several thousand repetitions to minimise the TWCSS for cluster numbers k = 2, 3, 4, 5… The Figure shows a preliminary result with nine clusters (k = 9). The clusters could be redrawn as quadrilateral seismic zones. The red rectangle again represents a hypothetical rupture area for an earthquake of magnitude 8, using the equations of Wells and Coppersmith (1994), as described in Figure 2-15. The size of these clusters along the spine of Nepal can readily contain the rupture extent of a magnitude 8 and larger earthquake

This exploration of seismic hazard mapping in Nepal is preliminary and ongoing. It does highlight some issues meriting development. The fundamental data underpinning any PSHA is the seismicity or earthquake catalogue and it seems possible that individual large earthquakes may be parameterised differently by different authors and in different earthquake catalogues, thus fuelling differences between hazard maps. The large 1916 earthquake may fall into this category and any significant infrastructure development in western Nepal could consider such an issue. The seismic zonation schemes that can underpin PSHA also merit

more investigation as earthquake magnitudes in excess of 8 M_w are considered possible along the Himalayan arc. The issue of suitable ground motion models will continue to stand while there is a dearth of strong motion recording in and near to Nepal; in our exploration we took the lead on ground motion modelling from the NSC, Kathmandu. While we do see ways forward to develop PSHA in Nepal, at this time it seems appropriate to respect and use the national seismic hazard map produced by NSC, Kathmandu, with the caveat, for instance, that this map may indicate values of PGA that may be too low in western Nepal.

2.4. CHIMNEYS AND MONUMENTS (STUPA)

A field mission of this kind provides opportunity to deploy seismological concepts and methods of observation that are both ancient and modern and yet both are relevant to seismic hazard and earthquake impacts on structures. For instance, how do monumental structures respond to earthquake? What ground motions induce a free-standing rock to leave, or remain, in its position? These questions in one form or another have interested observational seismologists for very many years. Mallet (1862) travelled to the Naples 1962 earthquake and reported on the rotation of monuments with respect to their foundation slab in churchyards. The Assam 1897 earthquake was investigated in detail by Oldham (1898), and he described evidence for both very high horizontal acceleration at the ground surface in the shearing of the Khasia standing stones, and also for very high vertical accelerations at the ground surface evidenced by boulders displaced from their embedment in gentle soil slopes in the Khasi Hills. Such monuments, standing stones and boulders are historical examples of significant disturbances caused by earthquakes that can be analysed. More recently, examples of significant *non*-disturbances have been analysed. For example, Brune (1992) examined “precarious rocks” in Southern California, inferred that acceleration of 0.3 g was sufficient to topple them, and therefore such accelerations had not occurred for a great length of time. Such observations can be considered a constraint on a seismic hazard map and are palaeoindicators of PGA. The dynamics and mechanisms of unimpeded rocking response of a rigid block have also been explored, by Housner (1963), and developed further (e.g. Anooshehpoor et al., 2004).

Figure 2-17 Kiln chimney and stupa, Kathmandu.

Kiln chimney and stupa, Kathmandu. a) Panorama of a brick making factory near to Kathmandu. b) Close-up of shear damage to the brick kiln chimney seen in panorama (a). The GPS waypoint coordinates given at the bottom of (a) and (b) are the photographer’s position. Waypoint (a) to (b) is 36 m. The bearing photographer-to-centre“X”damage is N08°E. c) A damaged stupa in the centre of Kathmandu. On inspection the stupa shows damage similar to the kiln chimney. The stupa was imaged in detail using a 3-D laser scanner. The GPS waypoint is beneath the tripod supporting the 3-D laser scanner in the foreground of (c)

The panorama of Figure 2-17a shows a brick making factory near Kathmandu. This panorama was photographed from the south of the site. The brick baking kiln chimney is near the centre of the panorama, and seen close-to in the photograph Figure 2-17b. The distance between the two GPS waypoints taken at these two photographs is 36 m. Shear crack damage to the

brick kiln chimney is very visible in Figure 2-17b. The bearing from the photographer to the centre of the "X" shaped damage is N08°E. This chimney was photographed from all four quadrants (not illustrated).

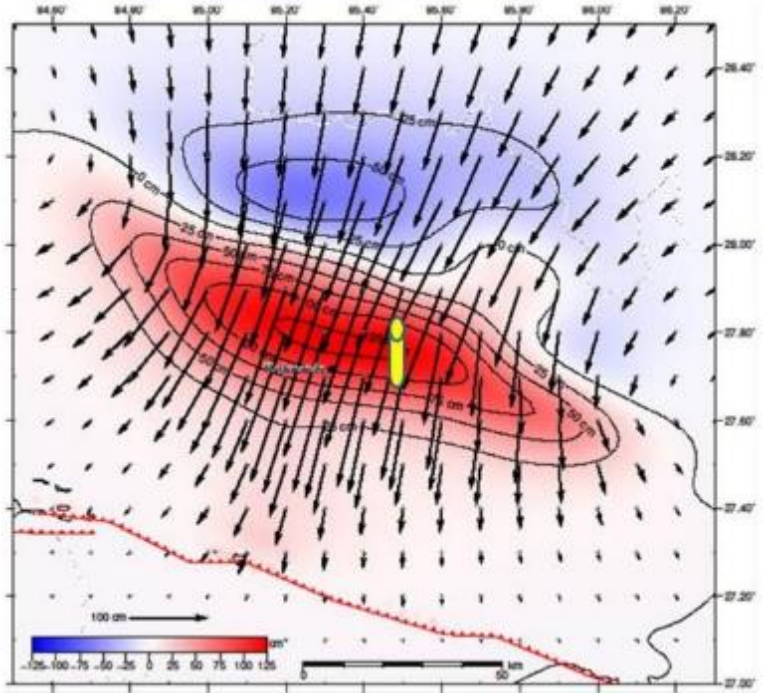

Figure 2-18 Total horizontal displacement field around Kathmandu.
The map contours are of final vertical displacement; red is up and blue is down, in cm on the graduated colour range in the map legend at the bottom of the map. The map arrows indicate resultant horizontal displacement vector on the 100 cm scale arrow in the map legend. The base of the yellow chimney-like symbol is the position of the damaged kiln chimney photographed in Figure 2-17b. This map depicts the final static displacements. The dynamic displacements to reach the static result in the map were recorded by a high-frequency continuously recording GPS network deployed around Kathmandu (Avouac and Adhikari). Dynamic displacement lasted about 5 s and was not uni-directional i.e. the E-W component showed reversal, moving first to the East and then to the West. (This map was kindly prepared and supplied by J. P. Avouac. The dynamic displacements were kindly described by L. B. Adhikari at the National Seismological Centre, Kathmandu)

The total horizontal displacement field (determined from analysis of satellite observations) caused by the Gorkha earthquake is illustrated in Figure 2-18 (from J. P. Avouac) on which is superimposed the position of the kiln chimney. At the position of the chimney, the total horizontal displacement was a little over 1 m in the direction N192°E. There are rare additional data as the NSC and Avouac (L. B. Adhikari, J. P. Avouac, pers. comm.) obtained results from their high-frequency continuously recording GPS network around Kathmandu. The recordings show ground displacement with a vertical component of ~160 cm achieved in the first 5 sec of disturbance, which stabilised at ~130 cm, a horizontal N-S component of ~180 cm to the South, and, vitally an E-W component with displacement first ~+80 cm to the East followed by a reversal of direction to ~-50 cm to the West, where it stayed. An interpretation of the dynamics to the kiln chimney, given the unusual quality and quantity of these observed displacement field data, is that it experienced shear by the reversal in the E-W displacement, displaced and rocked in a S-SE direction, in which diection it was close to being overtoppled. The stupa in Figure 2-18c was photographed in the centre of Kathmandu. The tripod in the foreground of Figure 2-18c is the mount for a 3-D laser scanner that was used to image this stupa in extreme detail (M. DeJong, later in this report), compared to the simple photography of the chimney and stupa in Figure 2-17.

2.5. CONCLUSIONS

The Gorkha 7.8 M_w earthquake and its 7.3 M_w main aftershock were caused by reverse (thrust) faulting associated with the decollement between the subducting India plate and the overriding Eurasia plate. Focal depths have been determined as 8.2 ± 2.9 km and 15.0 ± 1.7 km, respectively. These two epicentres are about 150 km apart, indicating a large seismic zone.

There were about 300 aftershocks (magnitude 4 and larger) in the six months to mid-October 2015, including four over magnitude 6, in addition to the main aftershock. This aftershock swarm measures nearly 200 km along the spine of Nepal, from west of the Gorkha epicentre, to east of the main aftershock. This is consistent with a Gorkha earthquake subsurface rupture length (RLD) of ~200 km. While small magnitude earthquakes tend to be a point source, the Gorkha earthquake is better visualised in combined terms of its epicentre and large rupture area.

The PGA observed in Kathmandu was ~160 cm s^{-2}, about 80 km southeast of the epicentre. This was at an installation in the compound of the US Embassy in central Kathmandu. Three seismic hazard maps have been published for Nepal and these are reproduced in Figure 2-9, Figure 2-10 and Figure 2-12. All three maps are surprisingly similar in general pattern. They display values of PGA (at bedrock level) with 10% probability of exceedance in 50 years, the usual 500 year average expectation. The national seismic hazard map prepared by the NSC, Kathmandu, indicates a PGA value around ~200 cm s^{-2} (500 year) near Kathmandu and the other maps indicate 0.475-0.524 g and ~0.33 g (g = acceleration due to gravity). The individual maps are based on different methodologies, different ground motion prediction equations and seismic zone schemes. There may also be differences in the parameters in the underlying earthquake catalogues analysed.

We have carried out exploratory tests of the Nepalese seismicity (using data sets from the NEIC USGS database) to consider issues in parallel to the three existing hazard maps. Our exploratory hazard map indicates a PGA ~475 cm s^{-2} near Kathmandu and considerably higher values in western Nepal that extend up to ~650 cm s^{-2} (500 year). A very different analysis was then deployed to partition Nepalese seismicity into earthquake clusters; these can be compared with the seismic zones that have been used to underpin the published seismic hazard maps. The earthquake clusters we elicited that embrace the spine of Nepal can readily accommodate the RLD of a magnitude 8 earthquake, whereas the individual zones in existing seismic zone models cannot. Note that magnitudes in excess of 8 are believed possible in Nepal, and indeed may have occurred in the last century. The seismic hazard map produced by the NSC, Kathmandu, remains the national standard map, it is reasonable and carefully produced, although there are caveats, for example it may indicate values of PGA that are low in western Nepal and Kathmandu.

2.6. REFERENCES

Anooshehpoor, A., Brune, J.N. and Zeng, Y. (2004). Methodology for obtaining constraints on ground motion from precariously balanced rocks, *Bull. seis. Soc. Am.*, **94**, 285-303.

Atkinson, G. M. and Boore, D. M. (2011). Modifications to existing ground-motion prediction equations in light of new data, *Bull. seis. Soc. Am.*, **101,** (3):1121–1135.

Bayliss, T.J. and Burton, P.W. (2013). Seismic hazard across Bulgaria and neighbouring areas: regional and site-specific maximum credible magnitudes and earthquake perceptibility, *Natural Hazards*, **68**, 271-319, DOI 10.1007/s11069-013-0590-5.

Bellier, O., Sebrier, M., Pramumijoyo, S., Beaudouin, Th., Harjono, H., Bahar, I. and Forni, O. (1997). Paleoseimicity and Seismic Hazard along the Great Sumatran Fault, *J. Geodynamics,* **24**, 169-183.

Bilham, R., Larson, K., Freymueller, J. and Project Idylhim members (1997). GPS measurements of present-day convergence across the Nepal Himalaya, *Nature*, **386**, 61–64 (1997).

Boore, D. M. and Atkinson, G.M. (2008). Ground-motion prediction equations for the average horizontal component of PGA, PGV, and 5%-damped PSA at spectral periods between 0.01 and 10.0s, *Earthq. Spectra.*, **24** (1):99–138.

Brune, J.N. (1996). Precariously balanced rocks and ground motion maps for Southern California, *Bull. seis. Soc. Am*., **86**, 43-54.

Burton, P.W. and Bayliss, T.J. (2013). Seismic hazard across Bulgaria and neighbouring areas: extreme magnitude recurrence and strong ground shaking, *Natural Hazards*, **68**, 1155-1201, DOI 10.1007/s11069-013-0699-6.

Burton, P. W. and Hall, T.R. (2014). Segmentation of the Sumatran fault, *Geophys. Res. Lett.*, **41**, 10 pages, doi:10.1002/2014GL060242.

Campbell, K. W. and Bozorgnia, Y. (2008). NGA ground motion model for the geometric mean horizontal component of PGA, PGV, PGD and 5 % damped linear elastic response spectra for periods ranging from 0.01 to 10 s, *Earthq. Spectra*, **24** (1):139–17.

Cattin, R. and Avouac, J. P. (2000). Modeling mountain building and the seismic cycle in the Himalaya of Nepal, *J. Geophys. Res.*, **105:** 13389-13407.

CEA (2005). China Earthquake Administration. *Training material on seismic hazard analysis for Engineering Sites*, (GB17741-2005), (in Chinese, not seen).

Chaulagain, H., Rodrigues, H., Silva, V., Spacone, E. and Varum, H. (2015). Seismic risk assessment and hazardin Nepal, *Natural Hazards*, **78**, 583-602, DOI 10.1007/s11069-015-1734-6.

Chiou, B. S. J. and Youngs, R. R. (2008). An NGA model for the average horizontal component of peak ground motion and response spectra, *Earthq. Spectra*, **24** (1):173–215.

Cornell, C.A. (1968). Engineering Seismic Risk Analysis, *Bull. seis. Soc. Am.,* **58**, 1583–1606.

De Joussineau, G. and Aydin, A. (2009). Segmentation along Strike-Slip Faults Revisited, *Pure appl. Geophys.*, **166**, 1575–1594.

EEFIT (2006). Peiris, N., Rossetto, T., Burton, P. and Mahmood, S. (2006). *EEFIT Mission: October 8, 2005 Kashmir Earthquake, Preliminary Report*, Earthquake Engineering Field Investigation Team. http://www.istructe.org.uk/eefit/files/EEFIT%20Mission%20Pakistan%20-%20prelim%20report.pdf, www.eefit.org.uk

EEFIT (2008). Peiris, N., Rossetto, T., Burton, P., and Mahmoud, S. (2008). *Kashmir Pakistan Earthquake of 8 October 2005, A Field Report by EEFIT*, Earthquake Engineering Field Investigation Team, Institution of Structural Engineers, London. www.eefit.org.uk, ISBN 978 1 906335 11 3, 119 pages.

Gelfand, I., Guberman, Sh., Izvekova, M., Keilis-Borok, V. and Rantsman, E. Ya. (1972). Criteria of High Seismicity, Determined by Pattern Recognition, *Tectonophysics*, **13**, 415–422.

GSHAP (1999). D. Giardini (ed.) 1999. The Global Seismic Hazard Assessment Program (GSHAP) 1992-1999, Summary Volume, *Annali di Geofisica*, **42**, 6, pp. 957-1230. Note: Giardini, D., Grünthal, G., Shedlock, K.M and Zhang, P. (1999), The GSHAP Global Seismic Hazard Map, **ibid.**, pp. 1225-1230.

Gupta, H. K. (2000). Major and great earthquakes in the Himalayan region: an overview, in: *Earthquake Hazard and Seismic Risk Reduction*, pp. 79-85, eds S. Balassanian et al., Kluwer Academic Publishers.

Housner, G.W. (1963). The behaviour of inverted pendulum structures during earthquakes, *Bull. seis. Soc. Am*., **53**, 403-417.

Krzanowski,W.J., and Lai, Y. T. (1988). A criterion for determining the number of groups in a data set using sum-of-squares clustering, *Biometrics,* **44**, 23–34.

Lava, J. and Avouac, J.P. (2000). Active folding of fluvial terraces across the Siwaliks Hills, Himalayas of central Nepal, *J. Geophys. Res.*, **105,** 5735–5770.

Mallet, R. (1862). *Great Neapolitan Earthquake of 1862: The First Principles of Observational Seismology*, Report to the Royal Society of London, two volumes, Chapman and Hall, London.

McGuire, R. K. (1976). *FORTRAN Computer Program for Seismic Risk Analysis*. U.S. Geological Survey Open-File Report, 76–67.

NSC (2012). *National seismological network and its contribution in seismological research in Nepal Himalaya*, Department of Mines and Geology, National Seismological Centre, Kathmandu, 16 pages.

NEIC. National Earthquake Information Center website. http://earthquake.usgs.gov/contactus/golden/neic.php

Oldham, R.D. (1899). Report on the great earthquake of 12th June 1897, *India Geol. Surv. Mem*., **29**, pp. i-xxx, 1-379.

Pandey, M. R., Tandukar, R. P., Avouac, J. P., Lave, J. and Massot, J. P. (1995). Interseismic strain accumulation on the Himalayan crustal ramp (Nepal), *Geophys. Res. Lett.*, **22** (7):751–754.

Pandy, M. R., Tandukar, R.P., Avouac, J. P., Vergne, J. and Heritier, T. (1999). Seismotectonics of Nepal Himalaya from local seismic network, *J. Asian Earth Sci.*, **17,** 703–712.

Pandey, M. R., Chitrakar, G. R., Kafle, B., Sapkota, S. N., Rajaure, S. N. and Gautam, U.P. (2002). *Seismic hazard map of Nepal*, Department of Mines and Geology, National Seismological Centre, Kathmandu, 8 pages.

Peiris, N., Rossetto, T., Burton, P., & Mahmood, S. (2005). The Kashmir, Pakistan earthquake of 8 October 2005. Retrieved from https://ueaeprints.uea.ac.uk/25475/1/Burton2008-PeirisEtAl_KashmirPakistanEarthquake8Oct2005_EEFITfinalReport.pdf

Scordilis, E. M. (2006). Empirical global relations converting M_s and m_b to moment magnitude, *J. Seismology*, **10,** 225-236, DOI: 10.1007/s10950-006-9012-4.

Sieh, K. and Natawidjaja, D. (2000). Neotectonics of the Sumatran fault, Indonesia, *J. Geophys. Res.,* **105**, 28,295–28,326.

Thapa, D. R. and Guoxin, W. (2013). Probabilistic seismic hazard analysis in Nepal, *Earthq. Eng. Eng. Vib.*, **12**, 577-586, DOI: 10.1007/s11803-013-0191-z.

Upreti, B. N. (1999). An overview of the stratigraphy and tectonics of the Nepal Himalaya, *J. Asian Earth Sci.*, **17**, 577–606.

USGS. United States Geological Survey website. http://earthquake.usgs.gov/.

Weatherill, G. and Burton, P. W. (2009). Delineation of shallow seismic source zones using K-means cluster analysis, with application to the Aegean region, *Geophys. J. Int.*, **176**, 565-588, doi: 10.1111/j.1365-246X.2008.03997.x.

Wells, D.L., and Coppersmith, K. J. (1994). New empirical relationships among magnitude, rupture length, rupture width, and surface displacements, *Bull. seis. Soc. Am.,* **84**, 974–1002.

Wikipedia. Wikepedia, the free encyclopedia website. http://en.wikipedia.org/wiki/United_Kingdom.

Youngs, R. R., Chiou, B. S. J., Silva, W. J. and Humphrey, J. R. (1997). Strong ground motion attenuation relationships for subduction zone earthquakes, *Seismol. Res. Lett.*, **68** (1):58–73.

Zhang, P., Yang, Z., Gupta, H.K., Bhatia, S.C. and Shedlock, K.M. (1999). Global Seismic Hazard Assessment Program (GSHAP) in continental Asia, *Annali di Geofisica*, **42** (6):1167-1189.

3. NEPALESE BUILDING STOCK AND CONSTRUCTION PRACTICES

The EEFIT team members involved in evaluating building performance spent most of their time in the Kathmandu Valley, but also spent two days evaluating building performance in rural areas in the district of Gorkha (nearer to the epicentre). Thus, the majority of observations are from the Kathmandu Valley for the urban context but some discussion of rural construction is also included.

The building typology distribution for the Kathmandu Valley is shown in Figure 3-1. As can be seen, the vast majority of buildings are unreinforced masonry, with fewer concrete buildings. However, the situation is much more complicated than Figure 3-1 suggests. In reality, as is typical with masonry structures in urban areas (particularly in locations where building codes are not regularly enforced), Nepalese buildings within a single category vary tremendously. For example, the categories do not account for the age of the structure, the quality, type, and integration of materials, and the geometry and detailing, which can all result in different levels of seismic performance.

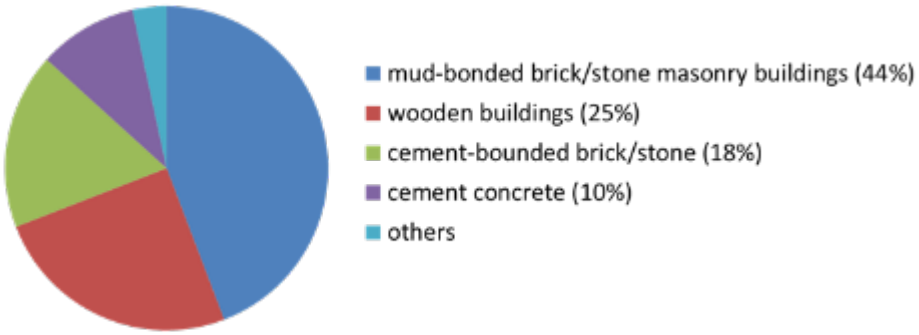

Figure 3-1 Building typology distribution in the city of Kathmandu.
Source: National Population and Housing Census (NPHC 2011).

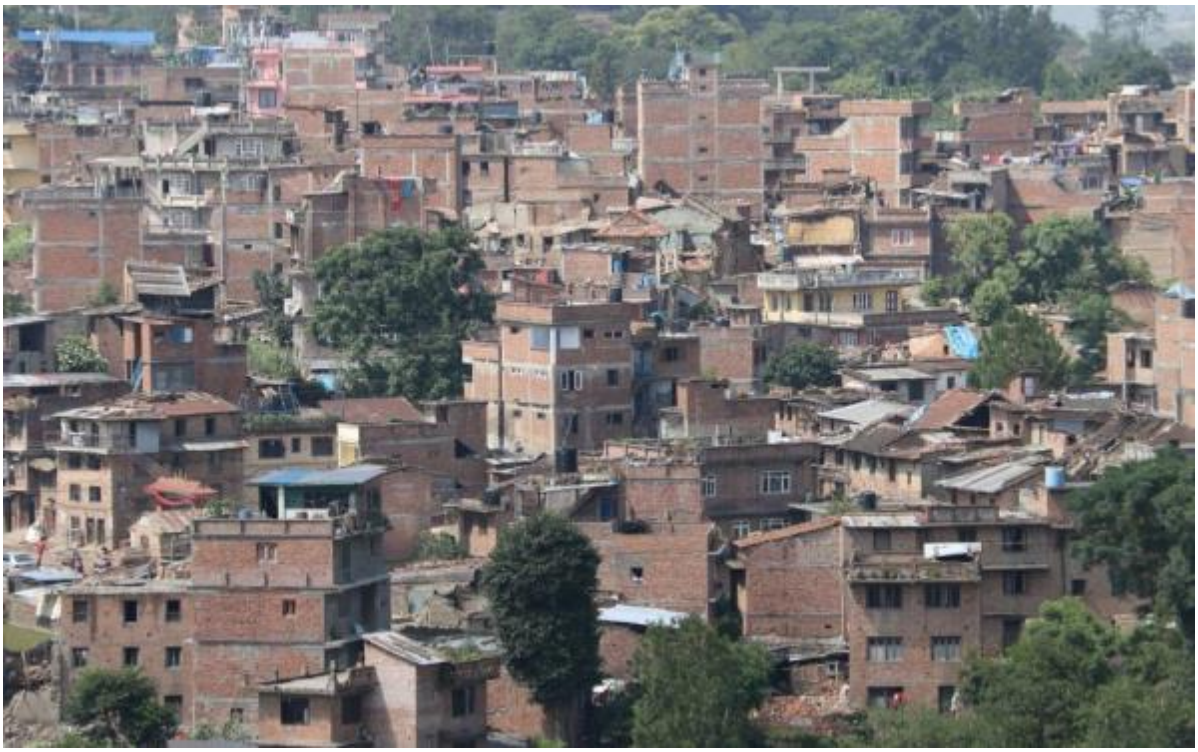

Figure 3-2 Typical urban construction in the Kathmandu Valley.

Additionally, the lines between these building typologies are blurred. For example, Figure 3-2 portrays a typical urban area in the Kathmandu Valley, which is dominated by 2-6 storey

buildings. Masonry is clearly the dominant building material, but many of the buildings are composed of some combination of brick, mud, lime or concrete mortar, timber and reinforced concrete. The use of these materials may also vary from floor to floor as buildings are often constructed progressively (upwards) and often resulting in irregularites such as overhangs. This also resulted is some very slender structures

Figure 3-3 is a photograph taken in Chyasal near Patan Durbar Square, and shows a representative variety of building typologies present in urban areas in Kathmandu. The legend in Figure 3-3 more adequately describes the majority of buildings observed by the EEFIT team, though of course the variation within each category remains large. In addition, many buildings in urban areas are built without building separations or built contiguously, so may not act independently in an earthquake.

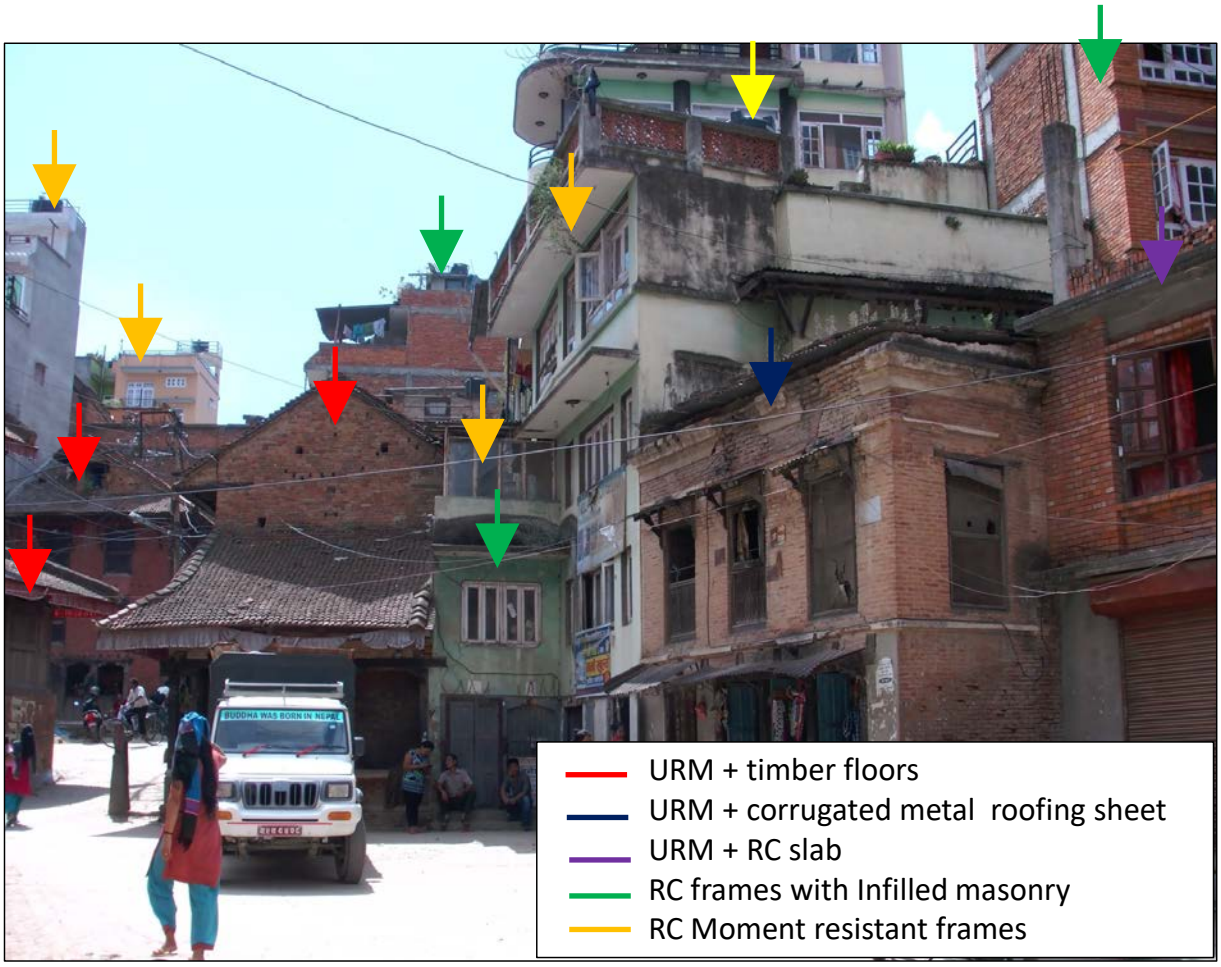

Figure 3-3 Buildings typologies observed in the district of Chyasal, Kathmandu.

The following subsections summarise observations regarding the various building types and construction techniques observed by the EEFIT team.

3.1. MASONRY STRUCTURES

3.1.1. Unreinforced masonry structures in urban areas

Unreinforced masonry (URM) constructions dominate the building stock in urban areas (see Figure 3-1). These constructions are distributed as clusters of low-rise units (one or two storeys) or medium rise units (between three and five storeys), of different dates of construction, using different construction materials and structural detailing, and of varying quality.

Despite the large variability in construction, some general observations could be made. The typical construction material for bearing walls was sun-dried bricks of approximate dimensions

of 210x105x50 mm or fired bricks of dimensions 210x105x50 mm with a trapezoidal cross section. Lime, mud, and sometimes cement are used for the mortar.

The original floors were typically made with timber beams (Figure 3-4a and Figure 3-4b). Roofs were typically constructed with timber trusses and tiles or light metallic corrugated galvanized iron sheets (CGI). Floors and roofs were often anchored with timber pegs (though the quality of detailing and prevalence of anchors varied significantly), which were used to try and prevent overturning failures of their bearing walls. In more recent construction or during retrofit, the original floors were often replaced with reinforced concrete slabs (see Figure 3-4c).

The traditional URM houses were mainly rectangular in plan (typical length of side being approximately 4-5m) with regular heights between 2.5 m and 2.8 m. These constructions were often altered in their plan with additional balconies and cantilevers, or in their heights with additional floors added at a later date.

Many masonry constructions were built with traditional techniques (Figure 3-5) named *Newari*'. It is characterised by using quality construction materials, well detailed connections and evidence of good levels of maintenance. However, in the majority of structures, the quality of construction, detailing, and maintenance was poor. Figure 3-6 shows examples of insufficient timber connections and poor interlock between the exterior and interiors wythes of the masonry.

As stated above, much of the construction in urban areas were located in close proximity to each other, causing the response of a structure to be largely influenced by the surrounding structures. Figure 3-7a shows the absence of seismic gaps between buildings, which was typical of the area. Further, adjacent (or connected) buildings were often constructed of different materials, as shown in Figure 3-7b. This could make interaction between structures more likely in an earthquake, leading to a higher risk of pounding damage.

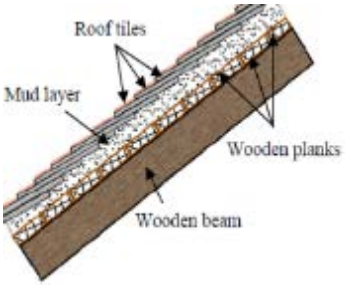

(a)

(b)

(c)

Figure 3-4 Construction details of URM buildings.
a) Structural detail of a timber beam adopted in traditional URM construction b) typical timber floor in traditional URM construction, c) URM with Reinforced Concrete (RC) floors

(a) (b) (c)

Figure 3-5 Buildings built according to traditional construction techniques.
a) Presence of timber pegs b) structural details of timber roof c) buildings with good constructional materials and good connections.

(a) (b)

Figure 3-6 Insufficient timber connections and poor interlock.
a) Bearing walls of one layers of fired bricks and two layers of sundried bricks tied with inadequate timber peg b) two layers of fired bricks filled up with cement mortar and bricks.

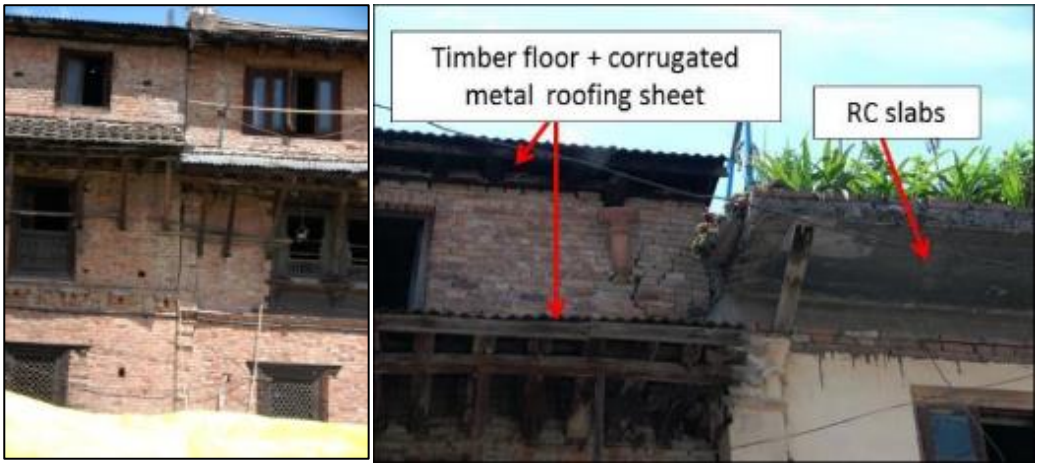

Figure 3-7 Absence of seismic gaps between buildings.
a) Absence of seismic gap in Newari construction. b) Damage due to pounding between buildings with different floor typology.

3.1.2. Unreinforced masonry structures in rural areas

Unreinforced masonry (URM) buildings were by far the most common typology identified in rural areas. These were constructed as isolated low-rise (one or two storeys) buildings. This typology is generally used as dwellings and rarely for commercial activities. The typical URM houses again have rectangular plan (typically 4x5m) with regular heights between 2.5 m and 2.8m.

The construction observed on site was usually built using local stones with approximate dimensions of 200x200x100 mm, or sun-dried or fired bricks with approximate dimensions of 210x105x50 mm, with a trapezoidal cross section. Lime or mud was typically used for mortar.

Floors were again typically constructed of timber beams, while roofs were constructed of timber trusses with tiles or light metallic CGI sheets. Original floors were sometimes substituted with reinforced concrete slabs, though this was not common in rural areas.

Some stone structures built with traditional techniques displayed high quality construction with good seismic detailing, and also showed no evidence of damage. For example, Figure 3-8 shows two structures that utilise high quality, larger stones, good interlocking between stones (particularly at corners), good dowel connections between timber floors and walls, evidence of good connection between the wythes of the wall (e.g. through stones), and lightweight roofs. These structures appeared to follow the National Society for Earthquake Technology (NSET) guidelines for building small residential dwellings in stone. However, such examples appeared to have been recently built, and were rare. Most of the URM stone buildings were shown to be vulnerable, as they were built using poor material, lack of mortar, lack of interlocking between stones, lack of connections between bearing walls and inner walls, and inadequate use of timber pegs. Damage due to lack of seismic detailing will be discussed later.

Figure 3-8 Stone structures built with traditional techniques.
Traditional stone houses exemplifying high quality construction with good seismic detailing, and which showed no evidence of damage.

3.2. VERNACULAR HOUSES

The majority of Vernacular houses in Nepal are either masonry or timber, or some combination of two. Thus, many of the observations made in Section 3.1 also apply to this form of construction. However, this section focuses more directly on this subset of structures, considering their history and construction in more detail.

3.2.1. Background

The Kathmandu Valley has been the home of the Newars for hundreds of years. During that time, this local amalgam of several ethnic groups developed its own unique traditional architecture (Blair 1983; Shrestha 2012), what will be referred to as *Newari* architecture (see later). The cultural significance of its structures has made the Kathmandu fit to be awarded

the status of The United Nations Educational, Scientific and Cultural Organization (UNESCO) World Heritage (WH) Site (DoA 2007).

As a seismically active area, it could be expected that traditional constructions will have adapted to the constraints of seismic shocks (Krüger et al. 2015). *Newari* architecture is characterized by a combination of load bearing brick walls and timber elements such as floors, roofs, windows, etc. This typology of buildings is one of the features that define the unique character of the Kathmandu Valley (Shrestha 2012).

Traditional settlements and structures observed during the EEFIT mission included the monument zones of Kathmandu, Patan (also known as Lalitpur) and Bhaktapur, as well as the historical centres of Patan and Bhaktapur, and the villages of Bungamati, Khokana and Sankhu.

Overall, three types of traditional buildings exist: temples, palaces, and domestic buildings. Temples and monuments are discussed in the following section. This section focuses instead on domestic buildings, which are inhabited and more prolific.

At the time of the investigation, smaller aftershocks were still occurring. Thus, it was deemed too risky to enter any traditional buildings, as there was no certainty as to the quality and soundness of their construction, and as their seismic performance remained uncertain. Furthermore, many observed buildings were in the process of being cleared of rubble. As a result, and due to the short length of the study, the observations mainly derive from external inspections, and need to be investigated further.

At the time of the mission, most of the rubble had been cleared away, with bricks and timber sorted into separate piles (see Figure 3-9), presumably to be used in reconstruction. It was typically not possible to know from which buildings the sorted elements came from.

It may be highly probable that the timber elements observed were only the ones deemed fit for reuse, with other badly damaged timber elements likely to have been discarded. Indeed, relatively few structural failures were found among the piles of timber. Furthermore, as the clearing was still underway, observations of the foundations was not possible.

Due to the short period of the investigation, observations were constrained to a limited number of buildings. By observation, it can be said that these buildings can be considered to be representative of the traditional construction and craft of the Kathmandu Valley. However, considering the variations in the building stock, statistical data cannot be extrapolated and the to the larger body of the Valley's historical built environment without further investigation.

Figure 3-9 Rubble to be used in reconstruction.
Stacks of building materials sorted for reuse were prevalent in heavily damaged areas throughout the Kathmandu Valley.

3.2.2. The *Newari* House

The *Newari* architecture distinguishes itself by the use of load-bearing brick walls and timber floors and roofs (see Figure 3-10 and Figure 3-11). Buildings are generally built in tight settlements, and typically do not exceed three floors above ground level (Blair 1983; Shrestha 2012; Romão, Paupério, and Menon 2015).

The construction also varied according to use. It was been observed that the quality of construction in the durbars (palaces), temples and other religious buildings was much higher than in domestic buildings.

One observation from the field was that common brick and timber structural principles linked the majority of buildings. However, this common pattern was found to be inconsistently applied, with some houses displaying a near complete set of details that would suggest that the building would act as one structural unit, while others only had some features of this system. As a result, each house can be regarded as a unique variation on the common pattern making it difficult to reach an overall conclusion for all structures of this typology.

In order to better understand the seismic response of the Newari traditional buildings, the following section introduces their main structural features.

Figure 3-10 A street lined with traditional Newari housing.
Sorted materials and propping are visible on masonry facades.

Figure 3-11 Elevation view of the front façade of a traditional Newari residence.

3.2.3. Wall Construction

The main vertical structural elements of traditional Nepalese houses consist of load-bearing brick walls. The walls are typically constructed using at least two types of brick, and sometimes three. The external wythe was composed of fired bricks. For significant buildings such as temples or palaces, bricks with a trapezoidal cross section, known as *daci apa* (or *dachi apa*), were used. These bricks produce thin hairline joints on the external face of the wall (Bonapace and Sestini 2003; D'Ayala 2004). For common buildings such as houses, rectangular section fired bricks are used, called *ma apa* (Beckh 2006; Romão, Paupério, and Menon 2015).

The internal face of the walls consisted sometimes of the same *ma apa* bricks, but more often than not, the internal face was made from air-dried bricks, known as *kaci apa* (Beckh 2006). Those bricks are also used for the infill layer between the two faces of the wall. Rubble infill was also sometimes used, but it was rarely observed during the mission.

Mud mortar is the principal binding compound in poorer construction, but it was noticed in several instances that repairs and alterations have made use of cement to replace it. This results in a heterogeneous construction using various types of bricks and mortars, with varying strengths. The most important observation is that no ties are used within the thickness of the walls, as most of the bricks are used as stretchers, and headers were rarely observed.

It was also observed that many wall corners were found to be unconnected, and adjoining houses have their walls only butt-jointed to each other (i.e. no effective connection).

3.2.4. Timber structure and details

Load-bearing brick walls support the horizontal structural elements which are usually made of timber (see Figure 3-12). At each floor level, a timber wall plate running parallel to the wall sits within the brick construction. Sometimes two wall plates are used, one for each face of the wall. Closely spaced floor joists typically span between two opposing walls and are seated on these wall plates. The joists are usually seated on the entire thickness of the brick wall. Where they meet the wall plate, a pair of timber pegs (*chokus*) run through every few joists on either faces of the wall (Korn 1976; D Ayala 2003; D'Ayala 2004). Sometimes only one peg is used and is inserted through both the joist and the wall plate, inside the thickness of the wall. These details enable the timber joists to tie together two opposing brick walls, thus partly preventing overturning of walls, as well as preventing floor joists from sliding off their vertical supports. When two pegs are used, one for each face of a wall, it also enables the joist to act as a wall tie at that specific height. Roof rafters are joined to the tops of the walls in a similar way.

Other features acting as wall ties are the windows and doors. These consist of two timber frames, one for each face of the brick walls. The lintels and sills of the window frames were observed to extend beyond the limits of the frame and were often well integrated into the wall, a feature that is mentioned in the Rules of Thumb for Unreinforced Masonry (Nepal Building Code, 1994). This added length allows for a timber element to tie both frames through the thickness of the wall, which is usually jointed with the frames using a dovetail.

In some buildings, such as resthouses (*pati*) or palace, the external walls are supported at the ground floor level by timber columns (Korn 1976; D Ayala 2003; D'Ayala 2004). Those columns extend into tenons at their extremities to join with timber wall plates in mortise and tenon joints. This enables for resistance against both in-plane and out-of-plane movement.

- Where timber lengths were insufficient, scarf joints were observed to be used. The latter were found to have the same form in all the observed instances. The complexity of the *Newari* scarf joint hints at a design that was conscious of a need to resist lateral forces.

Equally, the detailed jointing of the timber structural elements can be interpreted as an anti-seismic feature. Mortise and tenon joints, scarf joints, dovetails, pegs, are all recognized as designed to work under tension and the use of timber within brick walls also reinforces this idea. Thus, the local construction demonstrates a certain level of knowledge about resisting

lateral forces and achieving box behaviour through binding all structural elements into one structural unit.

The quality of craftsmanship and detailing of the majority of traditional structures observed was high, and provided evidence of a culture of meticulous detailing to provide connection between elements and improve earthquake safety, that had likely developed through history. However, in many cases, maintenance was lacking, often depending on the importance of the building.

Figure 3-12 Examples of timber detailing in vernacular structures.

3.3. TEMPLES AND MONUMENTS

The temples and monuments of Nepal attract numerous tourists each year, and have been well documented by architects and historians. The Kathmandu Valley Preservation Trust (KVPT) has done extensive work to document and preserve these structures. Discussions with KVPT were extremely informative when evaluating the seismic performance of these structures. One book that provides an excellent resource for the architecture of these structures is “The Traditional Architecture of the Kathmandu Valley” by Wolfgang Korn (reprinted in 2010).

The EEFIT team observed numerous temples, or *degas*, and monuments, primarily in Kathmandu Durbar Square, Patan Durbar Square, and Bachtapur Durbar Square. Perhaps the most commonly associated with Nepal is the multi-tier temple, an example of which is shown in Figure 3-13. These structures combine a supporting timber frame with load bearing masonry walls, which are again multi-wythe, with exterior bricks of trapezoidal cross section to minimise the width of visible exterior joints while allowing thicker mortar to penetrate between bricks at the interior.

Numerous other monuments were observed, but they vary significantly in their construction and cannot all be detailed here. Comments on the performance of selected structures follow in Section 4.3.

Figure 3-13 Example of a typical multi-tier temple, or dega.

3.4. CONCRETE STRUCTURES

The building stock of concrete structures in the Kathmandu Valley, and throughout Nepal, was primarily concrete frame with masonry infill (see Figure 3-14). The vast majority of buildings in Kathmandu are 2-6 storey buildings that either fall into this category or are unreinforced masonry. The other types of concrete structures observed were concrete bridges/flyovers and relatively few taller apartment buildings (e.g. Figure 3-15) and hotels (schools and hospitals are covered in a separate section).

The quality of concrete varied considerably between the structures observed. In many commercial buildings, where damage was relatively minimal, concrete appeared well-compacted and there was not noticeable damage due to excessive corrosion or lack of concrete cover. In many residential structures (and fewer commercial structures), spalled concrete indicated lack of concrete cover, and damaged columns indicated that shear reinforcing may not have been sufficient.

Nepal has a National Building Code, developed in 1994, which contains substantial chapters on seismic design. The code also contains mandatory rules of thumb for reinforced concrete buildings, both with and without masonry infill. In 2012, a draft of an additional chapter entitled “Ready to use guideline for detailing of low rise reinforced concrete buildings without masonry infill” was also proposed. Thus, the necessary design documents are in place, though they continue to need updating with progress in the field throughout the world.

However, discussions with locals confirmed the expectation that there is a significant difference between code and practice. Smaller buildings were rarely engineered, and while rules of thumb may be specified in the design, they are often neglected in the field. Based on our discussions, building inspection, which is especially important to ensure proper seismic detailing of RC structures, seemed to be almost non-existent for smaller structures. On the other hand, new larger structures were typically engineered, though inspection and quality control were still believed to be questionable. Significant variability in the construction of reinforced concrete buildings was observed by the EEFIT team with many examples of poorly detailed, failed concrete structures as well as evidence of good detailing in (such as long lap lengths and confining reinforcement) in surviving buildings that were partially constructed and therefore enabling the witnessing of the detailing of their reinforcement. Engineering design practice should also be questioned as there were examples of frames that seemed not to have been proportioned for seismic design (i.e. often columns are smaller than beams).

Figure 3-14 Examples of concrete frame structures with brick infill.

Figure 3-15 Park View Horizon Apartments in Dhapasi Kathmandu

4. PERFORMANCE OF BUILDINGS

4.1. MASONRY STRUCTURES

4.1.1. Urban URM structures

Many masonry structures built with traditional techniques, including good connections and the use of high quality construction materials, performed reasonably well in the earthquake. This is consistent with the low percentage of masonry constructions that actually failed in the city of Kathmandu, but can also, at least partially, be attributed to the earthquake energy being in the higher period region of the response spectrum and therefore less damaging to these short period structures.

However, severe damage in specific locations in the Kathmandu Valley, such as Shanku or Bachtapur, has shown that traditional URM houses made from poor materials and weak (or lack of) connections are highly vulnerable to seismic events. It is also possible that site effects played a role in these locations.

The majority of damage to URM buildings was out-of-plane failure, which typically occurs in structures with weak connections between adjacent bearing walls and between bearing walls and floors (see Figure 4-1b).

Another common type of damage observed in URM structures is in-plane shear failure of walls, which occurs when buildings have strong connections between adjacent bearing walls and between bearing walls and floors. These types of buildings, characterised by a box response to earthquakes, fail according to a crack pattern which involves the failure of the entire macro-element or by in-plane failure with X cracks on piers and on spandrels (see Figure 4-1a).

Combined mechanisms (Figure 4-1c) were also extensively observed. This type of collapse, which involves the overturning of one major element, tends to occur in structures, which have good connections between adjacent bearing walls, but where the connections between walls and floors or walls and roofs is inadequate.

4.1.2. Rural URM structures

The most typical failure observed in the rural areas was again out-of-plane collapse or wall delamination, due to: 1) very weak and badly bonded types of masonry (i.e. uncut stones in mud mortar) 2) the lack of connections between the main structural walls (see Figs. 4.2 & 4.3) and 3) out-of-plane arching failures due to the lack of connections between the main structural walls and floors and lack of connection between the wythes of the walls (see Fig. 4.4).

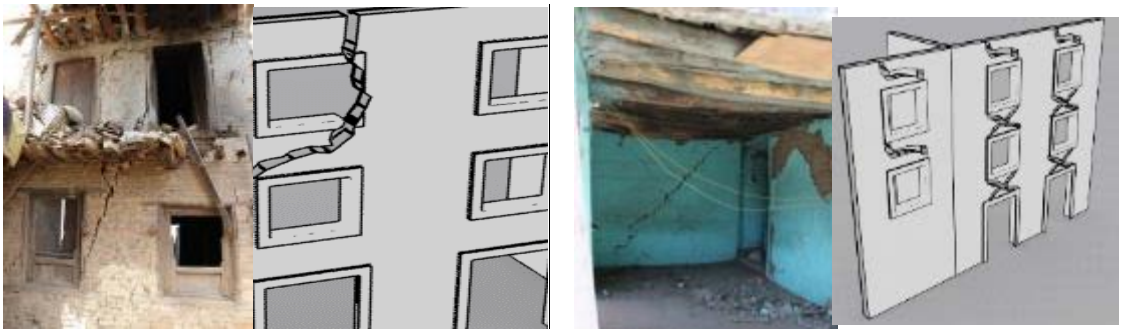

a) In plane failure (right: over multiple storeys; left: single wall beneath extremely heavy floor)

B1) Out of plane: Overturning due to insufficient connection of one side of the facade

B1) Out of plane: Overturning due to insufficient connections on both sides of the façade

C1) Combined failure: Corner failure overturning of two facades

C2) Combined failure: Overturning of three facades (left end of building)

Figure 4-1 Typical failure mechanisms observed for URM constructions in urban areas.

a b

c

Figure 4-2 Lack of connections between the main structural walls.
a) Lack of connection between bearing walls b) Lack of connection between bearing walls and inner walls c) Lack of connection between bearing walls and roofs.

Figure 4-3 Out of plane failure.
Out of plane failure due to lack of connections between adjacent walls and inadequate use of timber pegs.

Figure 4-4 Arch failure.
Arch failure due to the lack of connection between the floor and bearing walls and lack of connection between the wythes of the walls.

4.2. Vernacular Structures

There is unilateral agreement that the observed damage in traditional buildings greatly outweighs the damage to reinforced concrete frame buildings (Romão, Paupério, and Menon 2015). The large number of overturned façades encountered leads to the conclusion that the most common type of collapse was due to out-of-plane failure.

However, one important observation is that damage among traditional buildings was found to vary greatly. Some buildings seemed unscathed by the seismic shock while others were entirely destroyed, and everything within that spectrum was observed.

The damage not only varies between buildings, but is also unequally distributed between neighbourhoods. In some instances that one neighbourhood's houses fared quite well while the buildings in an adjacent neighbourhood completely collapsed.

Figure 4-5 Decay and delamination between wall wythes.
Examples of sorted timber that showed decay and delamination between wall wythes made from different materials.

Some signs of rot have been found in the sorted rubble (see Figure 4-5). But as mentioned earlier, there is no way to know whether a substantial amount of more rotted parts were discarded in the process of sorting out the rubble. Lack of maintenance could have been a cause of poor performance, but sufficient evidence could not be collected to make a definitive conclusion, nor what role site effects played.

Furthermore, the large range of quality of build in domestic buildings makes it difficult to assess the effectiveness of the structural system. As all buildings were constructed with slight differences, it is unknown whether the collapsed buildings had a complete set of structural elements that characterise the *Newari* house, or whether they failed because of missing elements.

The consistent lack of wall ties in the brick masonry walls, apart from the timber joists at floor levels, is one major weakness as also mentioned in the previous section. The structure of the brick wall makes it prone to delamination under lateral movement, which leads to bulging and eventually out-of-plane failure. Examples of restorations were found where cement was used to bind bricks within the thickness of the wall while mud mortar was used on the outside faces to retain the external appearance. Cement and mud mortar may not create a satisfying bond, enhancing the risk for delamination (see Figure 4-5 right). Combined with the lack of connections at wall corners, the fragile walls can easily experience overturning under lateral pressure, despite the presence of the timber floor joists, which could restrain out-of-plane movement if properly connected.

Though many structures collapsed, many others appeared to have significant wooden ties, providing good connection between elements, and although damage occurred, collapse was prevented (see Figure 3-10Figure 4-10 and Figure 3-11). In these cases, expected in-plane damage was often observed (e.g. Figure 4-6).

As mentioned earlier, most houses have been built so that they are abutting their neighbouring structures (these are independent structures i.e without any connections). The movement of the urban blocks during the earthquake would need to be further investigated, but is likely to have influenced the resulting damage due to pounding. Additionally, it was not uncommon to find RC structures and brick and timber buildings within the same block, also abutting each other.

Another concern with the construction was, as mentioned previously, the addition of storeys on existing traditional buildings, thus increasing both height and weight. The effect of this cannot be quantified, but it could significantly exacerbate other deficiencies.

4.2.1. Further risks

A further concern lies in the difficulty to determine the post-quake structural integrity of many remaining buildings. Indeed, many wooden pegs for example were only observable in the damaged structure, as they are hidden from view in usual circumstances, placed between the two external faces of a wall. This presents two main issues. First, it is hard to know whether pegs were used at all if no external ones can be seen. The other difficulty is that it is not possible to know whether the hidden pegs (which hold joists and wall plates together) are damaged without taking the structure apart.

4.2.2. Hope for the future

Despite the large variability in damage among traditional buildings, retrofits has been implemented in the past and these have now been tested by the earthquake. The work of the Kathmandu Valley Preservation Trust (KVPT) has shown a high success rate, with most of their retrofits (such as those in the Patan Museum) having survived the quake.

The KVPT's approach for historic construction is to take a sensitive approach that the balances risk reduction with retaining cultural heritage. They recommend making minimal contemporary additions that are distinguishable from the old fabric of the structure. This approach usually requires interventions that vary with each building.

However, their most common retrofit methods use steel bolts to replace or further assist timber pegs, and to insert steel wall ties into brick masonry walls.These examples show that dealing with one of the main weaknesses in the traditional construction system, namely the absence of wall ties, and improving timber joints can greatly improve the seismic behaviour of traditional buildings.

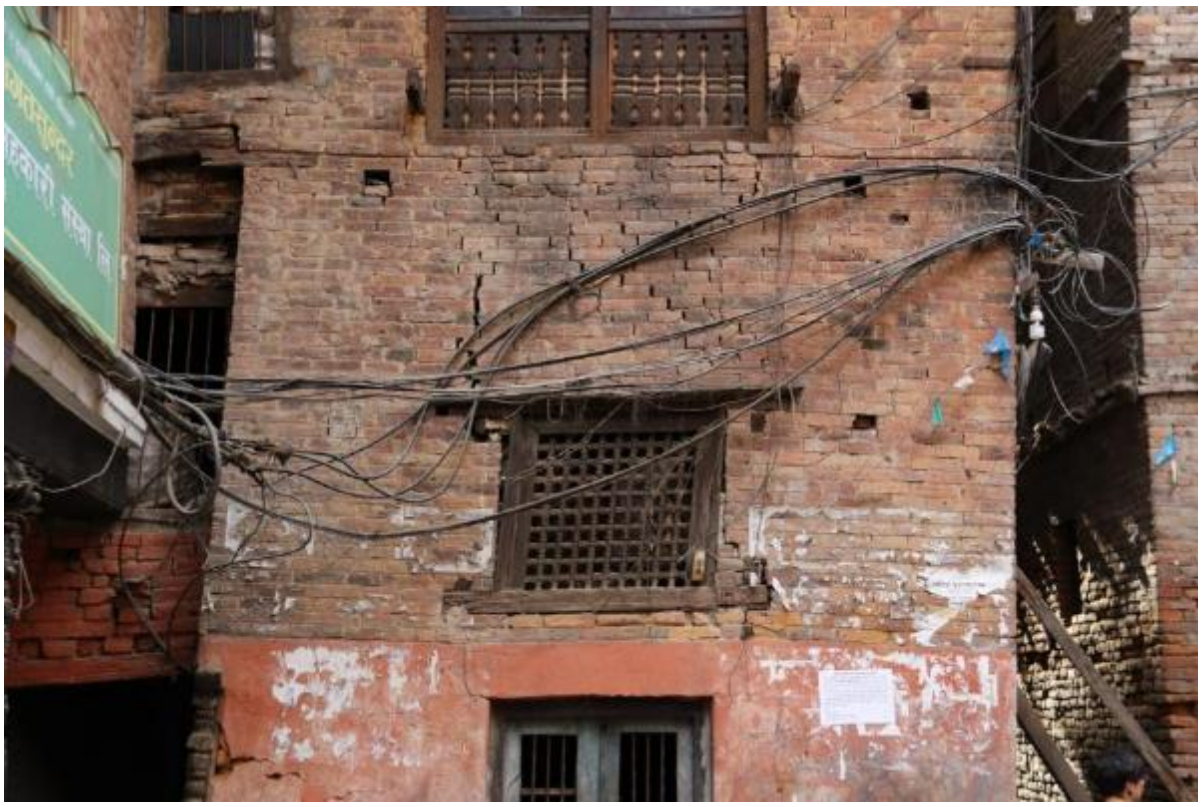

Figure 4-6 Example of In-plane shear failure of a typical Newari residence.

4.3. Temples and Monuments

The damage to temples and monuments was in some cases severe. Several of the temples had collapsed, and all that remained at the time of the EEFIT mission was their pedestals and well-sorted building materials (see Figure 4-7). However, numerous temples remained standing after the earthquake, with differing levels of damage. Anecdotally, the more slender structures were found to have been more likely to collapse, while the stockier temples remained standing which is consistent with the response spectrum of this earthquake (but this trend had notable exceptions).

The temples that remained standing appeared to be built with good materials, exhibited good craftsmanship, and appeared reasonably well maintained. Of these structures, in-plane damage (see Figure 4-8) was the most prevalent, and local out-of-plane failure of elements was rarely observed. This again indicated good connections within the structure. In order to document the damage in more detail, 3D laser scan data (see Figure 4-9) was collected in Kathmandu Durbar Square where extensive damage (but not collapse) had occurred.

Figure 4-7 Pedestal of a temple.
Example of pedestal where a temple used to stand, with well-sorted building materials ready for re-use.

Figure 4-8 Multi-tiered dega.
Example of a multi-tiered dega, or temple (left), which survived the earthquake but exhibited in-plane damage and evidence disconnection at corners (magnified view of top storey, right).

Figure 4-9 Laser scan data for Kathmandu Durbar square
Laser scan data for Kathmandu Durbar square which contains the three-dimensional geometry of damaged structures after the earthquake event.

For smaller monuments, evidence of direct rocking (Figure 4-10) or total or partial overturning (Figure 4-11) was also prevalent. The temple in Figure 4-10 had cracked diagonally in both directions, and showed evidence of toe crushing at the base, both indicative of rocking behaviour. This type of structural behaviour, for a monument of this size, was likely due to the very long period ground motion pulse, which could have generated significant rotational inertia for this structure, which appeared to be well connected. For smaller monuments (Figure 4-11), complete overturning was typical, also a potential result of long-period pulses in the ground motion, where the scale effect causes smaller monuments to be more vulnerable to overturning.) toppling (i.e. complete overturning) was typical, also a potential result of long-period pulses in the ground motion, where the scale effect would cause smaller monuments to be more vulnerable to overturning.

Figure 4-10 Evidence of rocking damage to a temple in Bachtapur Durbar.
Evidence of rocking damage to a temple in Bachtapur Durbar Square in the form of diagonal cracking (left) and toe crushing (middle),and laser-scan image of the damaged structure after the earthquake (right).

Figure 4-11 Evidence of rocking and overturning to monuments.
These base columns were embedded in the ground, so overturning occurred at the first joint above the ground.

4.4. CONCRETE STRUCTURES

There was no observed damage to concrete bridges, and no major bridge damage was conveyed to us in our discussions with local residents. Thus, this section will focus primarily on observed damage to concrete frame structures, most of which contain masonry infill.

The vast majority of concrete frame buildings showed very little or no damage, both in Kathmandu itself and throughout the country (although examples did exist). This was surprising, as the quality of construction varied considerably, and the team expected to see more widespread damage throughout the city. In general, the lack of damage should not be considered as indicative that the construction quality was high, particularly based on discussions that indicated that quality control was often lacking (see Section 3.4). Instead, it should be emphasised that the dominant period of the ground motion (i.e. the portion that significantly exceeded the design spectrum) was approximately 4-5 seconds. This long period motion significantly tested disconnected URM masonry structures, but does not resonate shorter structures that are reinforced (all structures in Nepal are < 20 stories). Thus, the demand placed on most 2-10 story structures in Kathmandu likely did not exceed design values, and these structures may well be more significantly tested in future earthquakes.

4.4.1. Balaju and Siddhitol neighbourhoods

Despite a lack of widespread damage to masonry structures, there were still numerous buildings that had collapsed or experienced very severe damage, and these tended to be concentrated in specific relatively small areas. For example, a large concentration of severe damage was observed in the Balaju and Siddhitol neighbourhoods of Kathmandu. These neighbourhoods are located in the northwest part of the city, adjacent to the Bishnumati river and so site effects may have been significant. The worst damage was observed close to the river in these neighbourhoods, though significant damage was also observed in the Balaju neighbourhood at a slightly higher elevation to the west of the river.

Many of the structures near the river may well have been constructed on made ground, or soft (uncompacted) soils adjacent to the river bed. These structures appeared to have experienced a combination of foundation bearing capacity failure, and soft/weak storey failure at the ground floor. Figure 4-12 exemplifies severe leaning, likely to have been at least partially caused by soil bearing failure. More moderate leaning of several other structures was observed where

the leaning was not accompanied by structural failure adding strength to the bearing failure argument.

Figure 4-12 Exemplifies severe leaning.

Figure 4-13 exemplifies the observed collapses with complete failure of the bottom storeys.

In this structure, reinforcing within the columns on the bottom storeys could be directly observed (see figure), and the shear reinforcing (in particular) appeared to be minimal.

In other locations, bearing capacity failure was less obvious, but soft storey failure was clear. Figure 4-14 typifies one such case, where the magnified view shows complete failure at the base of the ground floor columns. Again, the figure indicates lack of shear reinforcing at this location.

In this same neighbourhood, pounding damage between adjacent structures was also observed (see Figure 4-15). This was a common feature in this earthquake for all building types.

It should be emphasised that the cause of these failures could not be determined definitively, but the position close to the river indicates the potential of poor soil, which could have caused foundation failure as well as local site amplification effects. In addition, many of the failed structures did contain large ground floor openings characteristic of soft/weak stories, and the shear reinforcement in columns did not appear to be substantial (though this was not checked with calculations, and could have been removed prior to observation). Strong evidence of liquefaction was not observed by the team; however one road encountered by the team did seem to have suffered either lateral spreading or liquefaction.

In the Balaju neighbourhood slightly further from the river (up the hill to the west), similar severe leaning was not observed, nor was soft storey failure common. Instead, many structures appeared to be built from poorer materials, and contained upper stories that cantilevered out over lower stories (see Figure 4-16). In these buildings, local failure of cantilever members and extensive out-of-plane failure of brick infill was observed. Numerous structures had also collapsed or had been demolished, so little could be observed at the time of our visit. Based on the top-heavy geometry, it is possible that the concrete frames were inadequate, but this cannot be confirmed without detailed calculations.

Figure 4-12. Examples of combined foundation bearing capacity failure.
Left: Four storey building with soft storey failure. The gap to the right of the building did not exist before the earthquake. Right: Close up view of failure at the base of the right ground floor column.

Figure 4-13 Evidence of pounding damage between adjacent concrete buildings.

Figure 4-14 Examples of top-heavy concrete structures.
Examples of top-heavy concrete structures, where upper floors cantilever out and the concrete frames do not extend to the corners of the building.

4.4.2. Other areas in the Kathmandu Valley

The team also visited the Park View Horizon Apartments in Dhapasi, Kathmandu (see Figure 4-17). The apartments, which were located on a small hill, could only be observed from the outside due to safety concerns. Despite being tall, the natural period of the structure is likely to have been below the 4-5 second peak in the acceleration response spectrum. Although the building appears to be heavily damaged, no structural damage to the reinforced concrete frame was observed by the team from the exterior; however, extensive damage to masonry infill was observed. Of particular note was the dangerous damage that occurred where exterior

corners of the building were not supported by concrete columns. This meant that there was no frame to the infill, and consequently some of these infilled corners had collapsed out-of-plane and fallen to the ground. This would appear to be a detail to avoid in the future.

Other areas of the Kathmandu valley also experienced concentrations of damage, but all of these areas could not be visited by the team. One area that was very badly damaged was the Shankhu neighbourhood (see Figure 4-18). This area was characterised by a greater proportion of residential buildings, and fewer commercial buildings, that were lower rise than in the Siddhitol neighbourhood. This area again exhibited extensive and severe damage to what appeared to be poorly constructed URM structures, and extensive collapse of masonry infill within concrete frames was observed. As was typical with other areas, less damage was observed to the concrete frames themselves, and many of the buildings that were left standing had some degree of concrete framing (see Figure 4-18).

In some instances, local severe damage was observed to individual buildings, while surrounding buildings appeared unaffected by the earthquake. The most striking example of this was the pancake collapse of Morgan College (see Figure 4-19) in the Tokha region of Kathmandu. The seven-storey structure was only a few years old, and it was still standing after the main earthquake but collapsed in an aftershock 45 minutes later.

Figure 4-15 the Park View Horizon Apartments in Dhapasi.
The tallest structure visited by the team was the Park View Horizon Apartments in Dhapasi. The structural frame appeared undamaged from the outside. Typical in-plane and out-of-plane failure of the masonry infill was observed.

Figure 4-16. The Shankhu neighbourhood.
Panoramic view of the Shankhu neighbourhood. The majority of buildings had collapsed or been demolished, with primarily better quality concrete frame buildings still standing.

Figure 4-17 Pancake collapse of Morgan College -7-storey school in Tokha, Kathmandu.

4.5. REFERENCES

Booth, E., Saito, K., Spence, R., Madabhushi G. and Eguchi R. (2011). Validating assessments of seismic damage made from remote sensing. Earthquake Spectra 27, S1, Special Issue on the 2010 Haiti Earthquake, Earthquake Engineering Research Institute, Oakland, CA.

Bjorgo, E., (2010) GIS systems in Haiti. Presentation, Shelter Meeting 10a, 27th May, 2010, Geneva. http://sheltercentre.org/meeting/material/GIS+systems+Haiti+shelter+focus

Beckh, Matthias. 2006. 'Traditional Construction Techniques of the Newars at the Itum Baha Monastery in Kathmandu'. In Proceedings of the Second International Congress on Construction History, 1:325–39. Queen's College, Cambridge, UK: Short Run Press.

Blair, Katherine D. 1983. 4 Villages: Architecture in Nepal. Craft & Folk Art Museum.

Bonapace, Caterina, and Valerio Sestini. 2003. Traditional Materials and Construction Technologies Used in the Kathmandu Valley. Paris: UNESCO.

D Ayala, Dina. 2003. 'A Summary of the Report Seismic Vulnerability of Historic Buildings in Lalitpur, Nepal'. Earthquake Hazard Centre Newsletter 7. http://discovery.ucl.ac.uk/1379675/.

D'Ayala, Dina. 2004. 'Correlation of Fragility Curves for Vernacular Building Types: Houses in Lalitpur, Nepal and in Istanbul, Turkey'. In . Vancouver Canada: University of Bath. http://opus.bath.ac.uk/661/.

DoA. 2007. 'Kathmandu Valley World Heritage Site: Integrated Management Framework'. GoN, UNESCO.

Korn, Wolfgang. 1976. The Traditional Architecture of the Kathmandu Valley. Vol. 11. Bibliotheca Himalayica, III. Kathmandu: Ratna Pustak Bhandar.

Krüger, Fred, Greg Bankoff, Terry Cannon, Benedict Orlowski, and Schipper, eds. 2015. Cultures and Disasters: Understanding Cultural Framings in Disaster Risk Reduction. New York, NY: Routledge.

Romão, X., E. Paupério, and A. Menon. 2015. 'Traditional Construction in High Seismic Zones: A Losing Battle? The Case of the 2015 Nepal Earthquake'. In Seismic Retrofitting: Learning from Vernacular Architecture, edited by Mariana R. Correia, Paulo B. Lourenço, and Humberto Varum, Pap/Com edition, 93–99. S.l.: CRC Press.

Shrestha, Bal Gopal. 2012. 'The Significance of Newar Culture and Society'. In The Sacred Town of Sankhu: The Anthropology of Newar Ritual, Religion and Society in Nepal, 21–41. Newcastle: Cambridge Scholars Publishing.

5. GEOTECHNICAL ASPECTS (INCLUDING LANDSLIDES)

With steep slopes and deep sedimentary basins, Nepal has a clear predilection towards the most dangerous of onshore, geotechnical hazards. Both site effects and landslides have proven devastating to different communities in recent earthquakes (e.g. EEFIT 2009, 2011; Wilkinson et al. 2009). Thus, investigation into both these hazards was a priority for the mission.

For the rural communities, landslide & rock falls were reported to have had devastating consequences both during and following the earthquake. While not affecting resident communities, the most widely reported example being the avalanche on Mt. Everest which claimed at least 17 lives (Aydan and Ulusay 2015); however, this was not the most fatalities caused be a slip event. In rural hill communities, structural collapse was not reported to be the main cause of fatalities as many people were employed on the land and out of their homes. However, in the worst cases, landslides completely destroyed communities or at least cut off their main access routes. This has hampered rescue efforts (Goda *et al.* 2015), the only feasible route available being by air. Rock falls too had immediate damaging effects, for example, a bus was crushed by a boulder during the earthquake (Figure 5-1). Further details of landslide effects can be found in the landslide section.

Figure 5-1 Avalanche, landslide and rock falls.
(a) Avalanche reaching Everest Base Camp killing at least 17 people and injuring 61 more (Aydan and Ulusay 2015) (b) Damaged caused to a bus having been hit by a rock fall (Goda *et al.* 2015).

In the Kathmandu Valley a similar devastating picture was expected. The City of Kathmandu is founded on a Pleistocene lake bed similar to Mexico City. This was almost completely destroyed in 1985 by a $\mathbf{M_w}$ 8.1 earthquake, despite its epicentre being located more than 350 km away (Booth *et al.* 1986). Formed of heterogeneously layered clays, silts and sands, the Kathmandu Basin reaches over 500 m deep cross-section (Figure 5-2) and, because of the thick layers of soft sediments, it has been a concern to previous investigations (Piya 2004). Though boreholes have been drilled in the area, it is often difficult to link the deposits, partly as little testing has been carried out to determine the engineering characteristics and partly due to the fact that many are localised (Bhandary *et al.* 2014). Thus, strong shaking was expected in the valley and much damage had been predicted by most PSHA models (e.g. USGS 2015).

However, preliminary investigations found this was not the case. Goda *et al.*'s (2015) initial report noted devastating structural damage had occurred to the central historic buildings, but surrounding these the majority of the new buildings were structurally stable (Figure 5-3). It is speculated that due to the low-midrise nature of the buildings with a natural frequency of less than 1Hz, many escaped damage from the longer vibration periods the earthquake produced. In addition, the most critically damaged areas were localised conspicuously close to areas

around rivers and near to the edge of the basin. Site effects had been strongly implicated, but not conclusively determined (Goda *et al.* 2015).

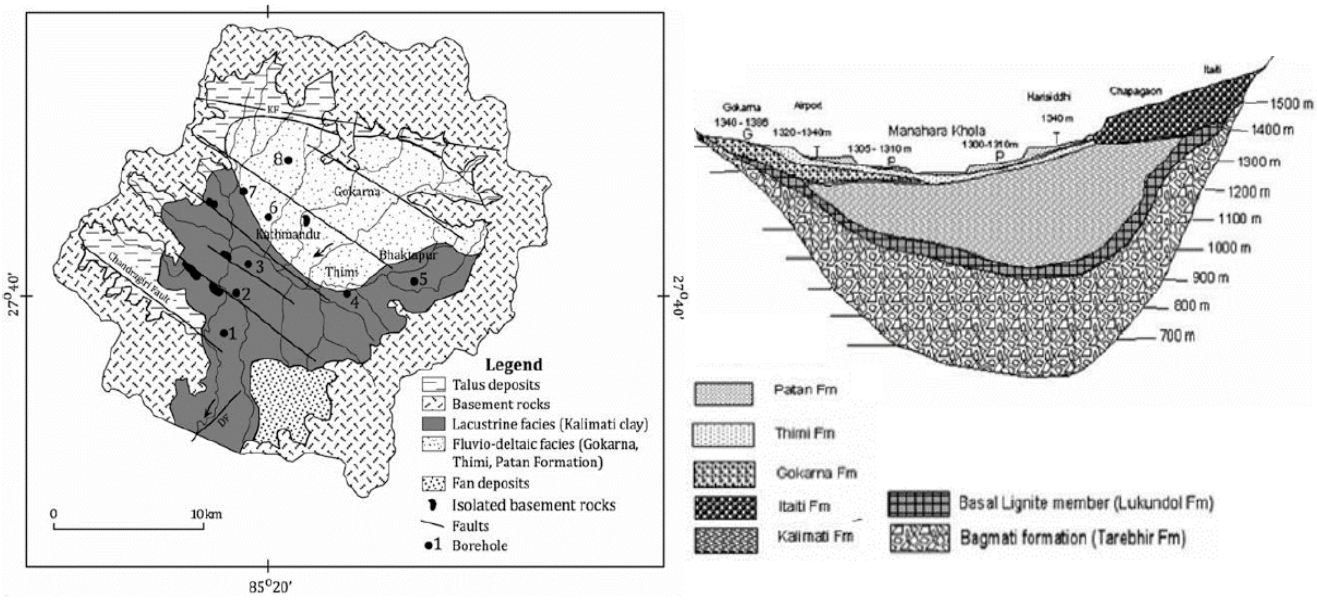

Figure 5-2 Geology of the Kathmandu Valley.
This is formed of soft sediments from the surrounding hills and has high potential for site effects, liquefaction and basin effects (Aydan and Ulusay 2015).

Figure 5-3 Damage in Durbar Square.
Much of the debris had been removed at the time of survey, but the front wall of the building had collapsed and in the background the white building had suffered severe shear cracking. (Left) View of Central Kathmandu. Structures probably damaged but still erect. Temple in the background with chimney remained standing (Right).

Due to the soft sediments of the valley, Kathmandu has high liquefaction potential, especially in the North Western and Central regions. The areas of high susceptibility follow the four major rivers in the valley (Piya 2004). During the survey, liquefaction had been found to occur during the earthquake, particularly in the region of Imadol (Figure 5-4) where lateral spreading is clearly visible.

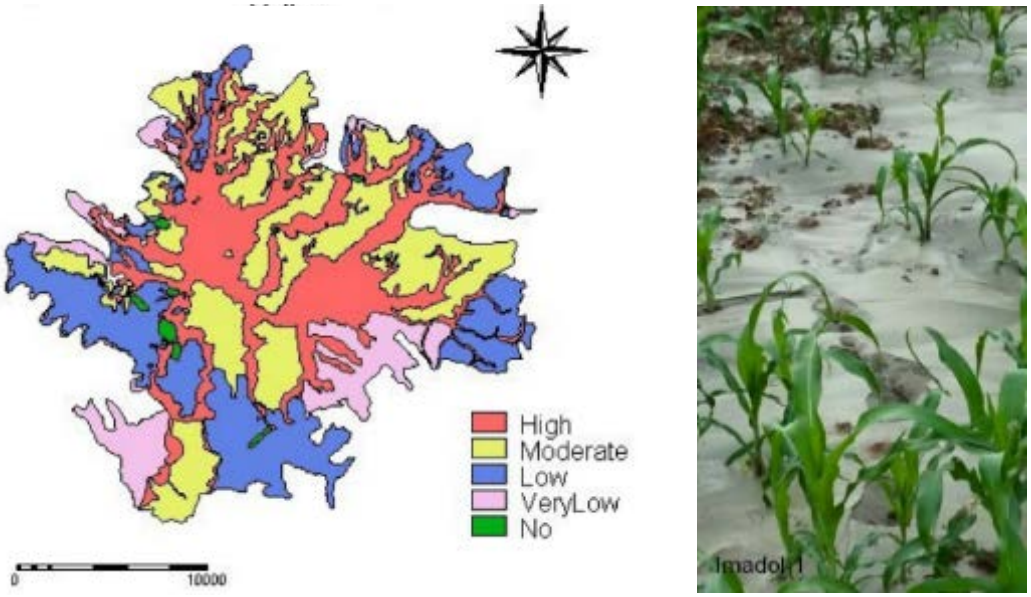

Figure 5-4 Liquefaction susceptibility for the Kathmandu Valley.
(Right) Piya's Map of Liquefaction Susceptibility for the Kathmandu Valley (2004) (Left) Liquefaction in the Imadol Region (Aydan and Ulusay) Agricultural land had been reported to be most affected by liquefaction (Right).

Several major pieces of infrastructure had settled significantly during the earthquake, for example a road embankment in the Araniko Highway at the edge of Kathmandu (Figure 5-5) and several dams including a hydroelectric power dam in Trishuli (Goda *et al.* 2015). Before the mission, it remained unclear how many foundation collapses had been implicated. Although there were several reports of utility, poles having suffered foundation collapse (Figure 5-5).

Figure 5-5 Infrastructure settled during the earthquake.
Settlement damage to Araniko Highway (Goda *et al.* 2015) (Left). Foundational Collapse of a utility pole (Aydan and Ulusay 2015) (Right).

In addition to examining geotechnical structure failures, the team aimed to investigate the extent of site effects including site amplification, liquefaction and topographical effects. It was also hoped to provide preliminary, but quantitative parameters, which would aid in initial PSHA for the earthquake.

5.1. Geotechnical Structures

The Nepalese Code is based on the Indian Standards for the design of foundations (NBC 1994b) possibly making them less clear and accessible compared to the rules of thumb provided in the structural codes. Indeed, there does not appear to be a specific section in the codes for foundations and other geotechnical structures, apart from the referencing of the relevant Indian Codes. In some cases this is fairly intuitive, for instance where the designs of pad foundations are included in the masonry code (NBC 1994a). However, the emphasis of good building practice is placed firmly on the structural aspects, which is echoed throughout the country, despite their extremely difficult ground conditions.

During the mission, the contribution of foundation failure was difficult to assess. Although in urban communities foundations for high-rise buildings, such as piles, were expected, in the rural communities it was often difficult to determine if foundations were present (Figure 5-6a and b). Yet, there were some clear signs of improvement with larger new buildings in rural areas appearing to have at least pad/strip foundations (Figure 5-6d).

Figure 5-6 Failure of buildings that could be related to the foundation.
(a) Rural building with base exposed, showing the difficulty in determining if foundations are present. (b) Failure of a reinforced concrete building likely to have been caused (or at least exacerbated) by liquefaction. (c) “Foundations” appearing to have come away from the soil; however this is a soft storey collapse with “foundations” actually being first floor. (d) Damage to floor slab, observed from road level, however, this is not the foundation of the building which can be seen two storeys below.

Most buildings, which had potentially suffered damage, due to foundation failure, were either deemed too dangerous to enter or had collapsed to the extent where it was not possible to determine the failure mechanism. Collapses, initially appearing to be foundation related, were often, after closer inspection, found to be related to other mechanisms. For example, slope failure appeared to have caused the building to move downslope (Figure 5-6b). Alternatively, several failures at road level were found to be structural rather than foundational, because the true base of the building was located some storeys below downslope (Figure 5-6d). In some cases, soft storey collapse had occurred where “foundations” appearing to have come away from the soil were actually an upper floor (Figure 5-7c).

The damage to the Araniko Highway was seen by the mission, but little could be added to the study of Goda *et al.* (2015) and the GEER reconnaissance team (Hashash *et al.* 2015), both covered this in detail. Several retaining walls were also seen on the main highway to Gorkha. Though these seemed in good repair, heavy building works were being carried out on them at the time of the mission. Thus, it was not possible to discover whether these had been built prior to the earthquake.

5.2. Site Effects

The Nepalese Building Code does give some guidance about siting the location of buildings to avoid site effects (NBC 2015b). This focuses particularly on liquefaction and topographical effects or slope instability. However, the documentation is brief. For example, in the liquefaction section, liquefaction is described and areas where it generally occurs identified (NBC 2015b), but, although mitigation measures are endorsed, no further details of what these could be or recommendations of further information given. Site amplification, liquefaction and topographical effects were all investigated by the mission and the results are presented below.

The team's assessment of site effects was limited by the lack of seismic recordings of the main shock. Though several instruments are known in the area, at the time of writing, only one recording, from the KATNP station, has been made publicly available. This prevents the team correlating damage patterns seen during the mission with potential site effects shown in the recordings. This highlights the importance of the installation of strong ground motion instruments in actively seismic regions as well as ensuring their maintenance.

5.2.1.Site amplification

Site amplification is the increase of the shaking experienced at the surface by the deposits in the near surface. Four areas in the Kathmandu Valley were investigated for site amplification during the mission, Figure 5-7. These surveys included testing with microtremor equipment - a non-invasive, passive, geophysical method that uses a digitalised seismometer to measure the components of elliptical, surface waves already within the ground. Using Nakamura's H/V method (1989), the ratio of the horizontal to vertical components can yield a peak at the lower limit of the fundamental frequency of the site. If this is further constrained by the thickness of the first layer of the soil, the shear wave profile can be calculated.

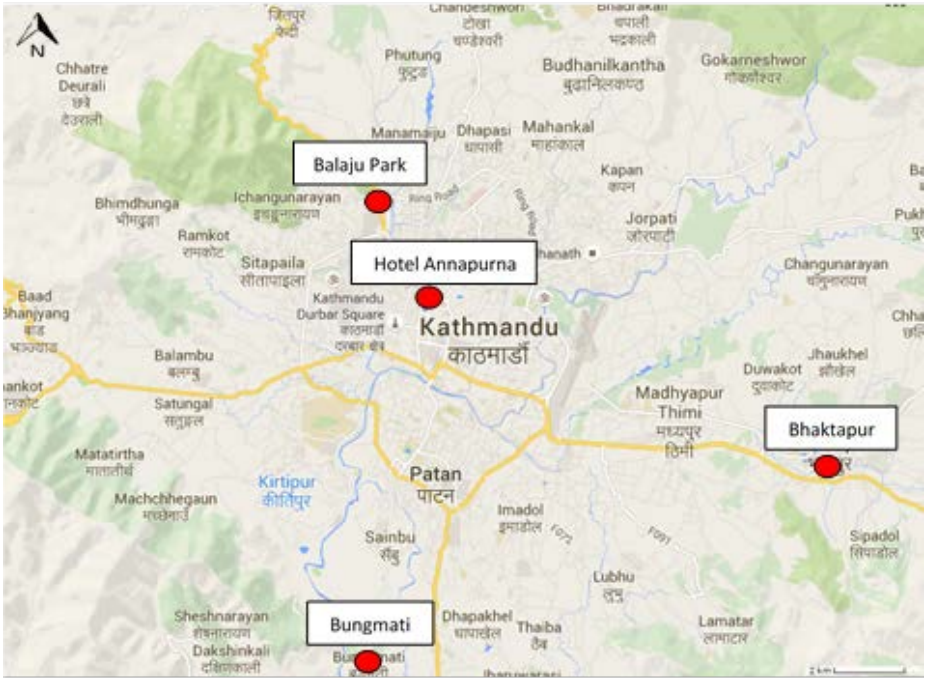

Figure 5-7 Areas investigated for site effects in the Kathmandu Valley
Adapted from Google Maps 2015.

The microtremor equipment was chosen for its flexibility. It is light and portable, while the measurements are of short duration. In addition to single site recordings, a number of measurements could be taken in a traverse allowing the pseudo seismic stratigraphy and the likely conditions of the deposits to be analysed.

However, this method is not without its limitations. It depends on surface waves within the ground from natural sources, which can be obscured by human interference, especially at higher frequencies which reveal the near surface. There was a significant amount of made ground in the valley which led to velocity inversions causing difficulties in processing and again obscured near surface data. Limited measurements could be made in the duration of the mission and those that were, should be constrained more fully by borehole data. Single readings contain larger uncertainty than transects due to inherent soil variability, but also due to human disturbance as they were more likely to be near people's homes. Thus, the results obtained are preliminary and should be used with caution.

The testing was conducted with a Tromino Zero instrument, kindly donated for the mission by Micromed Geophyscis (2013b), Figure 5-8. It was carried out according to Site Effects Assessment using Ambient Excitations (SESAME) guidelines (2004) to the best of the team's ability, given the difficult nature of the environment and the team's safety. All measurements were located in quite confined areas and so for the traverses, single stations measurements were carried out every 5 m. The data from testing were processed using Mircomed Grilla Software (Micromed 2013a).

Figure 5-8 Testing was conducted with a Tromino Zero instrument.
(L) Spot reading being taken by Tromino outside collapsed home in the Balaju region. Transect being carried out with Tromino in Balaju Park around 200 m from the collapsed home (C). Team members taking GPS reading for the Tromino measurement in Bhaktapur, close to the main temple collapses (R).

a) Results

Each of the areas suffered different damage patterns. In Siddhitol, where Balaju Park is located (Figure 5-9), the damage was in parts universal both to masonry buildings and reinforced concrete as well as high-rise and low-rise buildings. In Bhaktapur, the damage was again extensive, but variable. Buildings that had remained standing were often adjacent to collapsed ones. This was similar to the case in Bungmati, though possibly Bungmati had a larger proportion of full collapse. In the centre of Kathmandu, near the American Embassy (Foreign Consulate Club) and the Hotel Annapurna, the damage was more conservative.

Though the older masonry buildings of Durbar Square were critically damaged, the reinforced concrete in this region was affected, but repairable.

For the Balaju Park traverse in Siddhitol, the main hard layer, thought to be bedrock, was detected at approximately 27 m, Figure 5-9a. It is indicated to be dipping in the southern direction. This layer was underneath a thick deposit of lower impedance material. Although there was some disturbance in the near-surface, this is thought to be caused by a man-made drain, running close by, rather than significant layering in the material. However, in the Hotel Annapurna traverse (Figure 5-9b), the hard rock appeared over 40 m in depth. The rock is suspected to be located at over 100 m depth, but due to significant weathering and an inversion at the near surface this would need to be further confirmed.

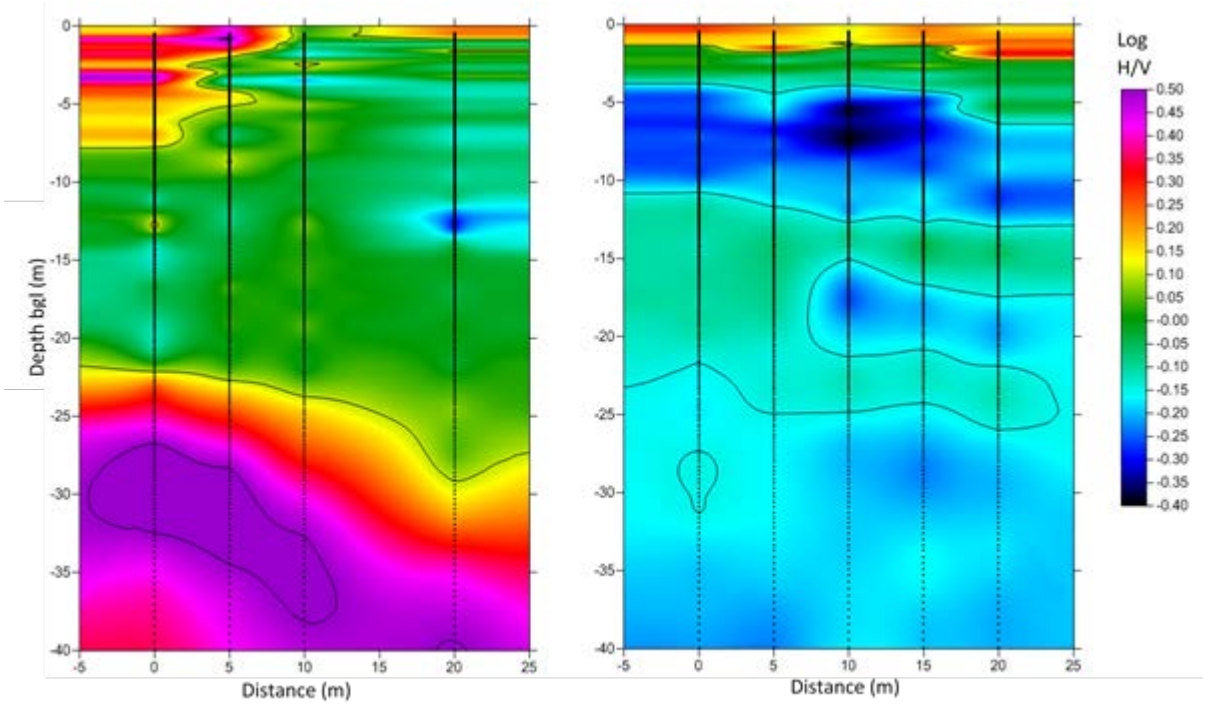

Figure 5-9 Logarithmic impedance ratio.
Graphical representation of the logarithmic impedance ratio for (L) Balaju Park and (R) Hotel Annapurna. Purple & red represent a stiff rock ranging to blue, which represents a less stiff more soil like structure.

AREA	INDICATED DEPTH TO BEDROCK	H/V FUNDAMENTAL FREQUENCY	V_{S30}	EUROCODE SITE CLASS (EN 2004)	RELIABILITY
Hotel Annapurna near American Embassy (KATNP)	>100m	0.31 Hz +- 0.13	305 m/s	C	Inversion in near surface may obscure effects on V_{S30} of near-surface soil column.
Balaju Park, Siddthol	~27m	2.65 Hz +-0.26	304 m/s	E	Layer at 27m considered to be bedrock but would need to be confirmed.
Bhaktapur	>250m	0.43 Hz +- 0.07	205 m/s	C	Only single recordings, no traverse.

Table 5-1 Preliminary results from microtremor measurements.
It should be noted that H/V fundamental frequency is a lower limit of the body wave fundamental frequency.

The depth to the hard rock has a large effect on the fundamental frequencies of these two sites, Table 5-1. When compared to the record of the spectral acceleration at KATNP station,

Figure 5-, the period for the Balaju Park matches a region of high acceleration, while the Hotel Annapurna traverse and the readings from Bhaktapur do not. Thus, it is likely that the area around the Balaju Park experienced strong shaking caused by site amplification and would be a good area for further investigation.

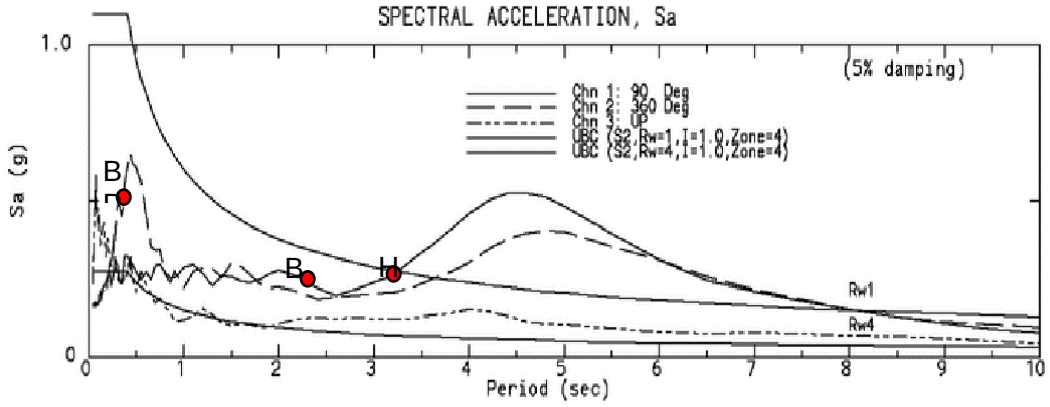

Figure 5-10 Strong motion data.
Center for Engineering Strong Motion Data (2015) 5% damped spectral accelerations (SA) determined from the acceleration recordings of KATNP. Fundamental frequencies of Balaju Park (BP), Bhaktapur (BH) and Hotel Annapurna (HA), plotted at maximum acceleration. As the Hotel Annapurna is located in the centre of the valley, the soil may not have been deep enough to resonate with the peak of the earthquake spectrum.

Though the region around the Hotel Annapurna may not have experienced site effects, the traverse was conducted there to model a time averages shear wave velocity for the top 30m of ground (V_{s30}) for the KATNP station. This is located in the American Embassy Foreign Consulate Club, to which the team could not unfortunately gain access. The transect that could be carried out was located approximately 100 m from the KATNP station which was the closest area of green land that could be found, located on the Hotel Annapurna grounds.

There were two difficulties with this location, the most notable being the layer of hard ground at the surface, possibly man-made. This caused an inversion in the record making the processing much more difficult and obscured near surface frequencies. The second was that a drill was being employed nearby which caused difficulties with the vertical trace. However, a preliminary result of 305 m/s was obtained, Table 5-1. This is consistent with work from Goda *et al*. (2015) and Bhandary (2014), the latter of which is based on borehole information. However, the near surface part of the record was obscured and further resonances, recorded by Paudyal *et al*. (2012) in the soil column may not be visible.

In Bhaktapur and Bungmati, the evidence was less clear. These regions had fewer areas of green space accessible around the damage buildings, so only short spot checks could be carried out in the short time available. These revealed the soil was also deep in these areas. Bhaktapur has seemed to have around 250 m of low velocity deposits. The Bungmati trace had similarly deep deposits, however, it did appear to have some intermediate layers. The shear velocities of the materials in the profiles from these sites were notably closer to that of Siddthol region, than central Kathmandu. However, the fundamental frequencies recorded in these regions were similar to that of the Hotel Annapurna tests and so it is thought site amplification had less of a role in these regions.

5.2.2. Liquefaction

Liquefaction is the reduction of strength and stiffness of a soil caused by earthquake shaking, which often results in the loss of the soil's capacity to bear load. The GEER team had recorded liquefaction throughout the Kathmandu Valley, mainly close to parks or agricultural land (Hashash *et al.* 2015). There was also considerable interest around the Bishnumati River. Located in the Siddthol region, it was speculated that the large number of housing collapses by the river had been caused by liquefaction as many had appeared to fail at the base of the structure, Figure 5-11.

Figure 5-11 Fail at the base of the structure.
(L) Building close to the banks of Bishumati River, near Goabu Bus Park, which has appeared to fail at the base of the structure. (R)Tromino spot check next to complete building collapse (around 4 storeys) of a reinforced masonary building on opposite side of the Bishnumati River. Building behind can also be seen to be tilted at the base.

A short traverse was carried out on the river bank which showed the bedrock to be around 30 m in depth. Similar to the deposits found in Balaju Park, the near-surface material was found to have a slightly higher impedance and to be more layered. This would be more consistent with a sand/gravel-like material.

There were no clear signs that liquefaction had taken place with no ejected material or lateral spreading seen, even in the open market place by the river bank. Though this could have been concealed by the significant layer of made ground which appeared to be around 7 m thick from the riverbank. In addition, as the earthquake happened at the end of the dry season, there was very little to no moisture in the upper few metres of the ground preventing liquefaction near to the surface. Many buildings had collapsed at the base of the structure in this area, but it was not possible to determine if this was foundational or structural collapse.

A simplistic, quantitative liquefaction potential calculation was carried out using Seed *et al*.'s method (2003). This assumed the water table was located at 9 m depth which was the level observed of the river and used the V_s to SPT correlations of sandy alluvium of Towhata (2008) and PEER (Wair *et al.* 2012). This gave values for the cyclic resistance ratio (CRR)/ cyclic stress ratio (CSR) of approximately 0.5 over the top few meters of saturated ground. This suggests that liquefaction should have occurred, though it should be noted this was carried out after the earthquake at post-earthquake density of the soil.

This location is an interesting contrast with the previously recorded locations of liquefaction in the Kathmandu Valley. Most of these appear to be on more natural ground which is less likely to have the made ground "crust" over the surface. This phenomenon has been commented on in studies before (e.g. Wotherspoon *et al.* 2013) and could warrant further investigation.

During the mission, it was observed that housing located on the steep topographical ridges fared worse than those in flatter areas. This was particularly noticeable in the region of Dolalghat, Chautara, to the East of Kathmandu. In this region, numerous ridge top communities had been almost completely destroyed, while those in the valley floors beneath remained standing, if damaged.

Initially, this was thought to have been caused by topographical site effects. Ridges have been known to focus waves, causing much larger ground acceleration experienced at the peak (e.g. Hough *et al.* 2010). These effects could have been compounded by the soil on the ridge tops. The surface deposits were found to be poor and surprisingly deep to reach engineering bedrock. From exposures in Dolalghat, the soil was at least a few metres in depth, Figure 5-12, while in Gorkha, a preliminary microtremor recording indicated that there could be up to 10 m of superficial deposits. Significant lack of foundations too was observed. However, these were not enough to explain the extent of the damage, particularly in Gorkha, the majority of damaged buildings were on slopes beneath the ridge top.

Figure 5-12 Exposures within villages of Dolalghat region.
Soils were found to be clayey and containing angular pebbles, suggesting colluvial deposits.

General guidance in national building codes for buildings on slopes is to avoid them (e.g. CEN 2004). Yet with 78% of Nepal's landmass being based on hilly or mountainous land (Pariyar 1998), this is unrealistic for the local inhabitants. The Nepalese codes give offsets from slope tops and bottoms to try to avoid slope instability (NBC 2015a). However, with rising populations and increased migration from villages to towns, many are forced to build on unstable hillslopes (Singh *et al.* 2015).

The team observed several types of failure specifically associated with 'hilly' construction (Singh *et al.* 2015). The main issue was the irregularity of the shape of the buildings in order to take into account the slope. Thus, failures included collapse of the columns located downslope and soft storey probably attributable to reduced ductility within the irregular building shape, Figure 5-13.

Figure 5-13 Building failures of Dolalghat region.
(L) Downslope column collapse First storey collapse, yellow, supporting column can be seen on the left. (C) Likely caused by ductility changes in the irregular structure. (R) Rebar and stirrups visible in the column.

Yet it could not be said these buildings were non-engineered. Many were observed to contain seismic detailing particularly in the rebar, with deformed bars for longitudinal and confining reinforcing at approximately 100 spacing, Figure 5-13 and several newer construction also had improved concrete material. The local inhabitants too showed a keen interest in improving the building styles and new buildings were seen to have some foundations, uncommon for more rural areas.

It can only be concluded that the building codes are failing these communities by not providing them safe design practices. As urbanisation increases in these seismically vulnerable, mountainous regions, this could be an area of research that could have significant, beneficial impact.

5.3 REFERENCES

Aydan, O. & Ulusay, R. (2015) *A Quick Report on the 2015 Gorkha (Nepal) Earthquake and its Geo-Engineering Aspects.* IAEG. [Online] Available from www.iaeg.info [Accessed 26/09/15]

Bhandary, N.P., Yatabe, R., Yamamoto, K., & Paudyal, Y.R. (2014) Use of a Sparse Geo-Info Database and Ambient Ground Vibration Survey in Earthquake Disaster Risk Study- A Case of Kathmandu Valley- Journal of Civil Engineering Research 4(3A): 20-30

Booth, E.D., Pappin, J.W., Mills, J.H., Degg, M.R. & Steedman, R.S. (1986) *The Mexican Earthquake of 19th September 1985. A Field Report.* London: EEFIT.

CEN (2004a). EN 1998-1, Eurocode 8—design of structures for earthquake resistance, part 1: general rules, seismic actions and rules for buildings. European Committee for Standardization, Brussels.

Centre for Engineering Strong Motion Data (2015) *CESMD Strong-Motion Data Set* [Online] Available from www.strongmotioncenter.org [Accessed 26/09/15]

EEFIT (2011) The Christchurch, New Zealand Earthqauke of 22 February 2011. An EEFIT Field Report, London, ISTRUCTE.

Goda, K., Kiyota, T., Pokhrei, R.M., Chiaro, G., Katagiri, T., Sharma, K. & Wilkinson, S. (2015) *The 2015 Gorkha Nepal Earthquake: insights from earthquake damage survey. Front. Bullt. Environ.* 1:8.

Google Maps (2015) [Online] Available from www.google.com [Accessed 26/09/15]

Hashash, Y.M.A., Tiwari, B., Moss, R.E.S., Asimaki, D., Clahan, K., Kieffer, D.S., Dreger, D.S., Macdonald, A., Madugo, C.M., Mason, H.B., Pehlivan, M., Rayamajhi, D., Acharya, I. & Adhikari, B. (2015) *Getechnical Field Reconnaissance: Gorkha (Nepal) Earthquake of April 25 2015 and Related Shaking Sequence.* Geotechnical Extreme Event Reconnaissance. GEER Association Report No. GEER-040 Version 1.1.

Hough, S.E., Altidor, J.R., Anglade, D., Gven, D., Janvier, M.G., Maharrey, J.Z., Meremonte, M., Mildor, B.S.L, Prepetit, C. & Yong, A. (2010) *Localised damage caused by topographic amplification during the 2010 M7.0 Haiti earthquake. Nature Geoscience* 3, 778-782.

MICROMED (2013a) *Grilla ver 6.4., spectral and HVSR.* Treviso, Italy: Micromed.

MICROMED (2013b) *Tromino.* [Online] Available from: www.tromino.eu [Accessed 16/10/14].

Nakamura, Y. (1989) Method for dynamic characteristics estimation of subsurface using microtremor on the ground surface. Quarterly Report of RTRI (Railway Technical Research Institute) (Japan), 30(1), 25-33.

NBC (1994a) NBC 109:1994 *Masonry: Unreinforced.* Kathmandu Nepal, Ministry of Physical Planning and Works, His Majesty's Government of Nepal.

NBC (1994b) NBC 108:1994 *Site Consideration for Seismic Hazards.* Kathmandu Nepal, Ministry of Physical Planning and Works, His Majesty's Government of Nepal

Pariyar, D. (1998) Country Pasture/Forage Resource Profiles. Food and Agriculture Organisation of the United Nations [Online] Available from www.fao.org [Accessed 30/07/2015]

Paudyal, Y.R., Yatabe, R., Bhandry, N.P. & Dahal, R.K. (2012) A Study of local amplification effect of soil layers on ground motion in the Kathmandu Valley using microtremor analysis. Earthquake Engineering and Engineering Vibration 11: 257-268

Piya, B.K. (2004) *Generation of a Geological database for the Liquefaction Hazard Assessment in the Kathmandu Valley.* MSc Dissertation. International Institute for Geo-Information and Earth Observation, Netherlands.

Seed, R. B., Cetin, K. O., Moss, R. E., Kammerer, A. M., Wu, J., Pestana, J. M., Riemer, M.F., Sancio, R.B., Bray, J.D., Kayen, R.E. & Faris, A. (2003) *Recent advances in soil liquefaction*

engineering: a unified and consistent framework. Report No EERC 2006-06, University of California, Berkeley.

SESAME (2004) Guidelines for the implementation of the H/V spectral ratio technique on ambient vibrations: Measurements, Processing and Interpretation. Deliverable D23.12. SESAME European Research Project WP12.

Singh, Y., Lang, D.H. & Narasimha, D.S. (2015) Seismic Risk Assessment in Hilly Areas: Case Study of Two Cities in Indian Himalayas. In: SECED 2015 Conference: Earthquake Risk and Engineering towards a Resilient World. 9-10 July 2015 Cambridge, UK

Towhata, I. (2008) Getechnical Earthquake Engineering (Springer Series in Geomechnics and Geoengineering), Springer Science & Business Media.

USGS (2015) *PAGER:M7.8-36km E of Khudi, Nepal* [Online] Available from earthquake.usgs.gov [Accessed 26/09/15]

Wair, B., DeJong, J.T. & Shantz, T. (2012) *Guidelines for Estimation of Shear Wave Velocity Profiles*. PEER Report 2012/09. Pacific Earthquake Engineering Research Center Headquarters, University of California.

Wotherspoon, L.M., Orense, R.P., Green, R.A., Bradley, B.A., Cox, B.R. & Wood, C. (2013) Analysis of liquefaction characteristics at Christchurch strong motion stations. New Zealand-Japan Workshop on Soil Liquefaction during Recent Large-Scale Earthquakes. December 2-3, 2013. DOI: http://hdl.handle.net/10092/8997

6. EDUCATION AND HEALTHCARE FACILITIES

6.1 Introduction

This section details key findings from visits to six schools consisting of 25 buildings in total, including some (both temporary and permanent) built in response to the earthquakes. An additional school serving a remote mountain community was also visited and this is included in Chapter 7. Key findings are based upon visual observation, where possible additional data was gathered through conversation with teachers or other school staff. A meeting with NSET provided valuable information with regard to damage assessments, local construction practice and activities before the earthquake. NSET[1] are a well-respected Nepalese non-govermental organization (NGO) focusing on seismic risk reduction since 1996, including for the education sector.

Figure 6-1 School sites visited.
Two schools were visited on the outskirts of Kathmandu in close proximity to each other,

6.1.1 Key findings

- **Rapid Visual Assessments**

By mid-June Rapid Visual Assessments had been conducted at all schools in the 14 affected districts, with approximately 50% deemed 'affected'. The impact of the earthquake in terms of injury and loss of life was thankfully minimised by the timing, as it struck on a Saturday when the schools were closed. These assessments were based upon a slightly adapted version of ATC-20, which was developed by NSET. The purpose was to determine whether or not a building was safe to re-occupy in the short term with Red and Green flags issued accordingly. Importantly these were issued as plastic flags that were tied to buildings, giving a clear visual indication of the recommendation. Yellow flags, as also included in ATC-20 as an intermediary category, were not used in these assessments. NSET played a key role in the process having provided training to local engineers as well as conducting assessments themselves.

[1] http://www.nset.org.np/nset2012/

Eleven of the buildings visited were flagged red (55%), five were flagged green (25%) whilst four did not have an observable flag (20%). Four of the buildings visited were built after the earthquake and did not have a flag. The assessments appeared to be broadly accurate, with the exception of two red tagged RC frame with fired clay masonry buildings. In this case the only damage appeared to be hairline cracking of plaster. This suggests that a minority of assessments may be overly cautious in their recommendations. Whilst it is unsurprising that those conducting the assessments might err on the side of caution this serves to place additional strain on the recovery process in terms of demand for temporary classroom space.

- **Structural Typologies**

School Building structural typologies are a loose function of year of construction and of geographic location, or ease of access. Use of concrete and fired clay bricks have increased with time in urban areas, but remain largely unavailable in rural and remote locations where stone rubble with mud mortar is widely used instead. All of the RC framed buildings visited were located in urban areas such as Kathmandu Valley or the town of Gorkha whilst all of the stone rubble buildings were in rural areas. Fired clay masonry was more evenly spread. The only adobe building visited (Figure 6-3) was built before 1970 and had been retrofitted by NSET.

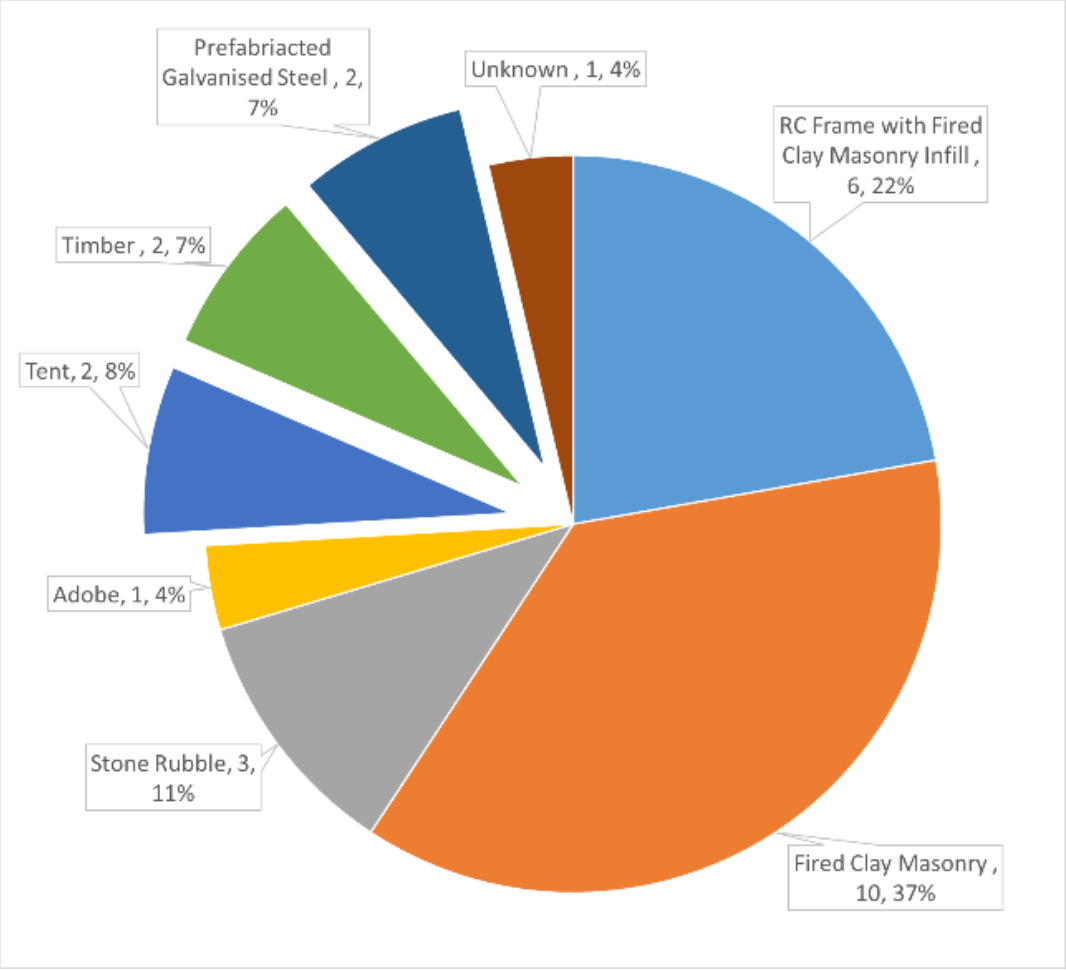

Figure 6-2 Structural typologies of the school buildings visited.
Pie chart illustrating structural typologies of the school buildings visited, extracted segments indicate buildings constructed in response to the earthquake

Fifteen (60%) of the school buildings visited were single storey, eight (30%) had two stories with a single three storey and a single four storey building. NSET reported that schools where additional stories had been added after construction had performed poorly, indicating either inadequate design of the extension or of the connection between the new and the existing

structure. They were hopeful that legislation to prevent this practice would be drafted in the future. Building plans were typically rectangular, although 'C' and 'L' formations were observed at larger schools. Seismic movement joints were sometimes included.

6.2.3. Building Performance

- **Retrofit**

NSET reported that they had been involved in the retrofit of 200 schools in the last five years at an approximate cost of 80USD/m^2. Two of the school buildings visited had been retrofitted, one was adobe block and the other fired clay brick (Figure 6-4). Both survived undamaged and were rated green. The adobe building retrofit scheme was designed by NSET. The fired clay brick retrofit was designed by a private consultant and then reviewed by NSET. Encouragingly NSET reported that all of the school buildings they had retrofitted had survived without damage, except for one where the foundations had failed.

Figure 6-3 Adobe building with 2014 retrofit solution designed by NSET.

Steel beams were installed under sagging floors whilst walls were jacketed on both sides with a mesh of steel bars @200mm c/c (tied through the wall) covered with cement render. The building survived undamaged, with green flag tied to the front.

Figure 6-4 A fired clay brick building retrofitted.

A fired clay brick building retrofitted by a private consultant, with the design approved by NSET. Seismic band beams are added either side of the walls. Consisiting of reinforcement and concrete they are tied together through the walls. The building performed well incurring no damage (R) – Internal view of seismic bands running vertically either side of openings and at cill level. The discreet nature of the band beams means this is likely to be a more economical retrofit that the full jacketing NSET design.

- **Reinforced Concrete Frame with Fired Clay Infill**

Of the six RC framed buildings two were green flagged and 4 were red flagged. Both green flagged buildings had incurred no visible damage, one of which had been designed by NSET and constructed in 2012 with funding from an international donor. There was limited evidence of seismic design in the other five, which exhibited varying degrees of cracking and collapse of non-structural fired clay brick infill. At the four storey school (Figure 6-5) severe damage of beam/column joints was observed as well as damage to the base of the columns and cracking of masonry walls (Figure 6-6).

Figure 6-5 A Four storey RC framed building with fired clay masonry infill.
Building constructed in 2010 without any seismic consideration. On the same site there is another school building designed with some limited seismic consideration following the 1988 earthquake, illustrating that seismic design awareness apparently reduced as the memory of the last earthquake dimmed. This is also symptomatic of weak enforcement of building regulations.

Figure 6-6 Damages in storey columns and walls in a RC-framed building.
(L) Four Storey RC-framed building continued spalling of concrete and deformation of rebar at column nodes (R) Propping installed since earthquake and cracking of infill walls.

- **Fired Clay Masonry**

Of the ten loadbearing fired clay masonry buildings visited, five were red tagged and two were green tagged, with a further three having no apparent rating. Four of the buildings were constructed to a typical design rolled out after the 1988 earthquake. Seismic features include a thin band of reinforced concrete at sill level whilst gable walls were made of CGI sheeting (see Figure 6-8). Critically there was no ring beam at the tops of the walls, leaving them to cantilever up to the roof instead (Figure 6-7). In two of the buildings this had led to the walls becoming unsafe, with cracking along the joint between the masonry and the sill level RC band beam (Figure 6-7). Both of these buildings had been red tagged.

Figure 6-7 A fired clay brick school building with gable wall failure.

The end wall has collapsed due to insufficient bonding at the corners as testified by the clean break with the surviving wall.

Figure 6-8 A fired clay brick school building with gable walls.
(L) A fired clay brick school building built to a typical design rolled out after the 1988 earthquake. A thin RC sill band can be seen below the windows whilst. (R) gable walls are constructed from corrugated galvanised iron (CGI) sheeting, a good detail for reducing weight and seismic vulnerability. With no ring beam at roof level the walls are un-restrained cantilevers.

- **Load bearing Stone Rubble Masonry**

All of the stone rubble buildings visited were red flagged highlighting the inherent vulnerability of this construction typology. Stone rubble was used by itself, but also used as walls for light gauge steel framed buildings (see Figure 6-9, 6-10 and 6-11). Stone rubble is used almost exclusively with mud mortar giving walls of very low strength. One had collapsed completely with materials already salvaged by the community by the time of the visit. The other two had suffered collapse of gable walls and exhibited significant cracking throughout.

Figure 6-9 Stone rubble with mud mortar school.
(L) A stone rubble with mud mortar school implemented by an international aid agency, it bears similarities to the typical desing seen in the photos on the previous page. (R) CGI sheeting has again been used in place of stone for the external walls.

Figure 6-10 Interior view of stone rubble with mud mortar school.
(L) Unfortunately the detail was applied inconsistently with the result that the internal rubble stone gable wall has partially collapsed with potentially deadly results. (R) Again the absence of a ring beam at the top of the walls is a critical design flaw meaning that the wall shown is an un-restrained cantilever.

Figure 6-11 Stone Rubble Masonry.
(L) Gable wall collapse of a stone rubble with mud mortar building (R) Damage to buttress

- **Temporary solutions**

Utilisation of schools as community centres for disaster response is a common occurrence around the world (see Figure 6-12). The role of schools as community centres for disaster response was highlighted at two of the schools visited, with the Red Cross having set up an aid distribution centre on the playground at one school. At another near Kathmandu, nearby residents whose homes had collapsed or were deemed unsafe were being sheltered in tents on the playing field.

Figure 6-12 Schools as community centres for disaster response.
(L) A Red Cross distribution centre set up on a school playground (R) A temporary school constructed by the local community from salvaged timber and CGI sheeting.

NSET reported that some schools were closed for up to one month following the first earthquake due to fear of aftershocks. With the trip occurring two months after the initial event the recovery had already begun. In two of the six schools visited the community had self-organised, clearing and sorting rubble and salvaging materials where possible, illustrating that recovery from a disaster is often led at a local level, especially in rural locations. In contrast an unsafe building in Kathmandu was demolished by the army. Tents were issued by agencies to two of the schools visited to replace classrooms that had collapsed or were deemed unsafe and were tagged red (see Figure 6-13). NSET reported that 61 bamboo and tarpaulin temporary schools had been completed. Of the 11 red tagged school buildings visited, 3 were still in use (see Figure 6-13). In each case, school staff cited the lack of alternative space as the reason, underlining that further work was required to meet the temporary need for classroom space whilst permanent reconstruction is planned and implemented.

Figure 6-13 Temporary solutions.
(L) Red buildings are being occupied in cases where there is no alternative. (R) Tents being used as temporary classrooms.

- **Permanent solutions**

Permanent re-construction was under way at two schools in and near Kathmandu. In both cases the donor and design was the same with materials and labour having been supplied by an Indian organisation (Radha Somai Satsang Beas, http://www.rssb.org/), who plan to construct 48 buildings in total. The designs consisted of a prefabricated, bolted, steel framed structure, with roof and walls to be clad with CGI sheeting. This included insulative material in order to provide some protection against heat and cold. Both materials and labour were imported from India, with the cost unknown. This imported prefabricated approach enabled them to construct a new school building in 10 days from start to finish (see Figure 6-14). Whilst the speed of response and lightweight and hence seismically resilient nature of the designs

are to be commended it appeared that in the rush to rebuild little consideration had been given to the location of the new buildings within the school site.

Figure 6-14 New prefabricated steel framed school vs. collapsed school.
(L) A permanent prefabricated steel framed school building under construction in Kathmandu. (R) The remains of a school building demolished by the army at the same site in Kathmandu.

In summary geographical location and access can be seen as key determinants in the response. Schools in and around Kathmandu had army assistance in demolition whilst an aid agency had nearly finished construction of two new prefabricated buildings. Outside of the capital demolition and temporary reconstruction was being led by the community.

6.2. Healthcare facilities

6.2.1. Introduction

This sections details key findings from visits to Chautara district hospital, which was badly damaged and four health posts, which were not. The hospital consisted of numerous buildings and the health posts typically consisted of two. Key findings are based upon visual observation as well as conversation with health workers.

There are nominally four levels in the hierarchy of health care facility in Nepal; (1) Regional or Zonal hospitals (2) District hospitals (3) Primary health centres and (4) Health posts. Health posts tend to be located in villages in rural areas. The location of health post is depicted in Figure 6-15.

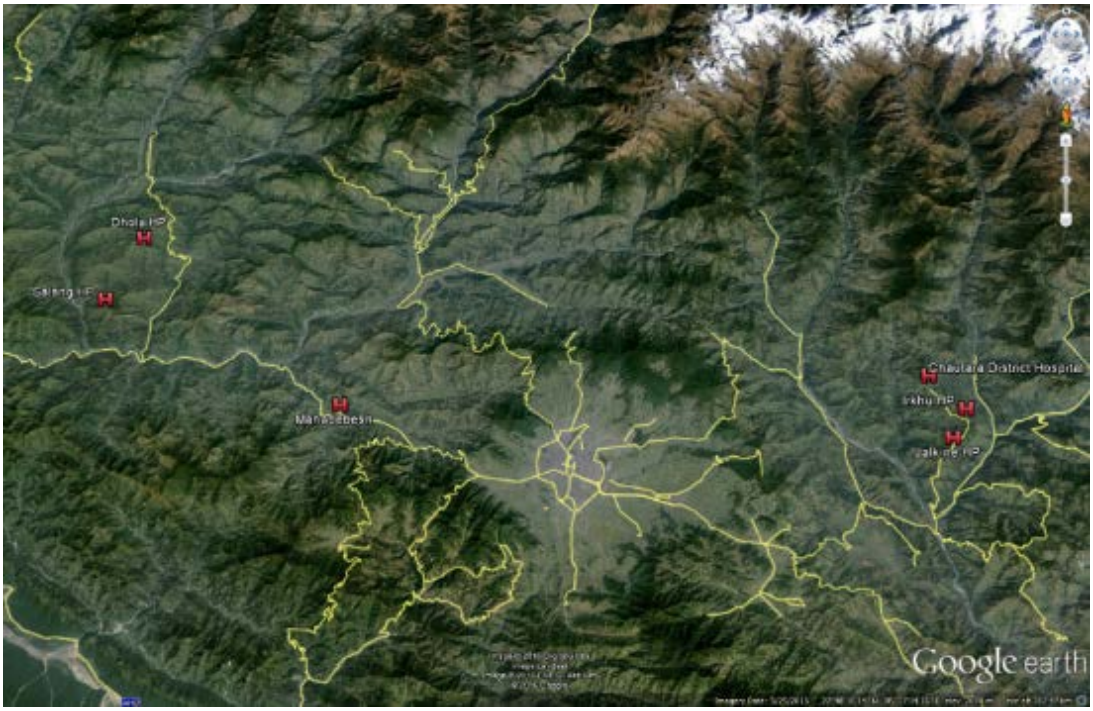

Figure 6-15 Health post locations.

6.2.2.Key findings

- **Rapid Visual Assessments**

Rapid initial assessments of health facilities were conducted by government officials in the weeks after the first event. The purpose of these assessments was to outline the scale of assistance needed to donors and were subsequently presented within the Post Disaster Needs Assessment (PDNA). They had three categories; completely, partially and un-damaged (see Table 6-1). 446 public health facilities (consisting 5 hospitals, 12 Primary Health Care Centres and 417 Health Posts, 12 others) and 16 private facilities were completely destroyed while a total of 765 health facility or administrative structures (701 public and 64 private) were partially damaged. Table 6-1 summarizes damage status in 14 highly affected districts. A total of 18 health workers lost their lives and another 68 health workers injured.

	Hospital		PHC		HP		Others		Private sector facilities	
Districts	Completely Damaged	Partially damaged	Completely Damaged	Partially damaged	Completely Damaged	Partially damaged	Completely Damaged	Partially damaged	Completely Damaged	Partially damaged
Bhaktapur	0	1	1	1	6	9	0	0	0	6
Dhading	0	1	1	1	33	12	1	1	3	5
Dolakha	1	1	0	1	33	16	1	0	3	2
Gorkha	0	1	1	2	35	24	6	6	5	3
Kathmandu	0	0	1	7	7	33	0	0	0	24
Kavre	0	1	1	2	32	50	0	1	0	2
Lalitpur	0	0	0	2	9	20	1	0	0	12
Makwanpur	0	0	1	2	14	13	0	0	3	6
Nuwakot	1	0	1	1	43	19	1	1	0	0
Okhaldhunga	0	0	0	0	17	17	0	0	0	0
Ramechhap	1	0	1	1	20	28	0	1	0	0
Rasuwa	1	0	0	1	14	3	1	0	1	2
Sindhuli	0	1	1	3	23	7	0	0	1	2
Sindhupalchok	1	0	1	2	62	17	1	0	0	0
Total (14 districts)	5	6	10	26	348	268	12	10	16	64
Source: PDNA findings presentation by MOHP										

Table 6-1 Post Disaster Needs Assessment (PDNA).
Source: the Ministry of Health and Population.

At the time of visit the Department of Urban Development and Building Construction (DUDBC) had conducted occupancy assessments of Hospitals but not of health posts. Detailed assessments of hospitals were being planned for July 2015 in order to determine whether a building should be repaired, retrofitted, reconstructed or relocated. The intention is that training and assessment tools will be provided by NSET.

The Ministry of Health had conducted rapid visual assessments of Health Posts with recommendations on whether they were safe to occupy given verbally to health workers. This was because only the DUDBC are legally entitled to provide written recommendations for Health facilities. Having completed occupancy assessments the Ministry of Health and Population (MoHP) had no plans to conduct more detailed assessments which would determine next steps in rehabilitation. In a bid to start the recovery various NGO's were engaging private engineering consultants to fill this need. In one case, the engineers involved had no previous experience in conducting damage assessments and had created their own assessment form based on internet research. The recommendations of these assessments were again given verbally and sometimes contradicted previous assessments, causing confusion and concern for health workers. The fragmented and contradictory health facility assessment process is in contrast to the assessment of schools, which appears to be benefitting from greater planning and organisation.

- **Structural Typologies**

The district hospital at Chautara consisted of a two and three storey RC frame with fired clay masonry infill. The health posts were single storey structures, with regular (nearly square) plans and internal cross walls subdividing the space, giving a relatively high wall density. The majority (seven) were constructed from rubble stone masonry with mud mortar, with wall thicknesses in excess of 350mm. Three buildings had a flat reinforced concrete roof, providing a roof diaphragm, albeit a heavy one. The only two buildings with apparent seismic design consideration were constructed by the Government. Government support during design and construction appears to reduce as you move away from urban areas. In the absence of government support rural communities had self-built non engineered structures.

Figure 6-16 Stone rubble buildings
(L) A stone rubble building with RC band beams at cill, header and roof level (R) A stone rubble building with a reinforced concrete roof slab

6.2.3.Building Performance

- **Hospitals**

Although the trip did not include a visit to Hospitals in Kathmandu, NSET reported that they were subject to only limited damage (see Figure 6-17 and 6-18). This did however result in a reduction of capacity at the police hospital, where some operations were moved to tents.

Chautara district hospital, consisting of an RC frame with fired clay infill, had incurred significant damage, with the main hospital building having been deemed unsafe by the DUDBC. The main building had been evacuated with operations moved to tents erected in the hospital grounds.

Figure 6-17Damages in a two storey RC framed district hospital.
Two storey RC framed District Hospital with damage to beam/column nodes evident throughout. Fired clay infill was cracked but had remained intact.

Figure 6-18 Damages in unreinforced mansony.
(L) This annexe building, consisting of unreinforced masonry, was particularle badly damaged (R) unlike the main building this structure had not reinforced concrete columns, instead relying on a single reinforcing bar in the corner.

- **Health Posts**

One of the rubble stone masonry health posts had collapsed, with the rest exhibiting minor cracking only. This may in part be attributed to relatively good passive design features such as regular plans, thick walls, high wall density and single storeys.

Each of the health posts sites visited were highly constrained by the topography, with flat ground at a premium. Of the nine health post buildings visited all were within 3-4m of a retaining wall or an unreinforced earth face, with three immediately on top or at the bottom of a retaining wall. Three of the five sites visited had cracks in the ground or in retaining walls ,as a result of one of the earthquakes. Three of the buildings visited exhibited cracking that could be attributed to ground movement, two of these were built immediately above a retaining wall. This could be caused by movement of the wall and or settlement of fill placed behind the wall to generate the terraces.

Figure 6-19 Health posts.
With flat ground at a premium in rural areas Health posts were commonly located close by to retaining walls and often within made ground associated with man made terraces.

Figure 6-20 Dhole health post.
(L) Cracking can be seen around opening in the plaster. The walls are stone rubble with mud mortar (R) Dhole health post is the furthest site from Kathmandu visited. In the absence of govermente support the community had designed and built a non-engineered building.

- **Temporary solutions**

All of the sites visited had been provided with tents, one of which (Irkhu Health Post) was not in use as it was too small to be useful (the bag label suggested it was intended as a family shelter). Of the sites visited this Health Post was the furthest from Kathmandu, again illustrating the relationship between support received and ease of access.

At Jalkine Health Post a local NGO facilitated a grant and instructed a team of local craftsmen to construct a temporary clinic in place of a collapsed stone rubble building. This consisted of a salvaged timber frame, salvaged CGI roof sheeting and bamboo lath walls rendered with clay and brick dust. This solution is non-engineered but low cost, utilises local labour and materials and its low weight means its performance in an earthquake is enhanced. The Health Post worker on site was glad that the new structure would be lightweight and hence safer, demonstrating that there is an understanding on the ground that heavy weight buildings are dangerous in an earthquake.

Figure 6-21 Field hospitals.
(L) All of the health posts and one district hospital visited had been issued with tents. The picture illustrates one of the largest tents seen at Chautara district hospital. (R) A local NGO temporary health post solution at Jalkine.

In many rural areas that only available material is stone, unfortunately there is an absence of seismic resistant designs. The MoHP response to this challenge has been to develop standard guidelines for health post-reconstruction, which provide concept design level detail for prefabricated transitional Health Post designs. They consist of steel frames with imported, pre-fabricated sandwich panels. Agencies wishing to build new health posts' will have to construct the Government designs or else will need to get a new design signed off by the MoHP. Anecdotal evidence suggest this is a politicised, bureaucratic and hence lengthy process.

Whilst these pre-fabricated designs are lightweight and should perform well in an earthquake they have a relatively short design life of 15 years. Importantly by importing materials and construction technology the construction process will exclude the local community who could never hope to replicate the design. The opportunity to build local capacity through implementation of designs that utilise local materials has been missed.

Figure 6-22 Prefabricated standard designs.
One of three proposed government prefabricated standard designs constructed from imported materials requiring construction technology that is new to rural Nepal. Note that the Image of the completed building was not taken in Nepal as construction was yet to start.

7. LANDSLIDES AND REMOTE HILLTOP VILLAGES

7.1. INTRODUCTION

From discussion with members of various NGOs and volunteers, the team had established that hilltop villages in the Gorkha region had been badly affected and that reports indicated that landslides were a significant cause of the fatalities in the region. It was also reported that these landslides were continuing to be a threat to the remote hilltop villages. Landslide casualties were also reported to be significant to the East of Kathmandu. As landslides have been observed as a poorly appreciated risk in previous events (Wilkinson et al. 2012) (Chian and Wilkinson 2015) and that there is likely to still be a significant seismic hazard in Nepal (Bilham 2015). The team hoped to visit the region affected by these landslides. The team coordinated with the UN Office for the Coordination of Humanitarian Affairs *(*OCHA) who confirmed that landslides were a serious concern in the region. The UN organised two team members to be flown by helicopter to the villages of Yamagaum and Lapsibot in the region of Gumda. The reason for this visit was to observe how the earthquake had impacted on remote mountain communities, and to ascertain any continuing threats to villages.

The urgent demand for helicopters, necessitated very short visits to each of these villages (less than one hour in each). A third village on the itinerary (Machikhola) was not visited as it had been evacuated due to the risk of further landslides and it was deemed too dangerous to land the helicopter for the extra information that an uninhabited village may produce.

The flight over the region enabled the team to see the scale of the situation in this region. Figure 7-1 shows a map with photographs taken during the helicopter flight and each photo shows either a village with damaged buildings or a landslide (note: these photos are available on request from EEFIT).

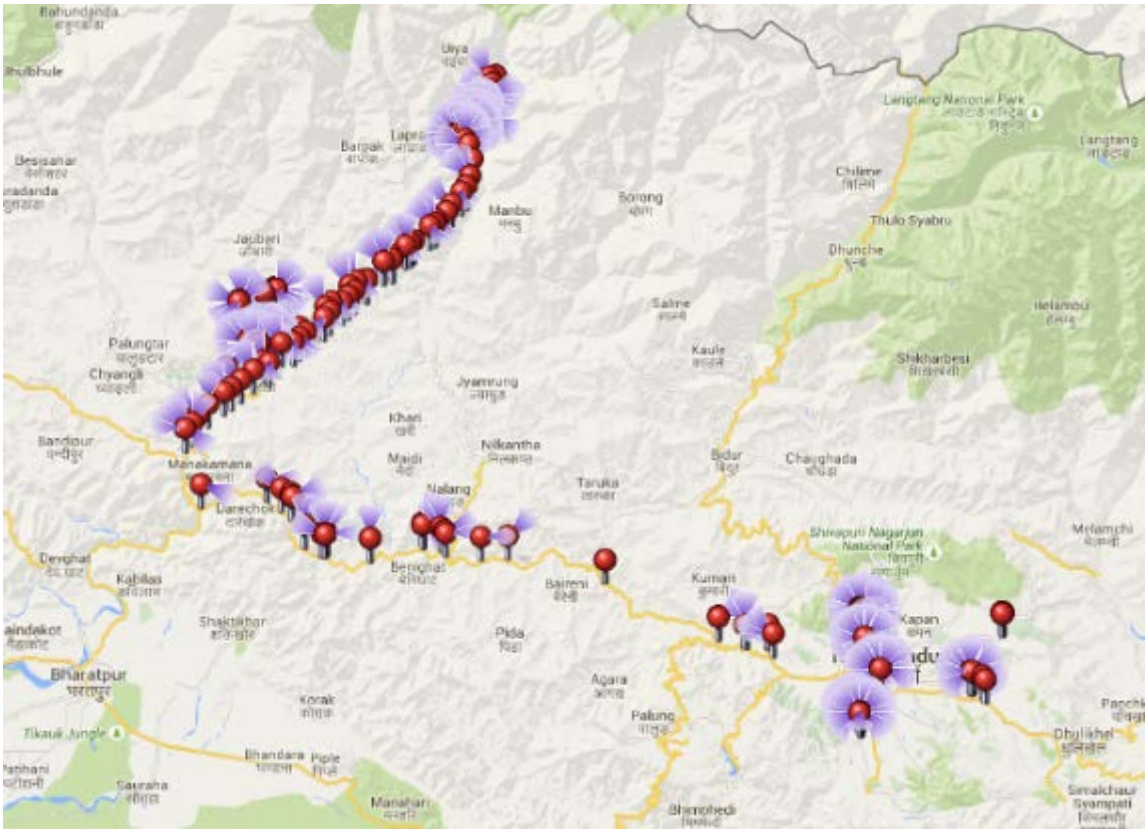

Figure 7-1 Flight path of the helicopter.
Each of the markers in the figure is the location and direction of a photoraph that was take during a helicopter flight to remote hilltop villages and each photo shows either a damaged village or a landslide. These photos are available from EEFIT upon request.

The villages ranged from only a few dwellings to quite large villages and most had tarpaulins on the roofs of many of the structures. Those villages that the helicopter flew close to enabled the team to see that many of the buildings had suffered serious damage or had collapsed. The two villages surveyed had similar levels of damage to those witnessed during the flight (the villages were chosen because of the landslide risk not because they had unusually high levels of building damage). Some examples of the villages that were overflown can be seen in Figure 7-2

a) Badly affected village. This village sustained heavy levels of damage but this was not unusual in the villages that were overflown. The coloured roofs are usual (but not always) tarpaulins. These were necessary due to roofs collapsing when rubble masonry walls collapsed or sustained heavy damage.

b) Very badly affected village. It is not known if this village was abandoned long before the earthquake and left to decay or whether it was caused by the earthquake, but the coloured roofs suggest the damage may have been recent.

C) Hill village

d)The village of Yamagaum. The buildings of this village were survey and are displayed in later figures. The locations of the various building mentioned in the report are indicated on this figure as a) new school building, b) temporary school building c) path to devastated school building (just out of shot).

e)The village of Machikhola. A survey was due to be conducted here, but was cancelled due to the ongoing threat of landslide

Figure 7-2 Villages that were overflown during the helicopter flight.

The landslides observed from the helicopter were many and some were very large. It was observed that many of the landslides cut across paths and this was later stated to be a significant impediment to relief operations. In general villages were located reasonable distances away from landslides, but a number of dwellings were observed to be in close proximity to significant landslides. A number of the landslides that were observed from the helicopter are shown in Figure 7-3.

a) Large Scale Landslide (scale can be judged from buildings in a small village on the right mid ground. Supply paths are also visible in the image and the landslides severed most of these

b) Landslide that has destroyed supply roads at a number of locations. This was reported to be extensive and a continuing threat which was severely hampering relief observations.

c) Shallow landslide of a similar size to the landslide in the above image.

d) Large landslide, size can be estimated from village at bottom right of the picture and the village above the landslide.

e) Thin landslide in close proximity to a village. Although most villages that were overflown by the helicopter were a reasonable distance away from the landslide, a number of villages were observed very close to significant landslides.

f) Deep landslide estimated to be over 200m in length.

g) Large scale landslide (scale can be judged from buildings in a small village on the right mid ground). Supply paths are also visible in the image and the landslides severed most of these.

h) Landslide that has destroyed supply roads at a number of locations. This was reported to be extensive and a continuing threat which was severely hampering relief observations.

i) Shallow landslide of a similar size to the landslide in the above image.

j) Large landslide, size can be estimated from village at bottom right of the picture and the village above the landslide.

K) Thin landslide in close proximity to a village. Although most villages that were overflown by the helicopter were a reasonable distance away from the landslide, a number of villages were observed very close to significant landslides.

L) Deep landslide estimated to be over 200m in length.

Figure 7-3 Landslide observed during the helicopter flight
Descriptions of features are presented next to individual pictures. GPS coordinates of camera location when photographs were take are available form EEFIT

Upon landing at each village a meeting was held with the villagers and a number of questions were asked to ascertain what impact the earthquake had on life in the village. It should be stressed that these questions were asked from an engineering perspective and there are many other important impacts resulting from the earthquake that we were not qualified to obtain. For example questions regarding health provision, food supplies, and other social impacts. A member of the United Nations (UN) was also part of the visiting team and she conducted detailed interviews on these matters (Robertson 2015). The villagers reported that 24 villagers had died as a result of landslides (most of the deaths had been farmers tending their herds) and nobody had died as a result of building collapse and only a few serious injuries had been sustained by this mechanism. The villagers reported that no one had yet supplied the village by overland routes (not even yaks or Sherpas) since the earthquake as landslides had swept away the road and rebuilding efforts were not successful as further landslides were continually severing the road. It was reported by the villagers that the only supplies provided thus far had been by helicopter.

7.2. YAMAGAUM

A rapid tour (approx. 30 mins) of the village and immediately surrounding slopes was made. This village is located on a steep sided hillslope In Gumda district. The village consists of a number (47 households according to the villagers) of dwellings and an aerial photograph of the village is shown in Figure 7-2d. These are mainly rubble masonry construction with timber and corrugated steel sheet roofs. The construction of these dwellings is very poor. The mortar was very weak although it did have some form of binding material (most likely either cement or lime). Most of the buildings suffered either partial or complete collapse (examples are shown Figure 7-4).

Figure 7-4 Examples of building and typical damage.

During the visit to this village, the local school was also surveyed. This buildings was of an even poorer construction. It is likely that no binder was used in the mortar (i.e. mud mortar) and the school suffered complete collapse (see Figure 7-5). A temporary school has been constructed towards the bottom of the village and lessons were taking place during the visit and this is shown in Figure 7-6. Near the collapsed old school and next to the temporary school, there was a new school under construction (shown in Figure 7-7). The construction of this school had commenced prior to the earthquake and while it was of much better construction with evidence of reasonable concrete reinforcement detailing, the rubble wall infill looked to have failed on this structure and therefore was inadequate (it should be noted however, that as the building was incomplete and there may have been a subsequent method of restraining the infill that had not yet been installed).

Figure 7-5 School building, showing complete collapse.
This building was one of the most poorly constructed in the village with no cement used in the mortar.

Figure 7-6 Temporary school building.

Figure 7-7 School building damaged.
New School building, showing concrete columns in the corner with longitudinal reinforcing and confining reinforcing (not apparent in this figure). The concrete appeared to be of reasonable quality and the lap lengths were reasonable length and there was evidence of confining reinforcing. The rubble infill did not seem to have binder and appears to have sustained damage. Whether further construction would have increased the stability of this wall remains unclear.

7.2.1.Landslide Risk in Yamagaum

Above the village, tension cracks were observed in the terraced hillslope. The width of the cracks varied between approximately 10mm and 40mm and they ran parallel to the slope for approximately 50m. It should be noted that accurate observations of crack widths were hampered as locals had attempted to fill in the cracks with clay. This operation was both observed and reported by locals who stated that the purpose was to prevent ingress of water. Other cracking was observed lower down the slope. Due to time constraints the exact extent and nature of observed cracks was not established.

7.3. LAPSIBOT

This village lies on an adjacent hillslope in a similar topography. it was reported to consist of 85 households. These buildings are of a similar typology to Yamagaum, are of a similar construction quality and suffered similar damage patterns. The structures and observed damage and failure patterns were similar to Yamagaum and can be seen in Figures 7-8.

Figure 7-8 Building Damage in Lapsibot

To the North East of the village is a trail that follows a ridge that eventually descends into the village of Machikhola. During a walk along the ridge (the route of which can be seen in Figure 7-9) a small landslide was observed on the other side of the valley and highlighted the unstable nature of the slopes. Further along this trail a series of tension cracks were also observed running along the ridgeline. These cracks were almost continuous along the ridge and examples are shown in Figure 7-10. Due to time constraints, the exact nature of this system

of cracks and landslide could not be established. The observations terminated at a large landslide shown in Figure 7-11.

Figure 7-9 Route of landslide survey.

Once beyond the village (seen at the left of the picture) significant tension cracks could be seen along the entire route traversed, although these were not necessarily continuous. Examples of these cracks are shown in Figure 7-10.

Figure 7-10 Tension Crack on the survey route.

Figure 7-11 Landslide at the termination of the survey.

7.4 References

April 2015 Nepal earthquake creative commons article available at, https://en.wikipedia.org/wiki/List_of_people_who_died_climbing_Mount_Everest, Retrieved 05/08/2015

Bilham, R; 2015; Raising Kathmandu, Nature Geoscience| Vol 8 | August 2015

Chian, SC; Wilkinson, SM; 2015; Feasibility of Remote Sensing for Multihazard Analysis of Landslides in Padang Pariaman during the 2009 Padang Earthquake; Natural Hazards Review 16 (1), 05014004

Goda, K; Kiyota, T; Mohan Pokhrel, R; Chiaro, G ;Katagiri, T; Sharma, K ;Wilkinson, S; 2015; The 2015 Gorkha Nepal earthquake: insights from earthquake damage survey; Frontiers in Built Environment; June 2015 | Volume 1 | Article 8

Robertson 2015, UN OCHA Field Trip Report to Gumda: 17 June 2015

USGS 2015 http://earthquake.usgs.gov/earthquakes/eventpage/us20002926. Retrieved 01/05/2015

Wilkinson SM, Alarcon JE, Mulyani R, Whittle J, Chian SC. 2012, Observations of damage to buildings from M_W 7.6 Padang earthquake of 30 September 2009. Natural Hazards 2012, 63(2), 521-547.

8. SOCIO- ECONOMIC IMPACT

In general, the event affected remote mountainous regions much more severely than urban regions around Kathmandu. Although very serious losses were experienced around the capital, these did not trigger social or economic crises of the scale apparent in the Northern provinces.

For prioritizing rescue and relief operations, 14 of the 75 Nepalese districts were tagged as 'severely hit' or 'crisis hit', as in Figure 8-1. In Kathmandu, supply of food and shelter, as well as supporting transport infrastructure and sanitation were not dramatically affected. During the team's visit in June, all economic and basic systems were working at standard or near-standard levels of operation. In contrast, villages in the mountains that had experienced severe devastation could not be reached easily by roads that had also been damaged by landslides. These situations posed the most severe challenge and it is these regions that have needed the most intense humanitarian response to re-establish food and shelter supply and basic sanitation. The flash appeal of US$422 million issued by UN OCHA to cover immediate relief operations was financed up to 66% as of January 2016.

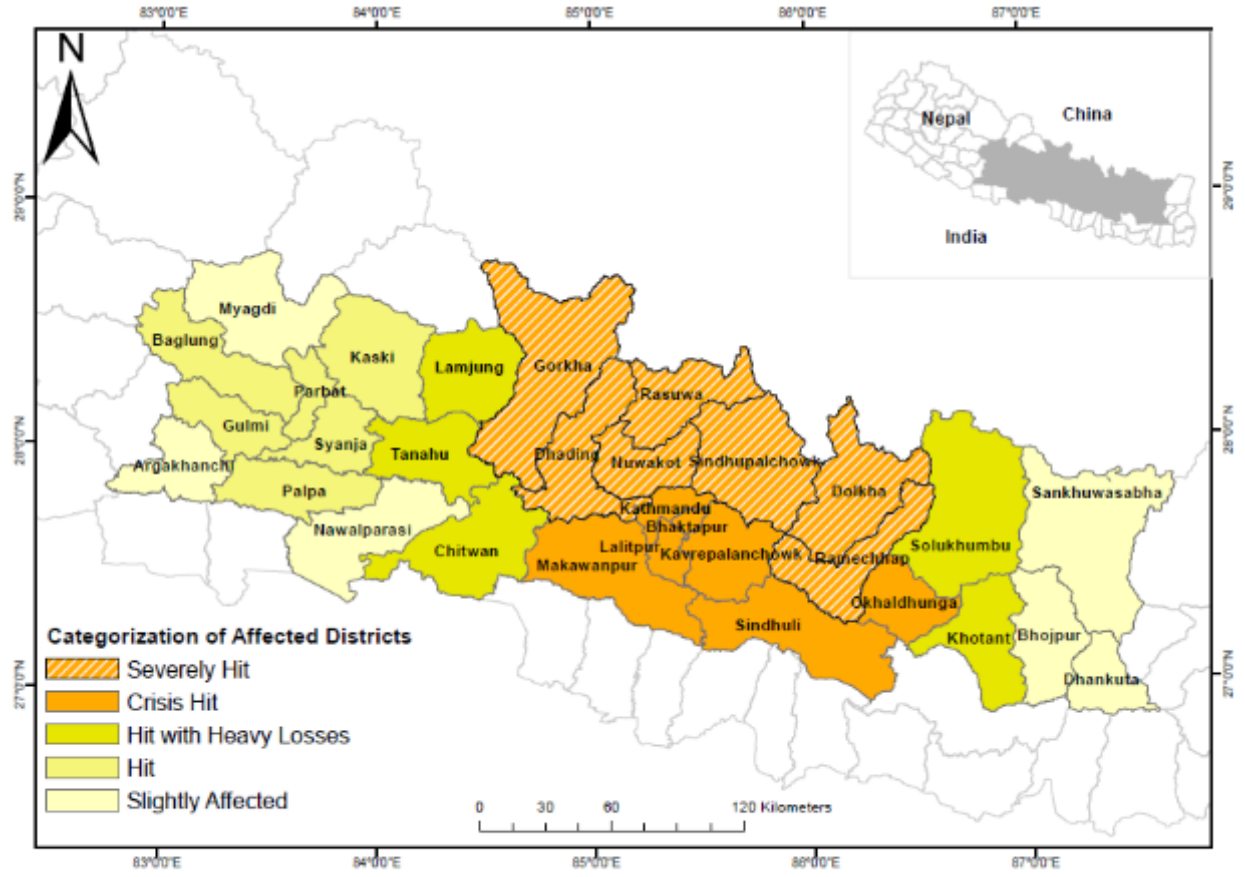

Source: GoN/MoHA as of 21 May 2015

Figure 8-1. Level of impacts throughout Nepalese regions.

TYPE	MEDIAN	ACCEPTED RANGE	DESCRIPTION	SOURCE
Deaths	8,254 (25.04)+ hundreds (12.05.)	ca. 350 missing	1,400-7,500* = initial estimate 7,560 (3,570-11,970)* = updated intensities 9,100 (5,700-14,000) = 2nd update	Daniell, CATDAT, EQ Report.
	**NB: 8,151 Nepal, 25 China , 75 India and 4 Bangladesh as of 16.15UTC 11.05			
Injuries	17,861	May rise	Still counting	News
Homeless/Displaced	1.3 million	1.2-1.7 million	Estimated 8 million affected, and 1.3 million homeless due to destroyed buildings	

*predicted

Table 8-1. Preferred social impact information.
Source: CEDIM (2015).

The EEFIT team visited some of the communities in Gorkha that were receiving aid in the form of packages containing building materials and cooking utensils (see Figure 8-2). Communities that were reachable in the lower parts of the mountains, albeit heavily hit by the event, seemed well organized and well supplied. However, those that were hard to reach, often only by helicopter, feared differently as the team could survey during a brief visit of three communities at high altitude (see Section 7 Landslides and Remote hilltop villages).

Figure 8-2. Package aid and distribution in Gorkha low-altitude communities.

Among the sectors most affected, two stand out: housing and tourism. These also reflect the juxtaposition between the effects in remote mountainous regions versus the Kathmandu valley.

Housing sector losses were large and completely dominate the distribution of loss (see Figure 8-3). Loss of housing was experienced in all regions affected, in some of Kathmandu's districts, around the immediate vicinity of Kathmandu in Bhaktapur, and in the Northern provinces of Gorkha, Nuwakot, Sindhupalchowk and others. Housing sector losses were frequently observed during the EEFIT field survey and are described in previous sections. They consisted of partial or total collapses of mid-rise reinforced concrete condominium structures in the most populated areas and of generalized collapses of weak masonry, non-engineered, low-rise residential buildings in more remote communities and entire city neighborhoods in historical districts.

According to the PDNA (World Bank), the housing sector accounted for about US$3.5 billion damages while tourism accounted for nearly US$1.0 billion. Cultural heritage buildings, whose existence is tightly linked to tourism income, suffered damages estimated at about US$300 million but, based on the EEFIT's team observations on the field (see section 4.3), this

estimate could be significantly underestimated and it the reconstruction of WH assets (assuming it takes place) could also severely hamper tourism revenue.

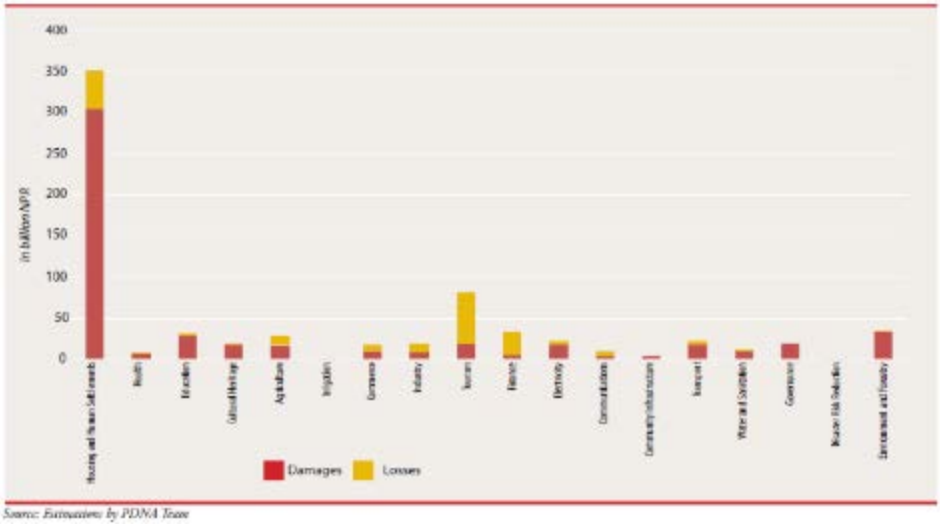

Figure 8-3. Disaster effects across sectors.
Source: World Bank 2015.

Total needs were assessed by the PDNA at about US$7.0 billion (see Table 8-2). About 73% (about US$5.1 billion) of these needs represented direct damages while the rest 27% (about US$1.9 billion) represented derived monetary losses. The direct damage estimates are in line with estimates calculated by the Centre for Disaster Management and Risk Reduction Technology (CEDIM) (see Table 8-3). Most of these losses were assumed by private individuals without any form of insurance or any other risk coverage mechanism. In fact, the losses suffered by the incipient insurance sector in Nepal amounted to about US$130 million, which is equivalent to a barely significant 2.5% of the direct damages experienced.

SECTOR	Total Needs (NPR million)	Total Needs (US$ million)	Share of Needs by Sector
Social Sectors	**407,747**	**4,077**	**60.9%**
Housing	327,762	3,278	49.0%
Health	14,690	147	2.2%
Nutrition	5,036	50	0.8%
Education	39,706	397	5.9%
Cultural Heritage	20,553	206	3.1%
Productive Sectors	**115,618**	**1,156**	**17.3%**
Agriculture	15,561	156	2.3%
Irrigation	467	5	0.1%
Commerce	20,051	201	3.0%
Industry	7,357	74	1.1%
Tourism	38,710	387	5.8%
Finance	33,472	335	5.0%
Infrastructure Sectors	**74,266**	**743**	**11.1%**
Electricity	18,586	186	2.8%
Communications	4,939	49	0.7%
Community Infrastructure	4,450	45	0.7%
Transport	28,185	282	4.2%
Water and Sanitation	18,106	181	2.7%
Cross-Cutting Issues	**71,875**	**719**	**10.7%**
Governance	18,442	184	2.8%
Disaster Risk Reduction	8,204	82	1.2%
Environment and Forestry	25,197	252	3.8%
Employment and Livelihoods	12,547	125	1.9%
Social Protection	6,398	64	1.0%
Gender and Social Inclusion	1,086	11	0.2%
Total	**669,505**	**6,695**	

Table 8-2. Estimation by the PDNA team of needs and losses by sector.
Source World Bank 2015.

TYPE	MEDIAN	ACCEPTED RANGE	DESCRIPTION	SOURCE
Replacement Cost (incl. triggered quake)	$5,930m	$4,880m-$8,440m	Replacement Cost (without indirect/life) - $2.5-3.2bn USD in building costs	CATDAT
Total Loss	$3,860m	$3,210m-$6,020m	Total estimate (using rapid loss model)	CATDAT/Daniell

Table 8-3. Loss information published.
Source: CEDIM (2015)

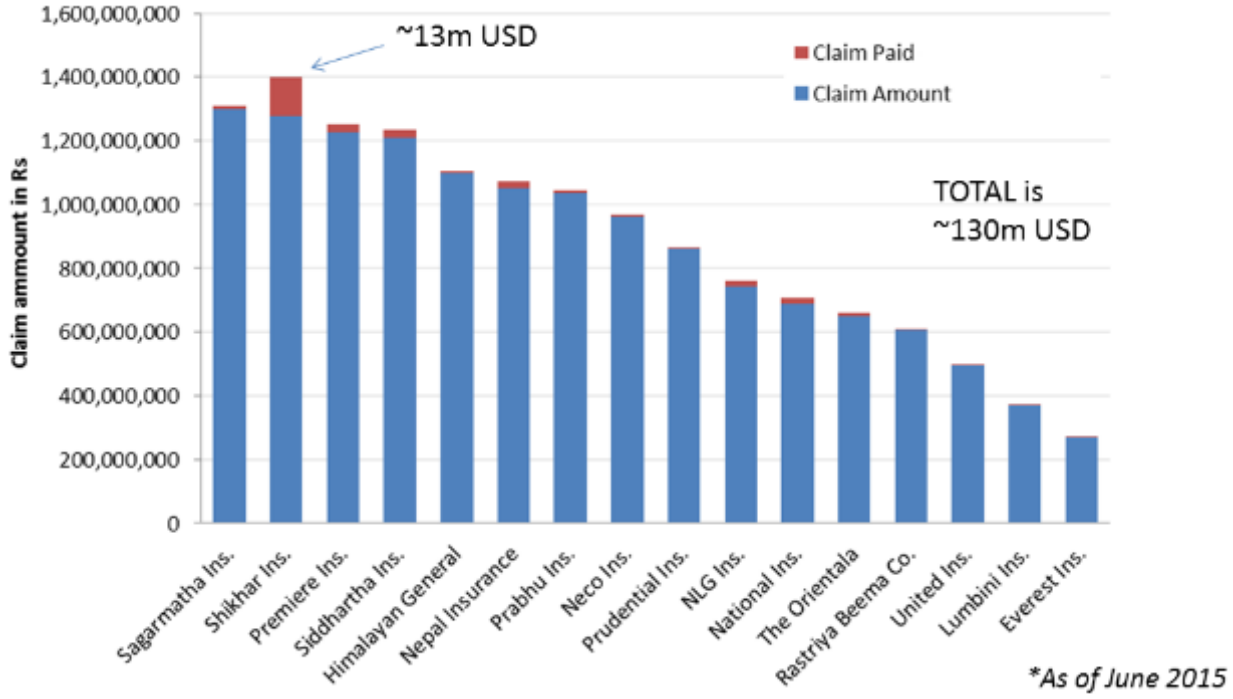

Figure 8-4. Distribution of insured losses among Nepalese insurance companies.

Most of the 16 insurance companies operating in Nepal (see Figure 8-4) did not have appropriate reinsurance coverage, so it is likely that, as a consequence of this event, some of them will suffer severe financial impacts that may trigger bankruptcies or defaults.

8.1. REFERENCES

World Bank. 2015. Nepal - Earthquake post disaster needs assessment : sector reports. Washington, D.C. : World Bank Group. http://documents.worldbank.org/curated/en/546211467998818313/Nepal-Earthquake-post-disaster-needs-assessment-sector-reports

CEDIM Center for Disaster Management and Risk Reduction Technology, Karlsruhe Institute of Technology, Forensic Disaster Analysis Group, CATDAT and Earthquake Report.com, Nepal Earthquakes, Report #3, http://www.cedim.de/english/2624.php

9. CONCLUSIONS

The Gorkha 2015 earthquake and its main aftershock had magnitudes 7.8 and 7.3 M_w respectively, were shallow and about 150 km apart. The subsequent aftershocks mapped out a zone nearly 200 km along the spine of Nepal, from west of the Gorkha epicentre, eastwards, to east of the main aftershock, consistent with a subsurface rupture length of ~200 km. While smaller earthquakes tend to a point source, the Gorkha earthquake is better visualised in combined terms of its epicentre and large rupture area.

The Gorkha earthquake and related aftershocks was a major event that caused significant damage, losses and social upheavals in a large region of Nepal between the epicentre and an area stretching to the East of Kathmandu. The earthquake also triggered numerous devastating landslides in the hills and mountains of the affected region as well as causing an avalanche on Mt. Everest which resulted in the deaths of Sherpas and climbers.

The ground shaking was unusual in that much of the energy was concentrated in the long period (4-6 sec) region and this is likely to have contributed to the less than expected damage observed in mid-rise engineered structures in Kathmandu and surrounding areas. The survey team witnessed many of the reinforced concrete structures to be very slender with small structural members and yet they had survived an M_w 7.8 earthquake. The extent of damage or impact on the communities in Nepal should not be downplayed however, as damage to masonry and rubble masonry structures and temples was typically severe and there were many people still living in tents at the time of the survey. In addition to the ground shaking being concentrated in the long period range of 4-6 seconds, other reasons for this less-than-expected damage are still unclear; however, some of the reinforcing detailing witnessed in reinforced concrete structures was good for a country at this stage of development and recent history, and this may have also contributed to the survival rates, but more work needs to be done to confirm the validity of these explanations as there were also large spectral accelerations recorded in the 0.2-0.6 second period range and many examples of poorly constructed buildings. It should also be noted that the timing of the earthquake of would have also influenced survival rates.

In certain locations, the geotechnical makeup of the region had a significant effect on the ground shaking with micro-tremor recordings indicating likely site amplification at locations such as the Siddhitol region near the edge of the Kathmandu Valley.

Liquefaction was not a significant feature of this earthquake although there were some isolated but significant liquefaction failures near the Bishnumati River.

School buildings often performed badly, especially in the more rural areas due to the dominance of poor quality masonry wall construction; however schools that had been constructed or retrofitted with NSET supervision with attention to construction quality and seismic details, generally performed well.

At the time of survey, the hill villages were still in a difficult situation. Supplying these villages with essentials was proving challenging for the Nepalese Government, the UN and NGOs. It was reported by the villages that were visited that overland supplies were not arriving as further landslides continued to sweep away the supply roads. A helicopter flight over the region showed that in every village a significant number of buildings (often most) had tarpaulins on their roofs and therefore had presumably suffered significant damage. This general observation was confirmed by the on-site inspection of two of the villages, where most masonry buildings had suffered partial or complete collapse (intensity IX). Finally, the landslide risk remains and the arrival of the monsoon will increase this risk. Landslide hazard and risk are endemic throughout the Himalaya and the fronting lower mountains. The villages described in this paper showed evidence of stressed hillsides and with the onset of the monsoon season the risk of further landslides has increased. Based on this event and others, it seems that globally, there is an underestimation of earthquake-induced landslide risk and insufficient resources being devoted to mitigating this risk. The observations of the earthquake impacts in Nepal suggest that this should be a cause for concern for us all.

Impact on the Nepalese economy was significant with considerable losses to housing and to the tourist industry both in terms of trekking, in the short term, and tourism related to cultural heritage in both the short and longer terms. There were also significant shortages in building material and labour in the construction industry which were hampering rebuild efforts.

EEFIT

Earthquake Engineering Field Investigation Team

EEFIT is a UK based group of earthquake engineers, architects and scientists who seek to collaborate with colleagues in earthquake prone countries in the task of improving the seismic resistance of both traditional and engineered structures. It was formed in 1982 as a joint venture between universities and industry, it has the support of the Institution of Structural Engineers and of the Institution of Civil Engineers through its associated society SECED (the British national section of the International Association for Earthquake Engineering).

EEFIT exists to facilitate the formation of investigation teams which are able to undertake, at short notice, field studies following major damaging earthquakes. The main objectives are to collect data and make observations leading to improvements in design methods and techniques for strengthening and retrofit, and where appropriate to initiate longer term studies. EEFIT also provides an opportunity for field training for engineers who are involved with earthquake-resistant design in practice and research.

EEFIT is an unincorporated association with a constitution and an elected management committee that is responsible for running it activities. EEFIT is financed solely by membership subscriptions from its individual members and corporate members. Its secretariat is generously provided by the Institution of Structural Engineers and this long-standing relationship means that EEFIT is now considered part of the Institution.

Earthquake Engineering Field Investigation Team (EEFIT)
c/o The Institution of Structural Engineers,
International HQ
47-58 Bastwick Street
London EC1V 3PS
Tel: +44 (0)20 7235 4535
Fax: +44 (0)20 7235 4294
Email: mail@eefit.org.uk
Website: http://www.eefit.org.uk